Lucas Lagerquist

Structure and Properties of Soda-type Lignin from a Modern Biorefinery Process

Åbo Akademi University

Structure and Properties of Soda-type Lignin from a Modern Biorefinery Process

Lucas Lagerquist

Organic Chemistry
Faculty of Science and Engineering
Åbo Akademi University
Åbo, Finland, 2022

SUPERVISORS
Docent Patrik Eklund
Laboratory of Molecular Science and Engineering
Åbo Akademi University
Åbo, Finland

And

Professor Chunlin Xu
Laboratory of Natural Materials Technology
Åbo Akademi University
Åbo, Finland

OPPONENT
Assistant Professor Mika Sipponen
Stockholm University
Stockholm, Sweden

REVIEWERS
Professor Mikhail Balakshin
Aalto University
Helsinki, Finland

And

Assistant professor Elias Feghali
Notre Dame University - Louaize
Zouk Mosbeh, Lebanon

ISBN 978-952-12-4194-9 (printed)
ISBN 978-952-12-4195-6 (digital)
Painosalama Oy – Åbo, Finland 2022

Stay Awhile and Listen

- Deckard Cain

Preface

This work was carried out between the years 2015-2021 at the Laboratory of Organic Chemistry, Åbo Akademi University. The financial support received from the Fortum foundation project 201700061 and 201800091, Rektor för Åbo Akademi, Forskningservice vid Åbo Akademi, Suomen Luonnonvarain Tutkimussäätiö, and Magnus Ehrnrooths stiftelse are greatly acknowledged.

I would sincerely like to thank my supervisor Docent Patrik Eklund for giving me the opportunity to delve into the beautiful field of lignin chemistry. I am truly grateful for all the support and encouragement I've received over these years. I am also grateful to my co-supervisor professor Chunlin Xu and former co-supervisor professor Stefan Willför for many fruitful collaborations. I would like to thank Professor Mikhail Balakshin (Aalto University) and assistant professor Elias Feghali (Notre Dame University – Louaize) for reviewing my thesis, and assistant Professor Mika Sipponen (Stockholm University) for being my opponent.

A special thanks to Dr. Jani Rahkila, particularly for Friday afternoon brainstorming sessions that led to multiple articles and many fruitful discussions. I am also very grateful to my colleagues at the Laboratory for Wood and Paper Chemistry, especially, Dr. Andrey Pranovich, Dr. Annika Smeds, and Jarl Hemming. I would also like to acknowledge my co-authors Dr. Tarja Tamminen, Professor Ilkka Kilpeläinen, and Dr. Ivan Sumerskii. I am also extremely grateful to my industrial collaborators Sebastian von Schoultz, Dr. Lari Vähäsalo, and Nicholas Lax from CH-Bioforce Oy.

I would like to thank my current and past colleagues (and good friends) at the Laboratory of Organic chemistry, in no particular order: Professor Reko Leino, Dr. Tiina Saloranta-Simell, Professor Leif Kronberg, Dr. Jan-Erik Lönnqvist, Päivi Pennanen, Teija Tirri, Dr. Denys Mavrynsky, Dr. Wojciech Zawartka, Dr. Risto Savela, Dr. Otto Långvik, Dr. Filip Ekholm, Jan-Erik Raitanen, Dr. Yury Brusentsev, Patrik Runeberg, Robert Lassfolk, Anton Örn, Veronika Badazhkova, Ellen Sundström, Atefeh Saadabadi, Annika Fougstedt, and many more.

I wish to thank my good friends Dr. Axel Meierjohann, Heidi Sundelin, and Magnus Perander for many adventures over the years. Professor Patrik Jern

and Dr. Ada Johansson for excellent company and Köklot visits. My sincere gratitude to my close friends Mikko Laikko, Miika Salo, Magnus Salo, Johan Ekström, Jan Lindholm, Markus Lervik, Patrik Hekkala, and Rasmus Wikman for your friendship over all these years.

My biggest thanks goes to my mother, father, and brother for always being there for me and supporting me. To my family Ida and Vidar, thank you for all the understanding, motivation, and support.

Åbo, May 2022

Lucas Lagerquist

Abstract

Due to the increasing concerns regarding the use of crude oil for fuel and chemical production, considerable efforts have been made to find renewable and sustainable alternatives. Lignocellulosic biomass is the most abundant carbon containing natural resource on earth and mainly consists of its structural components cellulose, hemicellulose, and lignin. Compared to the carbohydrate constituents, lignin is structurally completely different. It is derived from aromatic monomers which makes it an attractive feedstock for the production of renewable chemicals. For over a century the pulp and paper industry has been fractionating lignocellulosic biomass to isolate cellulose and to use the remaining hemicellulose and lignin for heat and energy production. To develop new products from lignocellulosic biomass, additional fractionation technologies need to be explored. The polymer structure of lignin is inherently complex and will structurally not only vary between plant species, but technical isolation methods will further alter its structure. As such each fractionation technology will yield a different type of lignin with different properties compared to other lignin. Due to these reasons, it is crucial to understand the structural features of different lignin to determine the best application area.

In this thesis three different lignin, one hardwood and two softwood lignin, from a pressurized hot water extraction followed by mild soda cooking biomass fractionation technology were thoroughly investigated. A precipitation and purification protocol were developed to yield lignin samples free of contamination. The different lignin fractions were analyzed and compared to native-like lignin samples. A wide variety of analytical methods were used and the combined information from the analysis could be used to determine key structural features and properties of the lignin. Also model compounds with specific structural features were synthesized and the spectroscopic data was used to assist in the structural elucidation of the analyzed lignin. As a proof of concept, the purified lignin was fractionated into even more homogeneous fractions by simple solvent fractionation. Chemical modifications were used to investigate how simple modifications affected the thermal properties of lignin and were also used for to assist the structural determination.

During this thesis a ^{31}P PULCON methodology was implemented to one of the most used lignin analysis methods, the quantitative determination of hydroxyl groups in lignin by ^{31}P NMR spectroscopy, which showed to have benefits compared to the standard protocol.

Abstrakt

På grund av oron kring användningen av råolja för produktion av bränsle och kemikalier har stora ansträngningar gjorts för att hitta förnybara och hållbara alternativ. Lignocellulosisk biomassa är den mest förekommande kolhaltiga naturresursen på jorden och består huvudsakligen av de strukturella komponenterna cellulosa, hemicellulosa och lignin. Jämfört med kolhydratkomponenterna är lignin strukturellt helt annorlunda. Lignin härrör från aromatiska monomerer och är därför en attraktiv råvara för förnybara kemiska produkter. I över ett sekel har massa- och pappersindustrin fraktionerat lignocellulosabiomassa för att isolera cellulosa och använda den resterande hemicellulosan och ligninet för värme- och energiproduktion. För att utveckla nya produkter från lignocellulosisk biomassa behöver ytterligare fraktioneringstekniker utvecklas. Ligninpolymeren är i sig komplex och kommer strukturellt inte bara att variera mellan växtarter, utan tekniska isoleringsmetoder förändrar ytterligare dess struktur. Detta leder till att varje fraktioneringsteknik kommer att ge en säregen typ av lignin med olika egenskaper jämfört med andra lignin. På grund av dessa orsaker är det väsentligt att förstå ligninets struktur för att avgöra det bästa tillämpningsområdet.

I denna avhandling undersöktes tre olika lignin, ett från lövträd och två från barrträd. Ligninet hade sitt ursprung från en biomassafraktioneringsteknik som använder sig av vattenextraktion under förhöjt tryck följt av en mild alkalisk sodaprocess. Ett tillvägagångssätt för att utfälla och rena ligninet utvecklades för att ge analytiskt rena ligninprover. De olika ligninfraktionerna analyserades och jämfördes med ligninprov med oförändrad nativ struktur för att förstå hur processen påverkade ligninets struktur. En mängd olika analysmetoder användes och den kombinerade informationen från analyserna kunde användas för att bestämma viktiga strukturella särdrag och egenskaper hos ligninet. Modellföreningar med specifika strukturer framställdes och deras spektroskopiska data användes för att underlätta strukturbestämningen av ligninet. För att vidare validera konceptet fraktionerades det renade ligninet till ännu mer homogena fraktioner genom enkel lösningsmedelsfraktionering. Kemiska modifieringar användes för att undersöka hur enkla modifieringar påverkade ligninets termiska egenskaper och för att underlätta strukturbestämningen.

I denna avhandling implementerades även ^{31}P PULCON-metodik för att kvantitativt bestämma mängden av hydroxylgrupper i lignin. Metoden visade sig ha vissa fördelar jämfört med standardprotokollet.

LIST OF PUBLICATIONS

I. L. Lagerquist, A. Pranovich, A. Smeds, S. von Schoultz, L. Vähäsalo, J. Rahkila, T. Tamminen, I. Kilpeläinen, S. Willför, P. Eklund, Structural characterization of birch lignin isolated from a pressurized hot water extraction and mild alkali pulped biorefinery process, *Ind. Crops Prod.* **2018**, 111, 306-316

II. L. Lagerquist, A. Pranovich, I. Sumerskii, S. von Schoultz, L. Vähäsalo, S. Willför, P. Eklund, Structural and Thermal Analysis of Softwood Lignins from a Pressurized Hot Water Extraction Biorefinery Process and Modified Derivatives, *Molecules* **2019**, 24, 335.

III. L. Lagerquist, J. Rahkila, P. Eklund, Utilization of ^{31}P PULCON for Quantitative Hydroxyl Group Determination in Lignin by NMR Spectroscopy, *ACS Sustainable Chem. Eng*. **2019**, 7 (9), 9002-9006

IV. L. Lagerquist, J. Rahkila, P. Eklund, Determination of chemical shifts in 6-condensed syringylic lignin model compounds, *Holzforschung* **2022**, 76 (3), 294-298

CONTRIBUTION OF THE AUTHOR

The author of this thesis is the main author and responsible for the planning and majority of experimental work of publications I-IV. With the following notable exceptions:

- Dr. Annika Smeds performed the gas chromatography analysis (short column GC, GC-MS, *py*-GC–MS and *py-THM*-GC–MS) in publication I.
- Dr. Andrey Pranovich performed the carbohydrate content analysis in publication I and together with Jarl Hemming performed HPSEC analysis in publication I & II.
- Dr. Jan-Erik Lönnqvist performed the elemental analysis for publication I & II
- Dr. Jani Rahkila performed the DEPT experiments in publication I and set up the PULCON experiments and performed the calculations in publication III.
- Dr. Ivan Sumerskii performed the methoxy group determination in publication I and thermal analysis in publication II.
- HRMS analysis was performed by Dr. Alex Dickens in publication IV.

SUPPORTING PUBLICATIONS

V. A. Sokolov, L. Lagerquist, P. Eklund, M. Louhi-Kultanen, Non-thermal Gas-phase Pulsed Corona Discharge for Lignin Modification, *Chem. Eng. Process.* **2018**, 126, 141-149

VI. Y. Zhang, S. Ni, X. Wang, W. Zhang, L. Lagerquist, M. Qin, S. Willför, C. Xu, P. Fatehi, Ultrafast adsorption of heavy metal ions onto functionalized lignin-based hybrid magnetic nanoparticles, *Chem. Eng. J.* **2019**, 372, 82-91

VII. L. Wang, L. Lagerquist, Y. Zhang, R. Koppolu, T. Tirri, I. Sulaeva, S. von Schoultz, L. Vähäsalo, A. Pranovich, T. Rosenau, P. Eklund, S. Willfor, C. Xu, X. Wang, Tailored Thermosetting Wood Adhesive Based on Well-defined Hardwood Lignin Fractions, *ACS Sustainable Chem. Eng.* **2020**, 8, 35, 13517–13526

VIII. D. S. Ryabukhin, L. Lagerquist, P. Runeberg, J. Rahkila, P. C. Eklund, One-pot propargylation and Claisen-type rearrangement for natural

lignans matairesinol and α-conidendrin *Chem. Heterocycl. Compd.* **2020**, 56, 949

IX. T. Jyske, H. Brännström, T. Sarjala, J. Hellström, E. Halmemies, J.-E. Raitanen, J. Kaseva, L. Lagerquist, P. Eklund, J. Nurmi, Fate of Antioxidative Compounds within Bark during Storage: A Case of Norway Spruce Logs. *Molecules* **2020**, 25, 4228

X. X. Lu, L. Lagerquist, K. Eränen, J. Hemming, P. Eklund, L. Estel, S. Leeneur, H. Grénman. Reductive catalytic depolymerization of semi-industrial wood-based lignin. *Ind. Eng. Chem. Res.* **2021**, 60, 47, 16827-16838

SELECTED CONFERENCE AND SEMINAR CONTRIBUTIONS

I. Flash presentation and poster at the Suomen Kromatografiaseuran, Åbo Akademin ja Nesteen Syyseminaari in Naantali, Finland 11-12th November 2015

II. Oral presentation at the PCC annual seminar in Åbo Finland, 25th August 2016

III. Poster presentation at the 1st International Conference Bioresource Technology for Bioenergy, Bioproducts and Environmental Sustainability in Sitges Spain, 23-26th October 2016

IV. Poster presentation at the 7th Nordic Wood Biorefinery Conference in Stockholm Sweden, 28-30th March 2017

V. Oral presentation at the 255th ACS National Meeting in New Orleans USA, 18-22nd March 2018

VI. Poster presentation at the 30th International Symposium on the Chemistry of Natural Products in Athens Greece, 25-29th November 2018

VII. Oral presentation at the SmartBIO annual meeting in Åbo Finland, 29th of October 2019

VIII. Poster Presentation CA17128 LignoCOST Meeting in Régua, Portugal, 13-14th November 2019

LIST OF ABBREVIATION

$CDCl_3$	Deuterated chloroform
$Cr(acac)_3$	chromium(III) acetylacetonate
Đ	Dispersity
DEPT	Distortionless enhancement by polarization transfer
DMF	Dimethylformamide
DMSO	Dimethyl sulfoxide
DTG	Differential thermal analysis
e-HNDI	endo-*N*-hydroxy-5-norbornene-2,3-dicarboxylic acid imide
FTIR	Fourier transform infrared spectroscopy
G (unit)	Guaiacyl
GC	Gas chromatography
H (unit)	*p*-hydroxyphenol
HPSEC	High-performance size-exclusion chromatography
HRMS	High-resolution mass spectrometry
HSQC	Heteronuclear single quantum coherence
i-PrOH	Isopropyl alcohol
IS	Internal standard
Me	Methyl
M_n	Average number molecular weight
MS	Mass spectrometry
MTBE	Methyl *tertiary*-butyl ether
M_w	Average weight molecular weight
MWL	Milled wood lignin
n-BuLi	*normal*-Butyllithium
NMR	Nuclear magnetic resonance
PHWE	Pressurized hot water extraction
PULCON	Pulse length-based concentration determination
Py	Pyrolysis
Rg	Receiver gain
S (unit)	Syringyl
TGA	Thermal gravimetric analysis
THF	Tetrahydrofuran
THM	Thermally assisted hydrolysis and methylation
TMDP	2-chloro-4,4,5,5-tetramethyl-1,3,2-dioxaphospholane
TPP	Triphenyl phosphate

Table of contents

1. Introduction

1.1. Background

Currently most chemicals, materials, and fuels are derived from fossil-based feedstocks. The reliance on these feedstocks is of concern due to the negative environmental impact, economic dependence of unstable regions, and limited amount of raw material.[1] Biomass is an alternative feedstock for these different products but in order to move towards a bio-based economy system biomass must be better utilized, both more efficiently and cost effectively. The purpose of biorefineries is to utilize biomass for production of various products and can be seen as analogous to the oil refineries, but fractionates and valorizes biomass instead of fractionating and distilling crude oil.[2] The International Energy Agency (IEA) Bioenergy Task 42 defined biorefinery as

"*Biorefinery is the sustainable processing of biomass into a spectrum of marketable products (food, feed, materials, chemicals) and energy (fuels, power, heat)*".[3]

The different types of biorefineries have been further classified according to four of their main features: feedstocks, platforms, products, and processes.[4] The feedstock, or raw material, can be anything from crop based (e.g. starch or sugar crops), lignocellulosic crops (e.g. wood or switchgrass), aquatic biomass (e.g. algae and seaweed) or various waste products (e.g. farm residues or forestry wastes). The feedstock can be processed to yield so-called platforms. These platforms are intermediary products between the end product and the feedstock. Examples of platforms are biogas, syngas, C6 and C5 sugars, oils, lignin, pyrolytic liquids, and cellulose. These platforms can then be converted to products via different processes. Even with this simplified classification system it is clear that there can be a wide variety between biorefineries. To be economically feasible each biorefinery should produce multiple platforms which can yield a wide spectrum of products, both of high and low value with little to no waste. Biorefineries are often considered sustainable due to the use of renewable resources; however, there are more factors to be taken into account to ensure sustainability. Examples of such factors are the utilization of all components of the biomass, land use, competition with food crops, accessibility to water, infrastructure etc. As such the versatility of biorefineries, and choice of feedstock, is somewhat limited due to the dependency on the geographical location. The pulping mills in Finland can be considered forest-based biorefineries. The mills mechanically and chemically process a renewable feedstock (managed forest) to platform chemicals (e.g. cellulose and fatty acids), which can be further processed to high value products. The hemicellulose and

lignin fractions of the biomass are used for energy production and the whole system is integrated to utilize all of the biomass and to reuse the process chemicals.[5] To diversify the products, from the forest industry, new technologies need to be explored in order to yield both new platforms and products. In this thesis the lignin fraction isolated from softwood and hardwood by a new fractionation technology have been investigated. The fractionation technology is able to yield all of the three main structural lignocellulosic components as platforms and different applications for these wood components are being explored. The natural lignin macromolecule is inherently complex and will structurally not only vary between plant species, but any type of technical fractionation and isolation approach will further alter the structure. As such the lignin from this fractionation process will yield a different type of lignin with different properties compared to other lignins and it is important to understand the structural features in order to identify the best application area for this lignin.

1.2. Lignocellulosic biomass

Lignocellulose is a complex material that builds the structural backbone of all plant cell walls. It is produced by photosynthesis and the lignocellulosic feedstock is the most abundant renewable bioresource on earth. The secondary cell wall compromises the majority of the wood biomass and provides the cell with the mechanical strength and rigidity. It is mainly composed of cellulose (40–55%), hemicellulose (20–40%) and lignin (15–30%).[6] Structurally cellulose is a high molecular weight linear homopolysaccharide and its repeating unit cellobiose has two D-glucopyranose units in $^4C_1$ chair conformation bonded together with a β-(1→4) glycosidic bond (Figure 1).

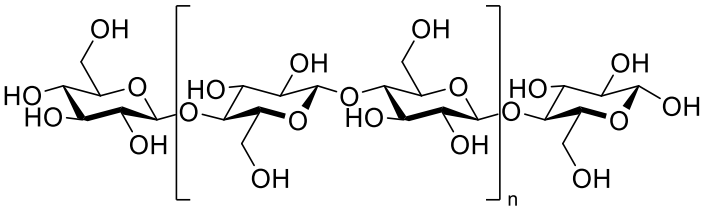

Figure 1. Structure of cellulose.

The cellulose polymer chains form supramolecular structures called elemental fibrils that are stabilized by intra- and intermolecular hydrogen bonding between the chains. Bundles of these elemental fibrils form so-called microfibrils that are packed and coated with hemicelluloses. The microfibrils can further form even larger macrostructures that are the structured skeleton of the wood cell.[7,8] Hemicelluloses are the second largest polysaccharide class in woody plant

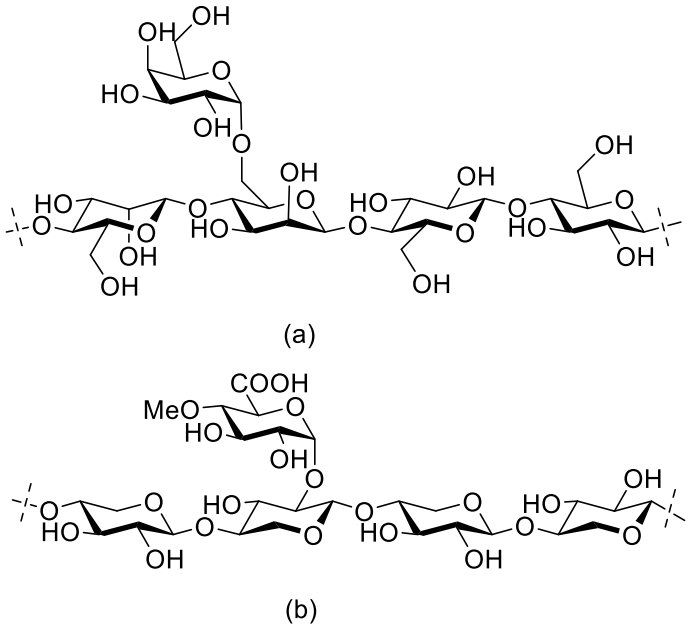

Figure 2. The structure of a) galactoglucomannans and b) 4-*O*-methyl-D-glucurono-D-xylan.

cells and structurally they differ greatly from cellulose. The hemicelluloses are a complex group of heteropolysaccharides, which can consist of multiple different monosaccharide units.[9] The monosaccharides can be pentoses, hexoses, hexuronic acids and deoxy-hexoses. They can exist in both the pyranose and furanose form and the hydroxyl groups can be functionalized with acetyl- and methyl groups. The hemicelluloses have a β-(1→4) linked backbone with the monosaccharides in equatorial configuration. The backbone can contain one unit (e.g. in xylan) or more units (e.g. in galactoglucomannans). These backbones often contain branching from the other hydroxyl groups via glycosidic bonds, such as α-(1→6) as in glucomannans (Figure 2a) or α-(1→2) as in 4-*O*-methyl-D-glucurono-D-xylan (Figure 2b) to other carbohydrates. The hemicelluloses exist in a matrix together with lignin in-between the cellulosic microfibrils and it has been proposed that glucomannans act as a cross linker between the microfibrils.[10] The structure of lignin differs greatly compared to the carbohydrates, cellulose and hemicelluloses. It is an amorphous aromatic polymer, which is mainly bonded with alkyl aryl ether bonds (Figure 3). Due to its hydrophobic nature, it has a crucial part in the transportation of water and nutrition in the plants. Lignin has often been seen as an adhesive, which "glues" the wood cells together, and it forms a matrix together with the hemicelluloses around the cellulosic microfibrils. It has been shown in intact maize stems that

lignin interacts with xylans via electrostatic interactions between lignin methyl ethers and sugar polar groups.[11] Evidence of direct covalent bonding between the lignin and carbohydrates has also been shown in Japanese red pine milled wood lignin.[12] Besides the three main components also minor quantities of extractives, pectins, proteins, and inorganics can occur in the lignocellulosic biomass. The quantities and occurrence of these components varies greatly between plant species.

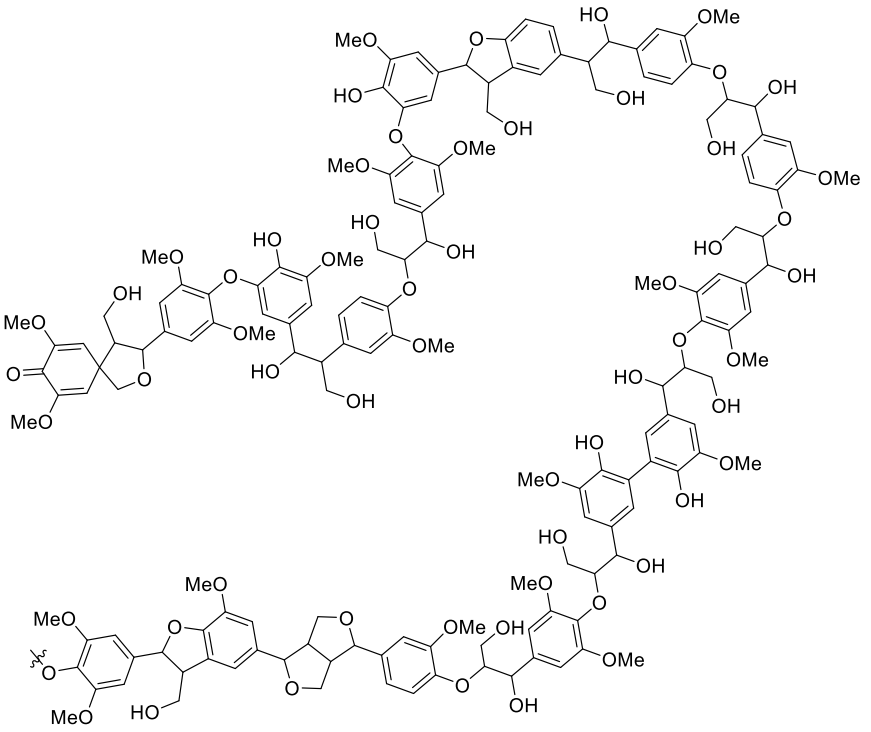

Figure 3. Structure of native hardwood lignin.[13]

1.2.1. Lignin structure and biosynthesis

The lignin biopolymer is formed by oxidative coupling reactions between its monomeric units. The monomers are *p*-coumaryl-, coniferyl-, and sinapyl alcohol, which are formed via biosynthesis from L-phenylalanine or L-tyrosine.[14] The difference between the monomers is the degree of methoxyl group substitution in the aromatic ring on the 3- and 5-position. The rings are often referred to as *p*-hydroxyphenol (H) unit if it is unsubstituted; guaiacyl (G) unit if monosubstituted; and syringyl (S) unit if disubstituted (Figure 4).

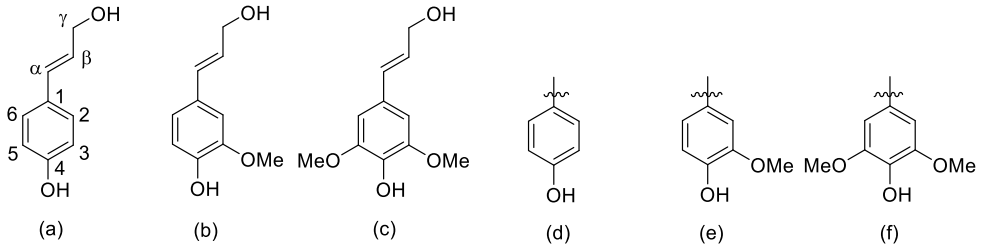

Figure 4. a) p-coumaryl alcohol, b) coniferyl alcohol, c) sinapyl alcohol, d) hydroxyphenol (H), e) guaiacyl (G) and f) syringyl (S).

The numbering of these so-called phenylpropane units, also called C_9 or C_6C_3 units, is assigned so the aromatic carbon that is attached to the propane chain as C-1 and in guaiacyl units the carbon that has a OMe-group attached is always assigned as C-3. The carbons on the propane side chain are assigned C-α, C-β and C-γ, where C-α is attached to C-1. The ratio and occurrence of the monomers vary among wood species. Softwood is mainly composed of guaiacyl units, hardwood both guaiacyl- and syringyl units, and grasses contain all three of the lignin units. Compression wood that is found on the lower side of leaning stems also contains hydroxyphenol units. The oxidative polymerization of the monomeric units starts with an enzymatically catalyzed one-electron transfer dehydrogenation reaction that result in a phenoxy radical (Scheme 1). The formed radical is resonance stabilized so that the electron density will be delocalized to positions O-4, C-1, C-3, C-5 and C-β. Due to the aromatic substitution pattern the O-4 and C-β positions will be mostly reactive together with C-5 in guaiacyl units and C-3 and C-5 in hydroxyphenol units. The radical coupling between the monomeric units will prefer to react between these reactive sites and the most common linkages will be β-O-4, β-5, 5-5 and β-β. In scheme 2 the monomer coupling between an O_4-radical monomer and a C_β-radical monomer can be seen. After the radical coupling, a quinone methide intermediate is formed, which is susceptible to nucleophilic attack on the C_α-carbon to regenerate the aromatic ring. Most often the nucleophile will be water, or hydroxyl ion, so that the most abundant β-O-4-linkage will be formed (Scheme 2d),

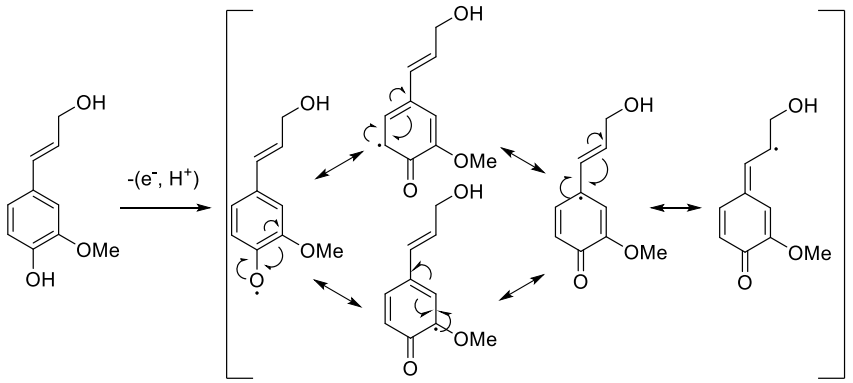

Scheme 1. Formation and resonance structures of the phenoxy radical.

but other nucleophiles can also attack the C_α-carbon to form α-O-4-linkages.[15] Due to the complexity of the lignin biosynthesis different types of lignin linkages (Figure 5a-k) and end groups (Figure 5l-o) have been proposed to occur in varying amounts.[16,17] A Synthetic lignin polymer, called dehydrogenation polymer (DHP), has been used to study the polymerization of lignin. This DHP lignin is synthesized *in vitro* by adding the monomer into a solution of hydrogen peroxide and an enzyme and has been an invaluable tool in understanding the structure and formation of lignin. Besides the lignin-lignin linkages lignin will also bind covalently to carbohydrates to form lignin-carbohydrate complexes (LCC). These can be formed by nucleophilic attack by the carbohydrates to the benzylic position of the quinone methide intermediate or by enzyme catalyzed glycosylation reactions. Due to the available functional groups the LCC will be linked by ester, ether, glycosidic or acetal bonds (Figure 5p-s).[18–20]

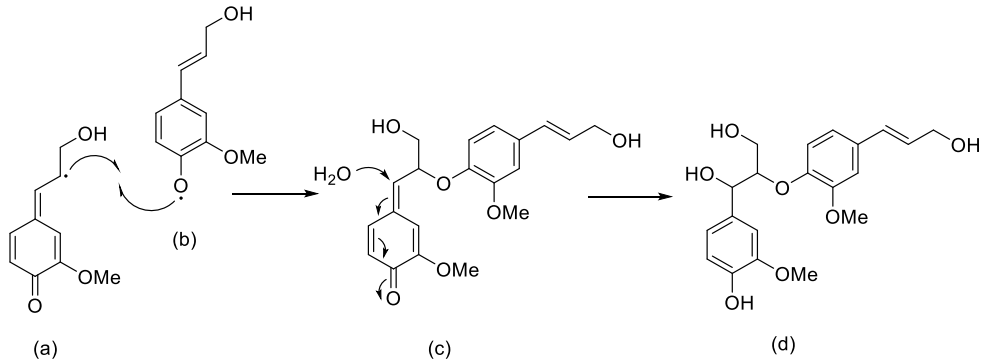

Scheme 2. Coupling of a) C_β-radical- and b) O_4-radical monomer to form the d) β-O-4 linkage via the c) quinone methide intermediate.

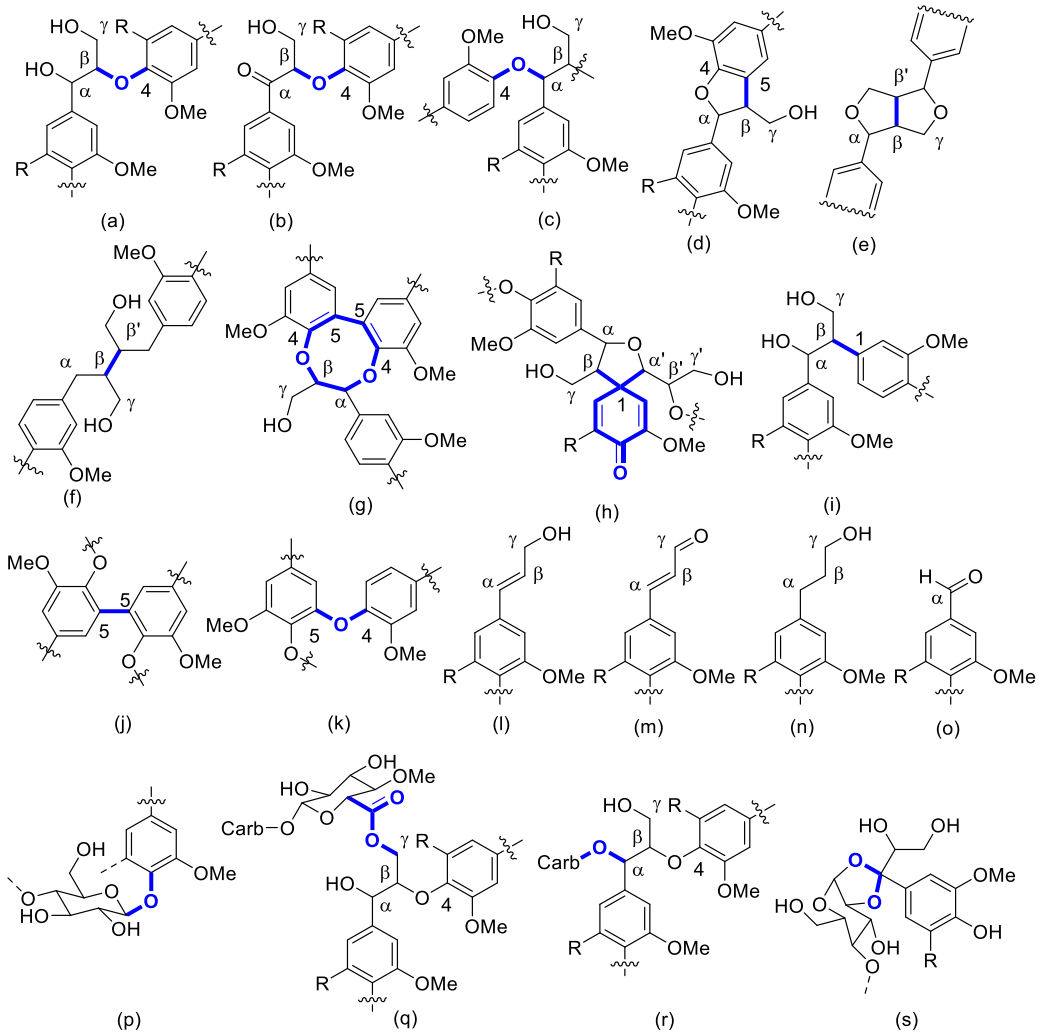

Figure 5. Structures of lignin linkages: a) β-O-4, b) C_α-oxidized β-O-4, c) α-O-4, d) β-5 (phenylcoumaran), e) β-β (resinol), f) secoisolariciresinol (β-β), g) dibenzodioxocin (5-5), h) spirodienone (β-1), i) β-1, j) 5-5 (biphenyl), k) 4-O-5. End groups: l) cinnamyl alcohol, m) cinnamaldehyde, n) dihydrocinnamyl alcohol, o) benzaldehyde. Lignin-carbohydrate linkages: p) phenyl glucosides, q) γ-esters, r) benzyl ether and s) acetal/ketal.

1.3. Isolation of lignin

As lignin is a structural component in the wood cell it has often been necessary to isolate it from the other wood constituents prior to any type of analysis. The quantification of the total amount of lignin in wood is usually performed by hydrolyzing the carbohydrates with strong acids to leave the acid-insoluble lignin. The most common of these hydrolysis methods is the Klason method. The

method first employs 72% sulfuric acid to hydrolyze the carbohydrates, after dilution a second hydrolysis step is performed, and the washed and isolated lignin residue is referred to as Klason lignin. While this gravimetric method determines the total amount of lignin its harsh conditions greatly affect the structure of the native lignin and other lignin isolation methods are needed for qualitative analysis. Laboratory methods for isolation of a more intact lignin usually ball mills the wood sample into a fine powder from which the lignin is extracted. The most commonly used method is the Milled-Wood lignin (MWL) method developed by Björkman.[21] In this method the wood is milled, in either dry state or in a non-swelling medium such as toluene, and a dioxane/water (96:4 v/v) solvent mixture is used for extraction of the lignin. The MWL is considered structurally close to native lignin found in wood, however, the isolated lignin yield in MWL compared to Klason lignin is relatively low (~30-40%). The mechanical energy of the milling can also induce structural changes to the lignin, such as oxidation of the α-carbon and cause cleavage of the β-O-4 bonds.[22] Another similar method, the Cellulolytic Enzyme Lignin (CEL), treats the milled wood with hydrolytic enzymes prior to solvent extraction and is able to isolated lignin in higher yields than MWL.[23,24] Enzymatic Mild Acidolysis Lignin (EMAL) uses enzymatic hydrolysis of the milled wood to remove the carbohydrates followed by mild acidolysis to cleave the remaining lignin-carbohydrates bonds, EMAL isolates a more intact lignin in higher yields than both the MWL and CEL.[25] While CEL and EMAL lignins yield a more presentative native lignin the procedures are more tedious than that of the MWL. Zinovyev et al.[26] showed that the main degradation of MWL occurs in its high molecular fractions and that the procedure can be reduced to a working day if accelerated solvent extraction is employed, therefore, MWL is still often used to study lignin and used as a reference sample.

1.4. Technical isolation of lignin

Most industrial pulping or pretreatment processes currently focus on the utilization of the carbohydrate fractions, mainly cellulose, from the lignocellulose matrix. To achieve this lignin is fragmented and solubilized, generally under either alkaline or acidic conditions, so that the cellulose can be isolated.

1.4.1. Kraft process

The kraft process, or the sulphate process, is the predominant pulping process and produces approximately 50 million tons of lignin annually. In a conventional kraft process the wood chips are cooked in a aqueous solution of NaOH and Na_2S (white liquor) at 170 °C for approximately 2 h.[27] The majority of lignin and

hemicelluloses are washed out and burnt in a recovery boiler to produce heat and electricity, and Na_2S is regenerated. As the electricity generation and process chemical regeneration is such an integrated part of the pulping mills only a fraction of the kraft lignin is available commercially, approximately 265 ktons annually.[28] The availability of commercial kraft lignin is increasing due to technologies that can isolate lignin from the black liquor in kraft processes, such as Lignoboost[29] and Lignoforce[30]. It is still necessary to secure the energy demand of the kraft mills but 5-20% of the lignin can be isolated by these processes.[28] The Lignoboost process has already been implemented in two full scale kraft processes, in Domtar's North Carolina mill and Stora Enso's Sunila mill, and in two demo plants, one in Klabin's Technology Center in Brazil and another plant in Bäckhammar, Sweden. Kraft lignin contains approximately 1-3% sulfur due to the incorporation of the pulping chemicals into the lignin. Another alkaline pulping method is the Soda process. The Soda process was the first chemical pulping process and was patented in 1854.[31] As it only uses NaOH as a pulping chemical the lignin obtained from the Soda-process is sulfur-free. It has largely been replaced by the kraft pulping due to the higher quality pulp but it is still used for non-woody annual plants and agricultural residues in small volumes.

1.4.2. Sulfite process

The second largest pulping process is the sulfite process and approximately 1.3 million tons lignosulphonates are annually produced for commercial use.[32] The sulfite process uses salts of sulfites or bisulfites as pulping chemicals and sodium, magnesium, ammonium and calcium have been used as counter ions. The pulping process is performed at 140-170 °C and the pH varies from acidic to alkaline depending on what counter ion is used. Considerable amounts of sulfur, about 4-8%, are incorporated into the lignin structure as sulphonates.[32] Compared to the lignin from the alkaline pulping processes lignosulphonates are water soluble below high pH (<12).

1.4.3. Acid hydrolysis

Acid hydrolysis lignin is the by-product of 2nd generation biofuels. To produce ethanol the carbohydrates need to be hydrolyzed to monomers so that they can be fermented. The process is called concentrated acid hydrolysis if higher concentrations of the acids are used (10-30%) and when lower concentrations (2-5%) it is called dilute acid hydrolysis. Concentrated acid hydrolysis process occurs at low temperatures and produces high hydrolysis yields (~90%), however, the use of large amounts of acids (often H_2SO_4) is the obvious drawback. Dilute acid hydrolysis uses lower amount of acids but is carried out at

high temperatures, which causes side reactions and the yields are lower.[33] Currently low amounts of hydrolysis lignin are produced compared to lignosulfonates and kraft lignin but due to the increasing demands for biofuels the production amount is expected to increase drastically.[34] Large amounts of hydrolysis lignin were produced by the Soviet Union for approximately 70 years but they were not able to find any economically feasible applications due to the heterogeneity, large amounts of impurities and condensation of the lignin.[35]

1.4.4. Organosolv process

There are many other promising fractionation technologies but these are not industrial scale processes.[36] One notable mention is the organosolv process.[37] Organosolv is an umbrella term for biomass fractionation using organic solvents (i.e. methanol, ethanol, acetone, THF, ethylene glycol) or organic acids (i.e. formic or acetic acid), often in water mixtures and can use acidic or alkaline catalysts.[38] The process operates at elevated temperatures (100-250°C) and is based on the fact that the lignin and hemicelluloses can be solubilized in some organic solvents. Organosolv processes can be used as a pulping process for the production of pulp or as a pretreatment with a subsequent enzymatic hydrolysis step to yield biofuel.[39] Organosolv has some advantages over traditional pulping processes, such as less air and water pollution, the possibility to isolate all biomass fractions, and the theoretical possibility to recover all of the organic solvent by simple distillation. Drawbacks of the process include costly washing procedures of the pretreated solids, substantial quantities of expensive organic solvents, and any loss of the solvents leads to both great economic losses and can be associated with explosion risks.[40] Aqueous ethanol is an attractive solvent system due to the price, being environmentally benign and possibility to be produced on site. A demonstration mill using the Alcell process (50% EtOH at ~195°C and ~28 bar) was operating in New Brunswick, Canada from 1989 to 1996. It was concluded that the mill produced high quality and easily bleachable pulp and that it could be economically feasible if it has a capacity of ~300 metric tons/day.[41] The Alcell technology and facilities was purchased by Lignol Innovations corporation, who are trying to commercialize the process.[42] Also other types of organosolv technologies are commercialized, such as the Formico technology developed by the Finnish company Chempolis. The technology is based on using formic acid and a biorefinary plant is currently being constructed in Assam, India. The biorefinary will use 300 ktons annually of bamboo to produce bioethanol, furfural, acetic acid and energy.[43]

1.5. Pulping chemistry

The chemistry behind the depolymerization, and subsequent repolymerization, of lignin during biomass processing strongly depends on the processing conditions. The chemical mechanism of the processing methods can be divided into a) base-catalyzed, b) acid-catalyzed, c) reductive, d) oxidative or e) thermal.[44] The acid- and base-catalyzed reactions are most important during biomass fractionation. The reductive mechanisms occur during reductive catalytic depolymerization of isolated lignin. The oxidative mechanisms occur during the bleaching of pulp and thermal mechanisms during pyrolysis. The process "severity" (i.e. time, temperature, concentrations etc.) will influence the extent of the chemical alterations.[45] Due to the importance of the chemistry during pulping, and other biomass pretreatments, detailed information regarding the mechanism have been acquired.[44,46,47] During these processes new types of structures can form by repolymerization reactions, these structures are often bonded by more stable C-C bonds and are called condensed structures and also new types of end groups can form during pulping processes (Figure 6).[48–52] Some of the already existing structures (Figure 5) can be enriched during these processes (e.g. 5-5 bonds Figure 5j).[53] While native lignin has a complex structure with multiple different linkages between the lignin units the most commonly occurring linkage is the β-O-4, and as such the main focus in pulping chemistry has been on its cleavage.

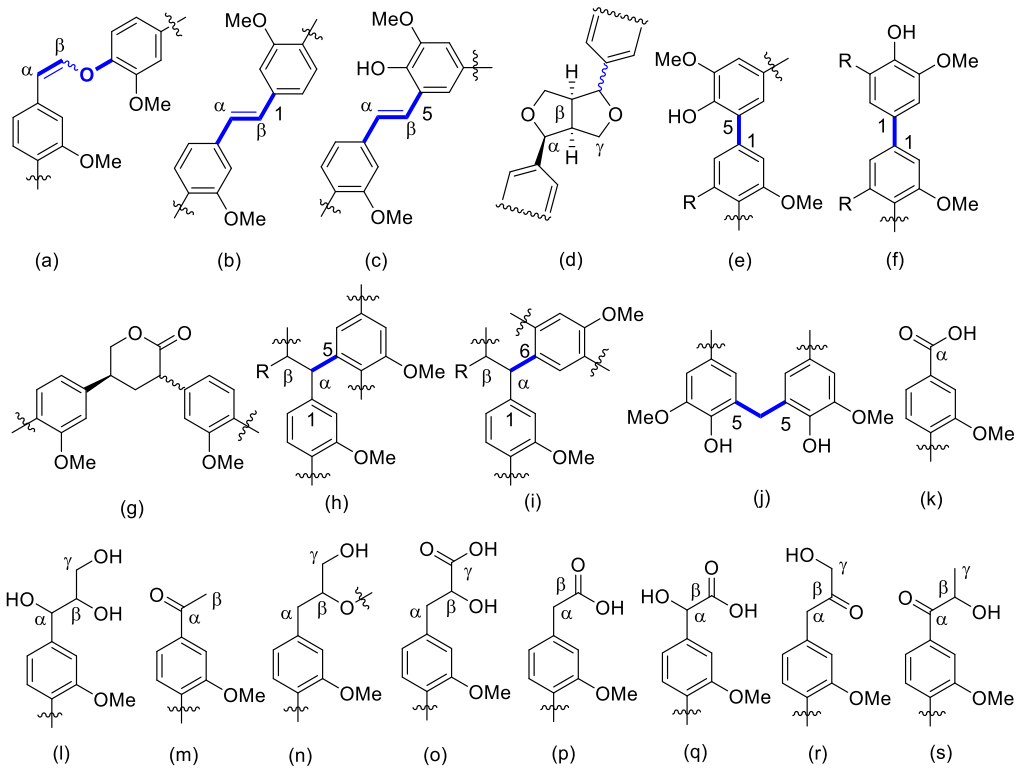

Figure 6. Examples of structures and end groups that can form during biomass processing: a) Enol ethers, b) β-1 stilbene, c) β-5 stilbene, d) epiresinol, e) 1-5, f) 1-1, g) lactone linker, h) α-5, i) α-6, j) diarylmethane, k) vanillic acid, l) aryl glycerol, m) acetovanillone, n) reduced β-O-4, o) β-hydroxy acid, p) guaiacyl acetic acid, q) mandelic acid, r) and s) Hibbert ketones.

1.5.1. Base-catalyzed pulping chemistry

A general scheme of the base-catalyzed depolymerization of lignin in kraft pulping can be seen in (Scheme 3). The initial β-O-4 cleavage proceeds slowly as the deprotonation, prior to the cleavage and epoxide formation, is from an aliphatic hydroxyl group (Scheme 3a). Nucleophilic attack on the formed epoxide (Scheme 3b) will yield the aryl glycerol (Scheme 3c) if the nucleophile is water or hydroxide ion. Other α-substitutions can also occur, for example condensation, if the nucleophile is another lignin fragment. The lignin fragment (Scheme 3d) has now a free phenolic hydroxyl group and can form a quinone methide structure (Scheme 3e) by eliminating -OH from the α-position. The quinone methide structure is extremely important for alkaline lignin chemistry and increases the electrophilicity on the α-position due to the desire to restore aromaticity. Nucleophilic attack on the α-position can yield condensed structures (Scheme 3f) if the nucleophile is another lignin fragment or benzyl

mercaptide (Scheme 3g) during kraft pulping if the nucleophile is hydrogen sulfide. The mercaptide can then ring close to cleave the β-O-4 bond and form the episulfide (Scheme 3h), which can react further. The quinone methide can also form the enol ether by cleavage of formaldehyde (Scheme 3i). The enol ether formation occurs mainly in soda pulp due to the lack of good nucleophiles, such as HS^- in kraft process, and is stable under alkaline conditions but is acid labile. The released formaldehyde can cause further condensation via formaldehyde-phenol condensation to form diphenylmethane structures (Figure 6j).

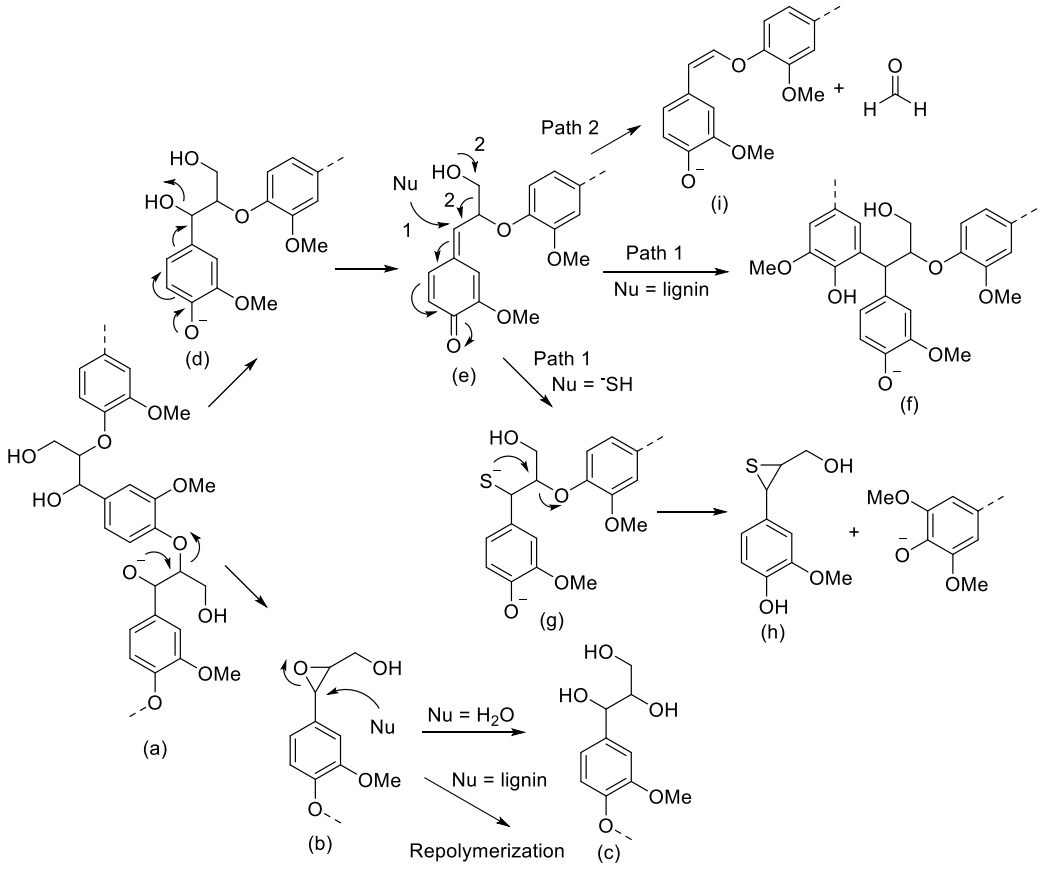

Scheme 3. Reaction scheme of base-catalyzed reactions adapted from Schutyser et al.[44]

1.5.2. Acid-catalyzed pulping chemistry

Considerable amount of condensation occurs during acid depolymerization compared to base-catalyzed. A general scheme of the acid catalyzed β-O-4 hydrolysis can be seen in (Scheme 4). Initially the hydroxyl-group on the α-position is protonated (Scheme 4a) and is eliminated to form the benzylic carbocation (Scheme 4b), that is stabilized by the aromatic ring. This position is

now susceptible to nucleophilic attack by for example another lignin fragment to form the condensed structure (Scheme 4c path 1). It can also form the enol ethers (Scheme 4c) and (Scheme 4d) by either eliminating the hydrogen on the β-position (Scheme 4 path 2) or by cleavage of formaldehyde (Scheme 4 path 3). These enol ethers are labile under acidic conditions and will be hydrolyzed to (Scheme 4e and 4f). The formed ketone (Scheme 4e) can isomerize into different types of ketones (Scheme 4g) and are called Hibbert's ketones after its discoverer Harold Hibbert.[54] Both the Hibbert's ketones and (Scheme 4f) can further react with other lignin fragments for further condensation.

These depolymerization mechanisms are also valid for the sulfite process but here the (bi)sulfites can act as nucleophiles. The specific mechanism will depend on the pH, which the sulfite process is using. The same is true for organosolv processes, here the solvent used can act as a nucleophile and be incorporated into the lignin structure.

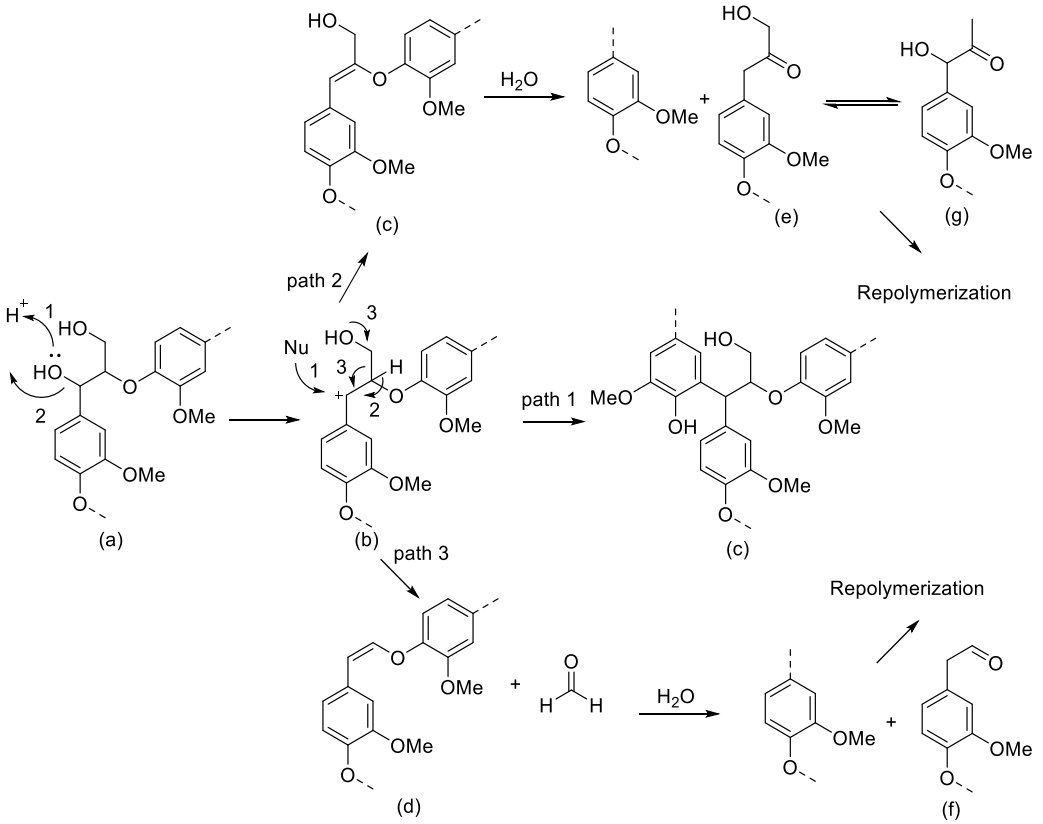

Scheme 4. Reaction scheme of acid-catalyzed reactions adapted from Schutyser et al.[44]

1.5.3. Lignin model compounds

It is challenging to study the chemistry that is occurring in biorefinery processes, or in lignin depolymerization reactions, due to the inherently complex lignin biopolymer. Synthetic model compounds of specific lignin structures have often been used to reduce the complexity and to simplify the chemistry. When depolymerization strategies are being developed, or when pulping chemistry have been investigated, the focus has often been on the most abundant alkyl aryl ether linkages (β-O-4).[55,56] This is apparent when looking at the minimalistic model compounds that are often used in depolymerization studies or studying pulping chemistry, such as the alkyl aryl ether (Figure 7a), aryl-aryl ether (Figure 7b), or simplistic β-O-4 models (Figure 7c).[13] Model compounds can also be used to assist in analysis and to verify structures detected in biomass samples,[49,50] and to study chemical reactions with lignin.[57] The main limitation of using model compounds is that the chemistry performed on these simplified structures are not necessarily applicable to lignin samples, due to the oversimplification of the structure. In more modern approaches the other abundant linkages such as the β-5 and 5-5 linkage are taken into consideration and substantially more complex model compounds are being used to give a better representation of lignin (Figure 7d).[58]

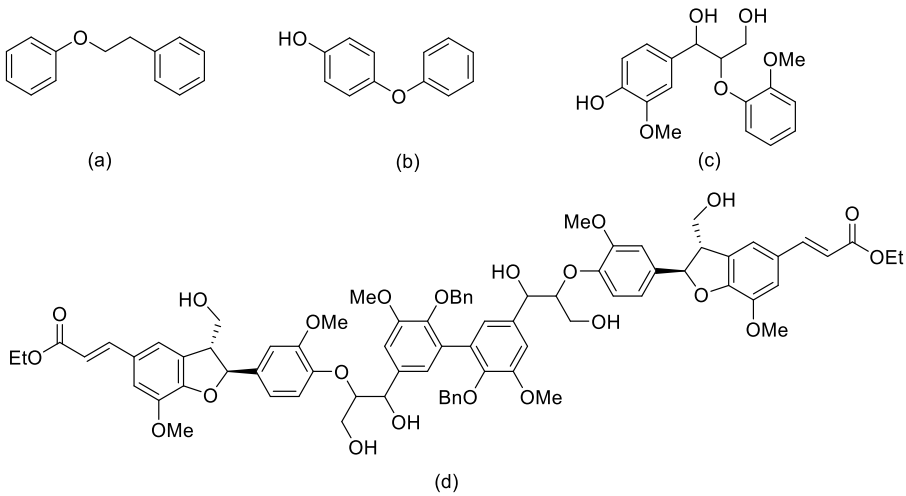

Figure 7. Examples of lignin model compounds.

1.6. Lignin analysis

1.6.1. Wet chemical analysis

Due to the complexity of lignin a wide variety of an analytical methods have been used to investigate its structure and properties.[59] Over the past century many structures of lignin have been suggested (e.g. by Freudenberg, Adler, Nimz etc.).[60] These proposed structures of lignin have continuously been refined due to the development of new methods for structural analysis. Traditionally different types of wet chemical methods have been used to measure specific functional groups (e.g. carbonyl-, carboxyl-, hydroxyl- and methoxy groups) and monomeric composition.[61,62] The functional groups were often measured by combining chemical modification and titration. For example, the determination of hydroxyl groups was done by acetylation followed by deacetylation and titrating the amount of formed acetic acid, the amount of methoxy groups was determined by demethylation of the methoxy groups with HI followed by determination of the formed methyl iodide; the amount carboxyl groups was determined by conductometric titration; and the total amount of carbonyl groups was determined by condensing the aldehyde or ketone functionalities with hydroxylamine hydrochloride and then determining the amount of formed HCl by titration. The methods for determining the monomeric composition employ degradative techniques (e.g. nitrobenzene oxidation, permanganate oxidation, thioacidolysis, derivatization followed by reductive cleavage (DFRC)) to cleave the lignin polymer into monomeric species, that can then be detected with chromatographic methods.[63] Nitrobenzene oxidation will mainly oxidize lignin to the monomeric units' vanillin, syringyl aldehyde and *p*-hydroxybenzaldehyde, which allows for the determination of the S/G/H ratio. Permanganate oxidation degrades all the aliphatic side chains, attached to the aromatic moieties, to carboxylic acids. This provides information about the aromatic substitution pattern and S/G/H ratio in the lignin sample. In the thioacidolysis analysis method lignin is depolymerized using boron trifluoride, as acid catalyst, and ethyl thiol as nucleophile. The method will mainly cleave the arylglycerol-β-aryl ether linkages to yield trithioethyl phenylpropane (C_6C_3) units, which allows for the determination of the β-O-4 content and the S/G/H ratio. The DFRC method provides similar information as the thioacidolysis method. The method proceeds by treating lignin with acetyl bromide, which will result in bromination of the benzylic position and acetylation of the hydroxyl groups. The alkyl aryl ether bonds can then be cleaved by reductive cleavage using zinc to yield C_6C_3 monomers. The wet chemical methods have played an important role in our current knowledge on the lignin structure. However, these indirect methods can be both time consuming and tedious to perform, and as

some methods give very specific information and multiple different methods are often needed. The chemical degradation reactions can also suffer from low yields, side reactions, low reproducibility and varying results based on what type of lignin is being analyzed. Due to these reasons and the increasing availability of spectroscopic instrumentation there has been a decrease in utilization and development of the wet chemical methods. Despite this, wet chemical methods are still routinely used for lignin analysis, for example Anderson et al.[64] used thioacidolysis to confirm the S/G ratio when researching lignin depolymerization and Balakshin et al.[65] used wet chemical methods in combination with spectroscopic methods when studying the branching of spruce MWL. The methods are still also being developed to give more structural information on lignin and to simplify the procedures. Examples of such improvements are to use Raney-nickel to desulfurize the thioacidolysis products. This simplifies the analysis as it reduces the number of products and improves the volatility, which allows for analyzation of dimeric fragments by GC or GC-MS.[66] A high-throughput and quantitative thioacidolysis protocol has also been developed by Harman et al., which allows for faster analysis times and quantification by using aryl glycerol standards.[67]

1.6.2. Spectroscopic methods

Spectroscopic methods are often direct methods that can analyze the whole lignin structure without the need of chemical degradation. Various spectroscopic methods have been used to analyze the lignin structure; however, NMR spectroscopy has had the greatest impact. A wide variety of experiments (i.e. ^{1}H, ^{13}C, ^{31}P, ^{19}F, HSQC, etc.)[68] can be measured with NMR spectroscopy providing detailed structural information about lignin. Signal overlap can be partially overcome by derivatizing lignin, by e.g. acetylation, and comparing the chemical shift of the unmodified to the modified lignin. Identification and quantification of some specific functional groups can also be performed by derivatizing lignin with suitable derivatization agents.[69,70] FTIR analysis is another spectroscopic method that has been frequently used to analyze lignin. FTIR provides substantial information on the chemical bonds present in the lignin structure, however, due to the complex signal patterns and peak overlap, it is mainly used for qualitative analysis to identify different functional groups. FTIR is still an attractive analysis method due to being relatively cheap, simple, fast, and available compared to other methods. Lancefield et al.[71] was able to accurately predict M_n, M_w and inter-unit linkage abundance in technical lignins with FTIR. This was performed by first analyzing a calibrating set of 54 technical lignins that had been thoroughly analyzed with GPC, NMR methods, and FTIR. Multivariate analysis techniques

could then be used to correlate structural characteristics to FTIR spectra of lignin samples.

1.6.3. ^{1}H NMR spectroscopy

^{1}H NMR spectroscopy has been an important technique for structural characterization of lignin. The proton nucleus has almost 100% natural abundance, which provides a high signal to noise ratio (S/N), hence the possibility to perform quantitative analysis without excessive experimental time. Many key features can be assigned from the spectral data such as carboxylic-, aromatic-, aliphatic- and the -OMe protons in underivatized lignin.[72] Signal overlap can be partially decreased by analyzing lignin acetates, which gives more information on the lignin side chains.[73,74] The amounts of aliphatic and phenolic hydroxyl groups can also be quantified by analyzing the lignin acetates.[75] The major drawback with ^{1}H NMR spectroscopy is the limited range of chemical shifts (0-12 ppm), which leads to extensive signal overlapping (Figure 8). Other NMR experiments have generally replaced ^{1}H NMR spectroscopy for lignin characterization and quantification but the method remains relevant for routine analysis due to its short experimental time and possibility to use benchtop NMR instruments.[76]

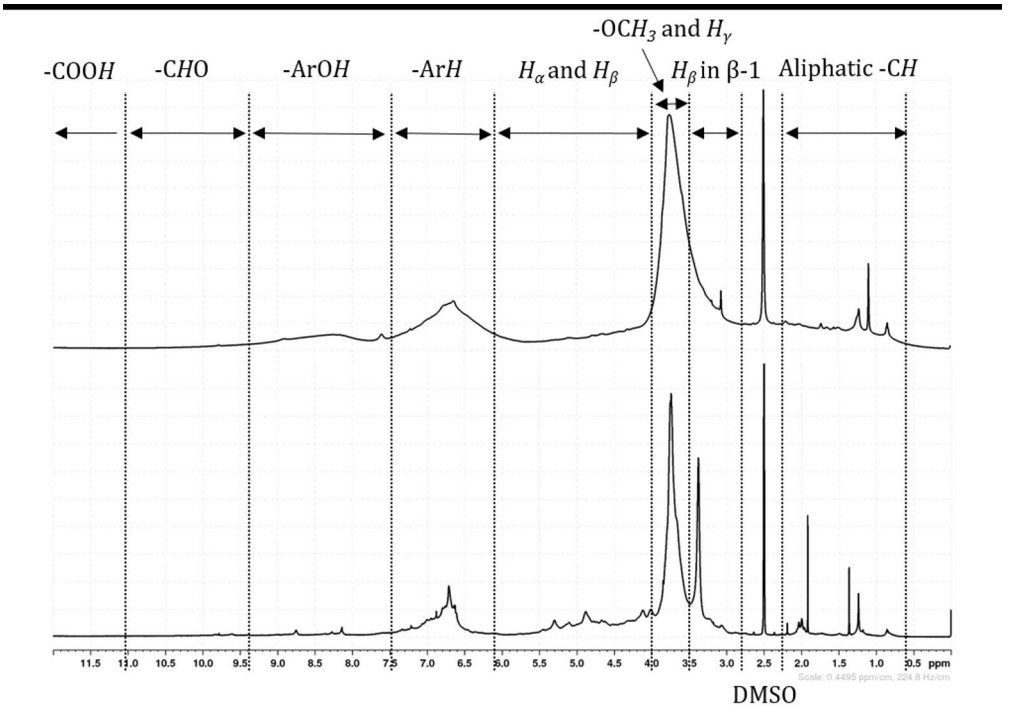

Figure 8. ^{1}H NMR spectrum of a technical birch lignin (above) and a birch MWL (below).

1.6.4. ^{13}C NMR spectroscopy

^{13}C NMR spectroscopy (Figure 9) has significantly broader chemical shift range (0-220 ppm), better resolution, and less overlap of signals compared to ^{1}H NMR spectroscopy (Figure 8).[77] The spectroscopic method can also detect aromatic carbon bonded with C-C and C-O bonds, which is impossible for proton-based measurements. Consequently, ^{13}C NMR spectroscopy can provide considerably more structural information on lignin. Model compounds have been used to prepare large libraries of ^{13}C NMR chemical shifts of various lignin moieties,[78,79] and a protocol for acquiring quantitative ^{13}C NMR spectra using 1,3,5-trioxane as internal standard was developed by Xie et al.[80] Balakshin et al. have performed comprehensive ^{13}C NMR spectroscopy method development for analysis on both native MWL and technical lignin, by analyzing acetylated and unmodified lignin.[48,81] In these studies they were able to quantify a wide variety of lignin moieties and structural features, e.g. aromatic C-H, S/G/H ratio, lignin linkages (e.g. β-O-4, β-β, β-5 etc.), carbohydrates, OMe groups, degree of condensation, conjugated and non-conjugated carbonyl and carboxyl groups, different types of hydroxyl groups, etc. Despite these advantages the measurement has drawbacks compared to other NMR experiments. The ^{13}C nucleus only has a 1.1% natural abundance, which leads to much longer experimental time. Performing quantitative ^{13}C NMR measurements prolongs the experiments even more due to the necessity to use an inverse gated decoupling sequence and increased relaxation delays between the pulses. The experimental time can be reduced by using relaxation agents, such as $Cr(acac)_3$, but are still considerably longer than e.g. ^{1}H NMR measurements.[80] Even with the wide chemical shift range there is still extensive amounts of signal overlap due to the heterogeneous nature of lignin. The high amounts of signals, especially in the aromatic region of technical lignin, can cause difficulties in baseline correction and subsequently effect peak integration. To assist with these data processing issues, Balakshin et al. have proposed a baseline correction protocol.[48] ^{13}C NMR spectroscopy is one of the most important lignin analysis methods due to the large amount of structural information that can be obtained with the method, and the possibility to perform quantitative analysis.[82]

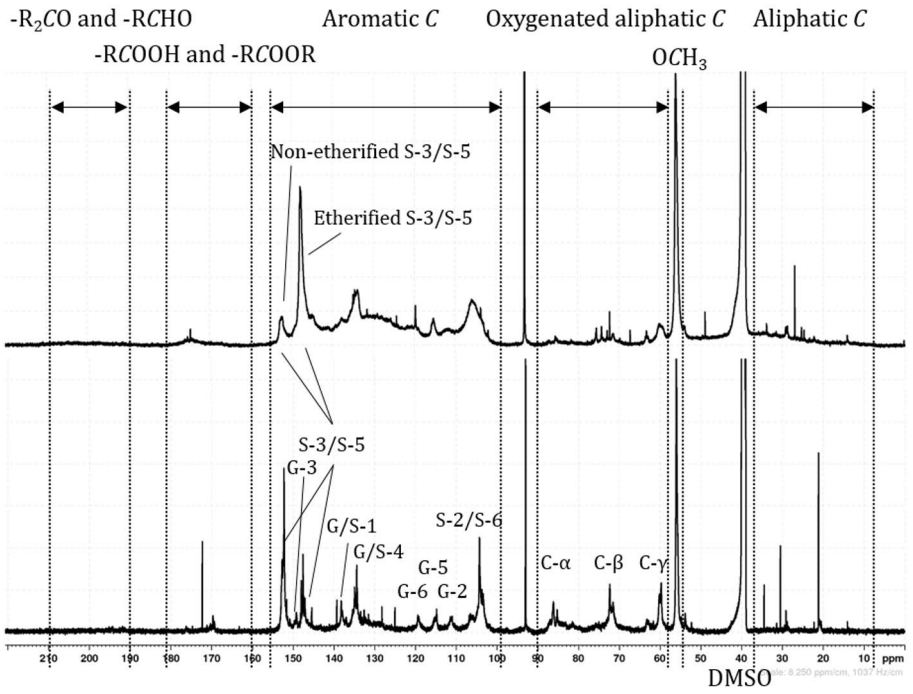

Figure 9. ^{13}C NMR spectrum of a technical birch lignin (above) and a birch MWL (below).

1.6.5. ^{31}P NMR spectroscopy

The quantitative hydroxyl group determination by ^{31}P NMR spectroscopy has become one of the most important routine NMR measurements for lignin chemists.[69] As lignin does not contain any phosphorus, the ^{31}P NMR method is made possible by preparing a phosphite derivative of the hydroxyl groups.[83] The chemical environment surrounding the different hydroxyl groups will affect the chemical shifts of the ^{31}P nuclei so that the aliphatic-, 5-substituted- (syringyl and 5-condensed structures), guaiacyl-, p-hydroxyphenyl hydroxyl groups as well as the amount of carboxyl groups can be detected separately (Figure 10). The hydroxyl group content is an extremely important parameter as it can be used to follow the structural changes caused by biorefinery processes, for stoichiometric calculations when performing chemical modifications of the hydroxyl groups, and to follow the progress of such reactions. The methodology was initially developed for identifying functional groups with labile hydrogens (e.g. alcohols, thiols, amines and carboxylic acids) in coal-derived materials by the Verkade group,[84–86] and was then applied to lignin in a series of publications by Argyropoulus et al.[83,87–91] Initially a first generation phosphitylation agent, 2-chloro-1,3,2-dioxaphospholane, was used but due to poor signal separation a

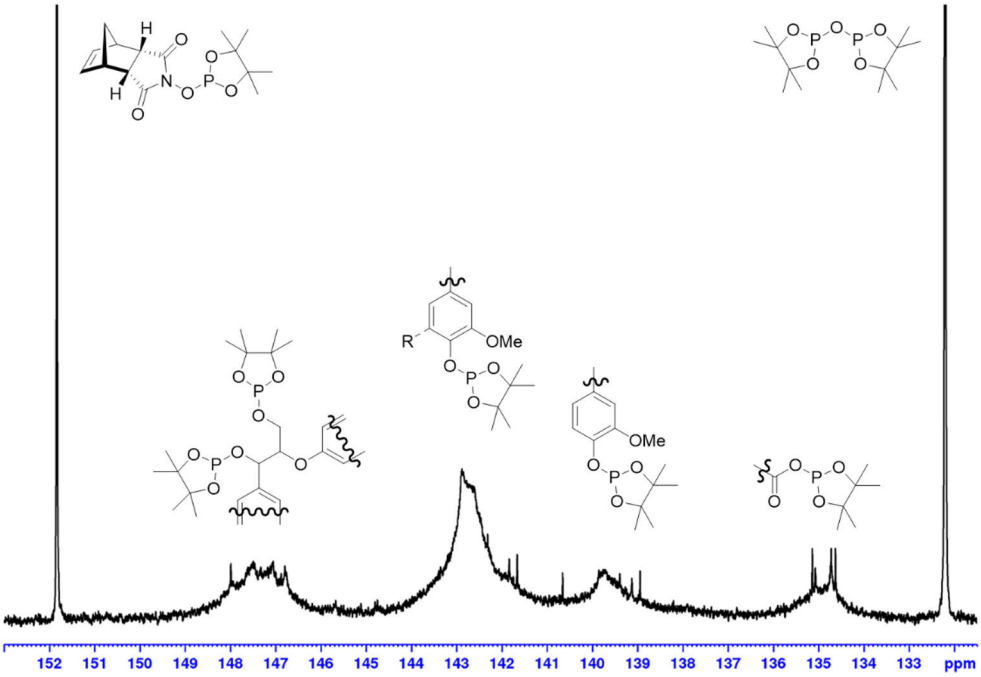

Figure 10. ^{31}P NMR of a phosphitylated birch lignin sample using e-HNDI as IS.

second generation reagent, 2-chloro-4,4,5,5-tetramethyl-1,3,2-dioxaphospholane, was applied to the procedure (Figure 11a and b).[83] The amount of hydroxyl groups are quantified using an internal standard (IS), and secondary alcohols (e.g. cholesterol and cyclohexanol) have often been used (Figure 11c and d). Due to the slight overlapping with the signals from lignin, another IS, endo-N-hydroxy-5-norbornene-2,3-dicarboximide (e-HNDI), has become a popular alternative (Figure 11e).[92] While there are no overlapping signals between e-HNDI and the lignin, some concerns regarding the stability of the phosphitylated e-HNDI have been raised, especially if the sample is not analyzed immediately after the preparation.[93] ^{31}P NMR benefits from almost 100% natural isotopic abundance and the chemical derivatization only takes 5-10 minutes for completion, which makes the method viable for fast screening of multiple lignin samples.[94] The quantification of phosphitylated products is ensured by using the relaxation agent, $Cr(acac)_3$ to suppress the long T_1 relaxation time of the ^{31}P nuclei, and an inverse-gated decoupling pulse sequence to eliminate any nuclear Overhauser effect (NOE) effects from coupling of ^{31}P nuclei to protons.[95] The method is continuously being developed to include different types of lignin (e.g. lignosulphonates),[96] biomass,[97] and in food analysis (e.g. vegetable oils, phenolics, tannins etc).[98–102] Some of the drawbacks with the method is the necessity for derivatization, the stability of the formed phosphites,

slight overlap of some signals, and the cost and commercial availability of the phosphitylation reagent.

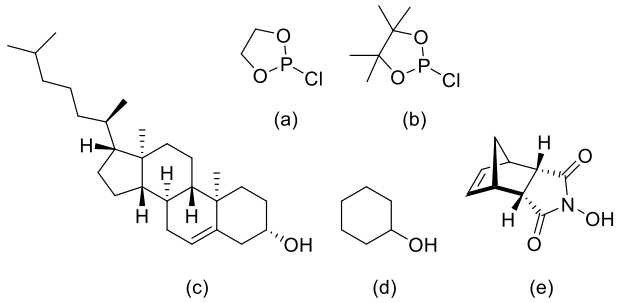

Figure 11. (a) Phosphitylating agents (a) 2-chloro-l,3,2-dioxaphospholane, (b) 2-chloro-4,4,5,5-tetramethyl-l,3,2-dioxaphospholane, and internal standards (c) cholesterol, (d) cyclohexanol and (e) e-HNDI.

1.6.6. 2D NMR spectroscopy

Two-dimensional $^{1}H–^{13}C$ Heteronuclear Single Quantum Coherence NMR Spectroscopy (HSQC) is at present one of the most frequently used spectroscopic methods for structural characterization of lignin. The additional dimension leads to significantly less signal overlap and more reliable assignation of structural components compared to ^{1}H- and ^{13}C NMR spectroscopy (Figure 12). HSQC provides comprehensive structural information on lignin samples such as naturally occurring inter unit linkages (e.g. β-O-4, β-β, β-5 etc.), end groups (e.g. cinnamyl alcohol, aldehyde etc), lignin-carbohydrate linkages, types of units (S-, G- and H-units) and structures formed during depolymerization processes (e.g. stilbenes, enol ethers, Hibbert's ketones, 4-O-5, α-alkoxy etc.).[49,50,103–105] It can also be used to identify impurities such as solvents, fatty acids, carbohydrates, amino acids, other extractives and to characterize products of chemical modifications of lignin.[106–108] The spectroscopic method has been used to identify new structures in lignin both native (e.g. spirodienone, tricin, and dibenzodioxocins)[109–112] and from industrial processes.[49] The inclusion of these new native linkages was of particular importance in recently proposed models of native lignin by Ralph et al.[113] Procedures for characterizing whole plant cell wall using HSQC have been developed, which allows for rapidly screen plant material and discern whole cell wall information without the need to deconstruct and fractionate the plant cell wall.[114,115] The 2D NMR technique also contributed significantly when Crestini et al.[52] proposed a new model structure of softwood kraft lignin based on in-depth analysis and quantification of lignin moieties.

Lancefield et al.[49] also investigated the structure of kraft lignin and identified previously unknown structures and structures that had previously only been proposed in kraft lignin. Prior to these improvements of our knowledge of kraft lignin, the previously proposed structure of softwood kraft lignin had been by Marton in 1971.[60] The verification of new structures can easily be performed by comparing the chemical shifts with model compounds. The NMR experiment is often used to calculate the amount of the different lignin linkages per C_6C_3 unit in a lignin sample. These are semi-quantitative values and use the correlation peaks of the aromatic C-H as IS representing the C_6C_3 units. Zhang and Gellerstedt improved this method by combining quantitative ^{13}C NMR spectroscopy and HSQC. In this method, the quantification is done with quantitative ^{13}C NMR spectroscopy and the relative abundance of the lignin linkages are calculated from the HSQC spectrum.[104,116] Many 2D NMR experiments are not quantitative as the peak integrals can vary between different types of C-H, however, new types of HSQC experiments and methodologies have been developed, such as QQ-HSQC and $HSQC_0$, which enable for better quantification using HSQC.[117–119] The main drawback with HSQC is that the method only detects $^1H–^{13}C$ cross correlation peaks and needs a proton to be attached to the carbon. Due to this valuable information, many of the aromatic carbons and quaternary carbons cannot be obtained.

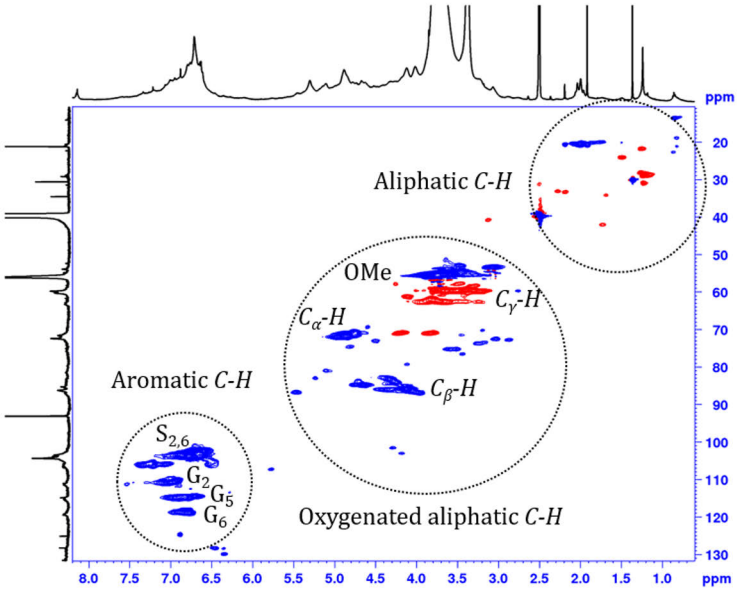

Figure 12. HSQC spectrum of Birch MWL with ^1H NMR spectrum projected on x-axis and ^{13}C NMR spectrum on y-axis.

1.6.7. Molar mass determination

The molar mass is an important physicochemical property of lignin polymers. The number average molecular weight (M_n) and the weight average molecular weight (M_w) are the averages used to describe the lignin polymer, and the dispersity ($Đ=M_w/M_n$) describes the molar mass distribution. Different techniques can be used for the determination of the molar mass but many of them can only determine either the M_w (e.g. light scattering, ultrafiltration and ultracentrifugation) or M_n (e.g. vapor pressure osmometry).[120,121] The most commonly used method for molar mass determination is high-performance size exclusion chromatography (HPSEC).[122] HPSEC which provides access to the whole molecular weight distribution (M_w and M_n), has short sample preparation and analysis time, and only milligram quantities of sample are required. Sulaeva et al.[123] showed that the analysis time could be reduced even more by using ultra-performance liquid chromatography instrumentation. The molecular weight is determined based on the elution time of the analyte, which is dependent on the hydrodynamic volume of the polymer. It is a relative method as molecular weight standards are needed for calibration to obtain the relationship between the hydrodynamic volume and the molecular weight. It can be necessary to derivatize lignin to increase its solubility in the eluent as unmodified lignin can have limited solubility or form aggregates in some solvents.[124] The most used HPSEC system uses THF as eluent using ultraviolet (UV) detection at 280 nm, and polystyrene calibration standards to analyze acetylated lignin.[125] In a collaborative study the intra- and interlaboratory variations in different HPSEC analysis systems were investigated.[125] It was concluded that high molar mass lignin with high polydispersity had the highest variations between the laboratories. The solubility of acetylated lignin was also a source of error, even with the chemical derivatization the solubility in THF of some high molar acetylated lignin was an issue.[124] Any derivatization will also affect the molar mass in varying degree based on the amount of free hydroxyl groups and there is a risk for side reactions. Asikkala et al.[126] investigated three similar derivatization systems (acetobromination, acetylation and partial acetylation) of lignin for HPSEC analysis. They concluded that acetobrominated lignin had the highest solubility in THF and considerably faster reaction times for the derivatization than the other methods. In an attempt to develop a standardized HPSEC system Lange et al.[127] investigated normal setup procedures for THF-HPSEC systems. They looked in to sample preparation methods (i.e. acetylation, acetobromination, benzoylation), choice and number of columns, detectors, calibration, and they also proposed correction factors to correct for the effect derivatization has on the molar mass. Multi-angle laser light scattering (MALLS)

is another promising method for molar mass determination of lignin. The method can determine the absolute molar mass, that is, no calibration standards are required as the molar mass can be derived from the intensity of light scattered by the lignin molecules.[128] MALLS can analyze lignin in solvents that can dissolve unmodified lignin, such as DMSO and DMF, and aggregation can be minimized by addition of LiCl or LiBr.[124] As UV-detectors are often used in HPSEC analysis, DMSO and DMF have been avoided due to their UV-dampening effect. The main limitation using MALLS is the interferences of fluorescence and UV/vis absorption from lignin, especially technical lignin.[128] It is also necessary to carefully determine a refractive index increment (dn/dc) parameter for each analyzed lignin. Gaugler et al.[129] investigated the use of a multi-detector HPSEC systems using MALLS and viscometry detectors. The use of such systems could prove beneficial as the different detector can provide different information about the lignin polymer. Other promising molar mass determination technologies that are being investigated include matrix-assisted laser desorption time-of-flight mass spectrometry. The analysis method has been used for qualitative analysis of lignin and molar mass determination in fractionated lignin with narrow polydispersity, but suffers from difficulties ionizing high molecular weight lignin.[130,131] Methods for determining the molar mass using NMR spectroscopy is also being developed, using diffusion ordered spectroscopy (DOSY) measurements.[132,133] DOSY measures the diffusivity of molecules in solution, which can then be related to their molar mass. The method is still in development and the diffusion coefficients in lignin and their relationship to the molar mass are not well defined.

1.7. Lignin applications

Approximately 1.65 Mt of commercial technical lignin is produced annually (excluding energy production), of which lignosulphonates constitutes ~80%, kraft lignin~15%, hydrolysis and soda lignin ~5%.[28] In Figure 13 the most prominent companies, their lignin brands, and applications can be seen.[134] The primary lignin applications currently use lignosulphonates, or sulphonated kraft lignin, as cement/concrete additives (~500 kt/y) or as miscellaneous dispersants and binders (~400 kt/y). Other current commercial products include vanillin (~30 kt/y), phenolic resins/derivatives (~35 kt/y), phenol (~5 kt/y), and additives in asphalt (~5 kt/y). All these applications are expected to have much higher potential production volumes than what they currently have. Other lignin applications that are not currently being produced at significant volumes but have great potential include carbon fiber, activated carbon, polyols, and BTX (benzene, toluene, and xylene). In a report by the Pacific Northwest National Laboratory and the National Renewable Energy Laboratory, lignin's

role as a renewable raw material resource was evaluated.[135] Three application categories were identified as possibilities in utilizing lignin: power, fuel, and syngas (generally near-term opportunities); macromolecules (generally medium-term opportunities); and aromatics and miscellaneous monomers (long-term opportunities).

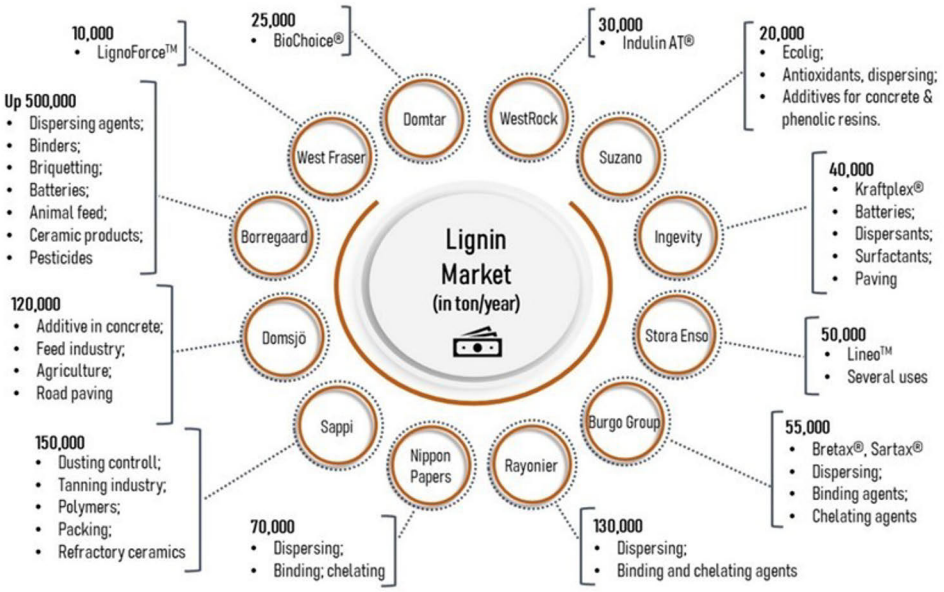

Figure 13. Lignin commercial brands and their applications by the prominent companies, figure from Suota et al.[134]

Besides combustion, which is practiced daily in paper mills, also other methods (i.e. gasification and pyrolysis) can be used to produce power and fuels. Syngas, which is a gas mixture consisting mainly of hydrogen, carbon monoxide, and carbon dioxide can be made by gasification of lignin, or biomass. Syngas can be used for production of methanol/mixed alcohols or green diesel by Fischer-Tropsch technology. Pyrolysis converts dry biomass to so-called pyrolysis oil, which can be used for production of syngas or incorporated into petroleum refinery processes. Pyrolysis oils are often prone to oxidation, which makes their use for chemicals and fuels problematic. Also other, more recent, technologies have been used to prepared fuels from lignin, such as the preparation of green diesel from kraft lignin by hydrogenation, followed by fatty acid esterification to yield a lignin residue that was soluble in light gas oil.[136] The main technological challenges gasification and pyrolysis of biomass are process scale-up and economic gas purification issues.

The majority of the commercial lignin applications that uses lignin as a macromolecule is generally of low value. Other application areas are lignin-based materials and adhesives, in these applications lignin can provide benefits to the products.[57,137–140] Due to the high amount of hydroxyl groups in lignin a common application is to use it as a polyol in different types of polymer formulations such as, polyesters via ring opening polymerization (ROP)(Scheme 5a) or polymerization with dicarboxylic acids (Scheme 5b), in polyurethanes (PU) by polymerization with diisocyanates (Scheme 5c). In lignin-based epoxy resins that can be prepared by polyether polymerization with ethylene- or propylene oxides (Scheme 5d), with epichlorohydrin (Scheme 5e), or crosslinking with diglycidyl ethers (Scheme 5f). Chemical modification is often used to alter the physico-chemical properties in lignin and to introduce new chemical functional groups and to increase the chemical reactivity. To increase the reactivity of technical lignin it can be necessary to prepare aliphatic hydroxyl groups by reacting the phenolic hydroxyl groups with epoxides (Scheme 5d) or to introduce amine groups via, for example the Mannich reaction (Scheme 5g). Lignin have also been used to partially substitute phenol in phenol-formaldehyde resins (PF), mainly for adhesive applications. The formation of the PF occurs by reacting the free 3- and 5-position in lignin aromatic ring with formaldehyde (Scheme 5h). As these positions are often blocked by methoxy groups or have reacted by condensation reactions, lignin is often derivatized by phenolation (Scheme 5i) to increase its reactivity. Lignin can also act as a co-polymer in graftpolymers where e.g. methyl methacrylate or styrene is grafted to lignin by radical polymerization. It can be necessary to functionalize the hydroxyl groups with polymerizable groups to facilitate the polymerization. Blending lignin, or as a substitute, with other polymers (e.g. polyolefins, vinyl polymers, polyesters, polyurethanes etc.) is another possible use of lignin in materials or plastics. The main objective of blending lignin with other polymers is to incorporate some of its properties to the new material. Besides affecting the physical properties of the material lignin has several other beneficial properties such as high thermal stability, antioxidant activity, absorbance of UV irradiation, antimicrobial activity and as a biomolecule it can possibly enable biodegradability in materials. To form miscible blends lignin needs to be compatible with the blended polymer, which can be problematic in non-polar polymer matrices. This can be overcome by increasing the compatibility by chemically functionalizing lignin by etherification (Scheme 5j) (e.g. methylation or ethylation) or esterification (Scheme 5b) (e.g. acetylation). Lignin can be used as a low-cost carbon fiber precursor, which opens up the possibility of utilizing large volumes of lignin for high-value materials.[141] Carbon fibers are currently manufactured from polyacrylonitriles (PAN) and while these fibers are of

excellent quality, the manufacturing costs limit the application areas. Carbon fiber made from lignin cannot compete with high end-applications of PAN carbon fibers, however, low-cost carbon fiber materials can find uses in for example the automobile industry.

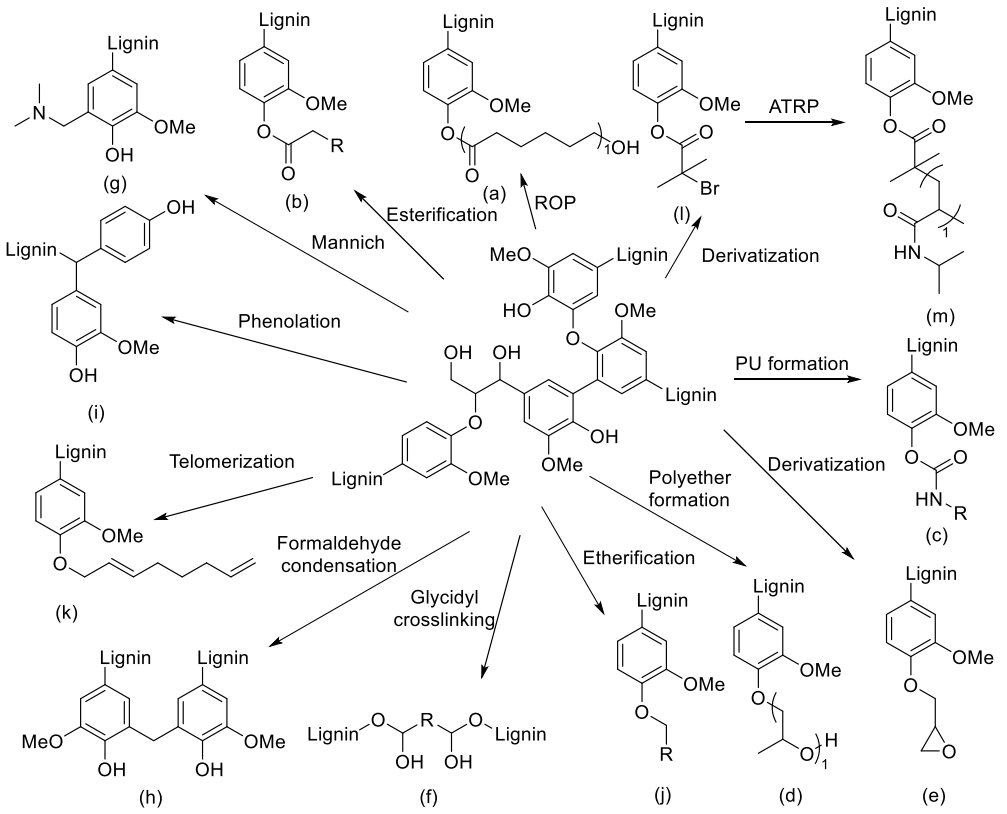

Scheme 5. Examples of lignin modification reactions.

The depolymerization of lignin into fuels and chemicals is one of the most promising ways of utilizing lignin.[142–145] This is a sustainable alternative to the petrochemical industry and a wide variety of depolymerization strategies have been employed e.g., acid/base catalyzed depolymerization, thermal (pyrolysis, gasification), hydrotreatments (reductive), oxidative and biochemical degradation. Some of the most desirable depolymerization products are so-called BTX aromatics, these compounds are produced from petroleum so there is an existing infrastructure for further valorization into products. Production of other types of lignin-based monomers (e.g. propyl guaiacol, vanillin) with greater structural complexity than BTX aromatics are also investigated. Applications of these types of compounds could be the same as other lignin

applications (epoxy resins, polyurethanes, or PF resins) but also starting materials for novel types of polymers and products.

1.8. Recent trends in lignin research

1.8.1. Lignin first

In the carbohydrate-oriented philosophy of traditional lignocellulosic biorefinaries, lignin has been seen as a waste product that impedes the efficient valorization of carbohydrate fraction(s). In these conventional biomass fractionation processes the native lignin is depolymerized and repolymerized into technical lignin, that has generally greatly reduced amounts of alkyl aryl ether linkages and increased linkages bonded by C-C bonds. As there are a broad range of application areas for lignin, there are also possibilities for valorization of technical lignin, however, condensation of lignin will greatly interfere with effective depolymerization of lignin into fuels and chemicals. To circumvent this problem different strategies, that consider the lignin fraction when fractionating the biomass, have been employed. One such strategy is to fractionate biomass under mild conditions, often with organosolv processes, to preserve the native β-O-4 linkages. The drawback with this type of "passive preservation" is the generally low yield of lignin. Another emerging strategy are so-called "lignin first", or active stabilization strategy.[146,147] This strategy aims to disassemble lignin prior to carbohydrate valorization by actively preventing the condensation of lignin during biomass fractionation. This is performed by so-called reductive catalytic fractionation were the lignin is solubilized, depolymerized, and the reactive intermediates are reductively stabilized to yield a depolymerized lignin oil. The technique still needs to be refined and overcome certain limitations such as separation of the catalyst from the de-lignified pulp. Another strategy to avoid the repolymerization, and is also considered a "lignin first" strategy, is to block the reactive benzylic positions with a protecting group during the pre-treatment.[148,149] Aldehydes have been used to stabilize the α,γ-diol group as a cyclic acetal during an organosolv-type pre-treatment of beech and birch wood, with a subsequent second depolymerization step to yield monomers in high yields. The main limitations with the method is the use of aldehydes and possible side reactions.

1.8.2. Biomass sources

The biomass itself can be genetically engineered to produce lignin that is more susceptible to depolymerization under mild conditions. This is accomplished by up- or downregulating genes in the phenylpropanoid pathway, this way they can for example grow softwoods with only S-units, which avoids condensation on the

5-position, or plants with unconventional lignin monomers such as C-lignin or zip-lignin (Figure 14).[150–152]

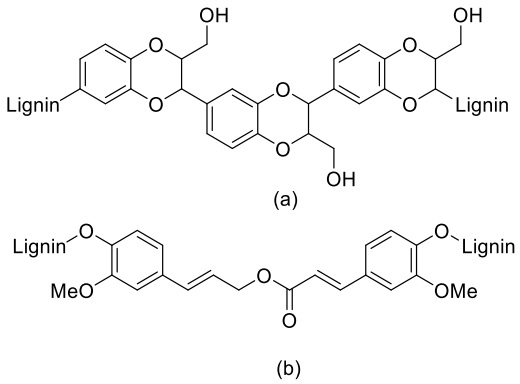

Figure 14. a) C-lignin and b) zip-lignin.

1.8.3. Lignin modification and novel applications

As many novel applications rely on chemical modification of lignin, new types of derivatization methods are being developed, one such example is the lignin palladium-catalyzed telomerization reaction developed by Dumont et al. (Scheme 5k),[153] but some of the most promising modification methods in preparing lignin-based materials is lignin co-polymerization.[154] In lignin graft polymers the lignin macromolecules act as macromonomers and there are two general methodologies used for their preparation: "grafting from" and "grafting to". In the ''grafting from" technique, lignin is used as macro-initiator for the polymerization and usually monomers react with functional groups on lignin (e.g. hydroxyl groups) and the polymer chain is assembled on the lignin core. Ring opening polymerization Scheme 5a), radical polymerizations and atom transfer radical polymerization (ATRP) can be used for "grafting from" method. It can be difficult to control radical polymerizations, but ATRP has largely overcome these limitations by esterifying an initiator (Scheme 5l) to the lignin from where the monomers can be grafted (Scheme 5m). In the "grafting to" method the polymer chain is synthesized first and is then grafted to the lignin core. The coupling between the polymer chain and lignin can be done with e.g. Cu(I)-catalyzed azide-alkyne cycladdition or via boronic acid functionalized polymers that are linked with cyclic boronate ester bonds to the lignin core. Lignin-based smart materials are emerging as next generation of value-added applications and chemical modification of lignin has been a key step in the material preparation. In a recent review, Moreno and Sipponen identified sensors, biomedical systems, and shape-programmable materials as promising applications areas for lignin-based smart materials.[155]

1.8.4. Structure-property relationship

A common trend in lignin research is to establish its structure-property relationship. This is often done by fractionation of lignin into more defined and homogeneous fractions that can then be tested individually for applications.[156,157] The fractionation can be done by membrane filtration, pH- or solvent fractionation, and is often based on molecular size but the different fraction can be enriched with certain functional groups.[158] Another way of reducing the heterogeneity of lignin is by transforming the crude lignin into lignin nanoparticles with uniform size and shape. This is an emerging field that shows great promise in utilizing lignin and in application development. There are different ways of producing lignin nanoparticles (e.g. anti-solvent precipitation, acidification, interfacial crosslinking, etc.) and they can be used in a wide range of industrial applications e.g. dispersants, emulsifiers, coatings, adhesives and composites.[159] Another application field for lignin nanoparticles are biomedical applications where the lignin nanoparticles act as capsules for biologically active substances. These carrier systems can be used for plant protection, nanomedicine, and biocatalysis applications.[160]

1.9. CH-Bioforce biorefinary process

The lignin that was investigated in this thesis originates from a novel biorefinery process. The process uses pressurized hot water extraction (PHWE) followed by mild alkali pulping for the biomass fractionation on a pilot plant scale (Scheme 6).[161,162] A key feature is its ability to isolate high purity extract of polymeric hemicellulose and can as such be considered a “hemicellulose first” biorefinery. The extract is isolated in high concentrations from the cellulose fibers, with absorbed lignin, by PHWE. The extraction water is circulated in the reactor in order to more efficiently remove impurities, to reduce the amount of water needed, to enable the lignin to be absorbed on the fibers, and to prevent degradation of the structural components. The circulating loop also enables the process to proceed under mild conditions (temperature ~150°C, pressure ~8 bar and pH ~4.5-5), and by using the same extract multiple times increases the concentration. The removal of all of the oxygen from the reactor, especially from the pores of the biomass is crucial for the process efficiency, as it reduces oxidation and subsequent degradation of the hemicelluloses and lignin. This is done by reducing the pressure in the reactor and by adding oxygen scavenger(s) to the aqueous solution prior to heating. Lignin can then be extracted from the remaining fibers once the hemicelluloses have been separated. This is performed by first displacing the hemicellulose extract with plain water, adding an oxygen

scavenger, heating the reactor, and then adding the pulping chemical in a single dose. The pulping process also proceeds at mild conditions (temperature ~150°C, pressure ~6-7 bar and pH ~13) using NaOH as pulping chemical and the liquid phase is circulated during the extraction to more efficiently separate lignin from the cellulose fibers. The remaining black liquor is then membrane filtered to remove inorganics and is concentrated. It is from the remaining concentrated liquid that the investigated lignin was isolated and analyzed. The biorefinery process has all the features expected from a modern biorefinery such as environmentally benign (using low amounts of water at relatively mild temperatures, and NaOH as pulping chemical) and uses all of the structural components in the biomass. Hemicelluloses are often fragmented during other types of biomass fractionation conditions to smaller carbohydrate fragments or/and to toxic compounds. Purity and low concentration extract is another problem for similar types of fractionation technologies but this technology yields pure polymeric hemicelluloses as a platform chemical.[163] The cellulose fraction from the process is also isolated in high purity without impurities and excessive degradation.

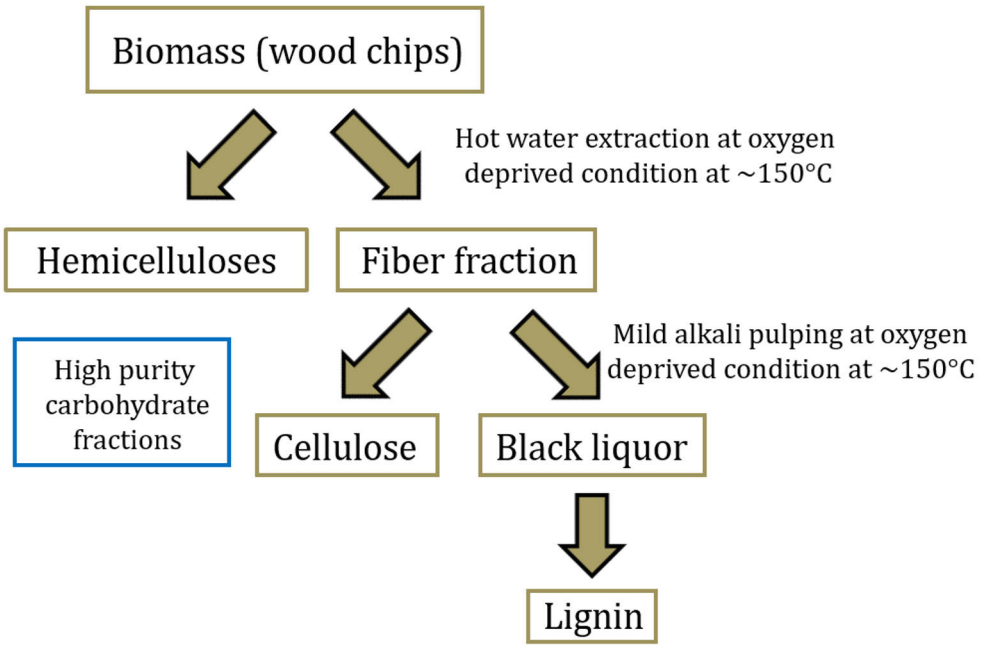

Scheme 6. Schematic flow-chart of the CH-Bioforce biorefinary process.

1.10. Objectives of this thesis

The key objective of this thesis has been to perform an in-depth structural characterization of lignins isolated from the modern biorefinery process developed by CH-Bioforce Oy. In this thesis, lignin from hardwood and softwood was analyzed, but straw and other waste products have been successfully fractionated using the same technology. As both carbohydrate fractions are isolated in high yields and purity, new high-value applications are being developed for these fractions, however, this thesis will not focus on the carbohydrate fractions, nor the process. As the lignin was supplied in the black liquor, the first objective was to develop a protocol to isolate the lignin from the other organic and inorganic impurities. A wide variety of analysis methods were to be used to investigate the structural features of the isolated lignin (i.e. HPSEC, pyrolysis GC-MS, pyrolysis-THM-GC-MS, GC-MS, elemental analysis, carbohydrate content, methoxy group quantification, TGA, FTIR) but with a focus on advanced NMR-techniques (i.e. ^{13}C NMR, ^{31}P NMR, HSQC, and DEPT experiments). Besides using established NMR-techniques for quantifying and characterizing lignin, another objective was to explore the possibilities for method development of the NMR-techniques. Simple chemical modification was also to be used to assist with the analysis and characterization of the lignin. Another objective was to investigate the possibility to fractionate the lignin into more homogeneous fractions with simple solvent fractionation. Structural properties of these fractions, as well as other isolated fractions, were also to be investigated. A secondary objective was to acquire broader knowledge of so-called condensed structures that can form during these types of processes. This knowledge should hopefully not be limited to the investigated lignin but also applicable to lignin from other types of processes.

2. Experimental

2.1. Materials and fractionation methodologies

Chemicals were purchased from commercial sources if not stated otherwise and used without further purification. Milled wood lignin was prepared according to a previously published procedure.[164] The phosphitylation agent 2-chloro-4,4,5,5-tetramethyl-1,3,2-dioxaphospholane (TMDP) was purchased from commercial sources or prepared according to the literature procedures.[102,165]

2.1.1. CH-Bioforce biorefinery

Wood chips of Norway spruce (*Picea abies*), Scots pine (*Pinus sylvestris*) or silver birch (*Betula pendula*) were first extracted at oxygen starved conditions with hot water to remove the hemicelluloses. The remaining fibers were further cooked with NaOH, also at oxygen starved conditions, to give the black liquor that was separated from the pulp (i.e. the cellulose fibers). The black liquor was then concentrated, and the dry content of the lignin solution was 19.3% at pH 12.

2.1.2. Lignin precipitation and MTBE fractionation (papers I & II)

The lignin was precipitated from the black liquor by addition of 1 M HCl until the pH was 2.5. The lignin was then collected either by careful filtration or by centrifugation. The lignin cake was then washed and collected five times with water acidified to pH 2.5 with HCl. After the final wash the lignin slurry was extracted 10 times with MTBE. Both the insoluble lignin fraction and the MTBE-soluble fraction was dried and analyzed.

2.1.3. *i*-PrOH fractionation (paper II)

The dried MTBE insoluble fraction (1.0 g) was stirred with *i*-PrOH (40 mL) for 1 h and then centrifuged. After centrifugation the *i*-PrOH was decanted off and the process was repeated 10 times. The *i*-PrOH insoluble and *i*-PrOH soluble fractions were collected separately, dried, and analyzed.

2.2. Chemical modifications and synthesis

2.2.1. Acetylation of lignin (papers I & II)

Lignin (100 mg) was dissolved in pyridine (1.0 mL) and acetic anhydride (1.0 mL) was added. The mixture was stirred in darkness for 3 days before the reaction mixture was cooled and quenched by addition of MeOH and evaporated under reduced pressure. The crude product was re-dissolved in $CHCl_3$, extracted three times with 0.1 M HCl, twice with water, dried with Na_2SO_4, and finally concentrated under vacuum with isolated yields over 90%.

2.2.2. Methylation of lignin (paper II)

A previously reported method for methylation of the phenolic hydroxyl groups was used.[166] In short, the lignin (1.0 g) was dissolved in 0.7 M NaOH (15 mL) and Me_2SO_4 (0.95 mL, 10.0 mmol) was added. The mixture was stirred for 30 min at room temperature followed by 2 h at 80 °C while 0.7 M NaOH was continuously added to keep the solution alkaline according to the procedure. The amounts of Me_2SO_4 were calculated from the total amount of free phenolic groups from the ^{31}P NMR analysis, approximately 2.5–3.0 equivalents of Me_2SO_4 per phenolic hydroxyl group was used in this work.

For the complete methylation the lignin (2.0 g) was dissolved in dry DMF (30 mL). An appropriate amount of 60% NaH in mineral oil (5 equivalents with respect to the total amount of free hydroxyl groups) was measured and washed three times with hexane. The NaH was then stirred to a suspension with 10 mL dry DMF and added dropwise to the lignin solution on ice bath. The methylation agent MeI (5 equivalents) was then added dropwise. After 16 h the reaction was cooled on an ice bath and the excess NaH was quenched by addition of MeOH. The solution was then poured into a large volume of water and acidified to pH 2.5 with 1M HCl. The lignin was collected by filtration and was purified twice by stirring the mixture in acidified water (pH 2.5) and filtering in between. After the final filtration the cake was thoroughly washed with distilled water and freeze dried prior to analysis.

2.2.3. Synthesis of model compounds (papers IV)

The synthesis of the model compounds used previously developed methodologies. The lithiation reactions were performed according to Costa and Saa.[167,168] The etherification of syringyl alcohol and subsequent bromination was done according to the procedure of Ellerbrock et al.[169] The bromination of syringyl aldehyde was performed according to Davidson and Barker[170] and the methodology for the Suzuki coupling to yield the phenylic products was done according to Priestley et al. 2013.[171]

2.3. Characterization methods

2.3.1. High-performance size exclusion chromatography (papers I & II)

Molar-mass characteristics were analyzed using a Shimadzu HPLC system (SCL-10AVP system controller + DGU-14A on-line degasser + FCV-10ALVP low-pressure gradient valve + LC-10ATVP HPLC pump + SIL-20AHT autosampler + CTO-10ACVP column oven) equipped with a sequentially connected guard column (50 mm × 7.8 mm) and two Jordi Gel DVB 500A (300 mm × 7.8 mm) columns in series. Eluent: THF with 1% acetic acid, flow rate: 0.8 mL/min,

column oven temperature 40 °C. Injection volume of the autosampler was 50 µL. Detector: LT-ELSD detector (SEDEX 85 LF Low-Temperature Evaporative Light Scattering Detector. Detector parameters: HPLC nebulizer, 40 °C, air pressure: 3.5 bar, gain 3, no-split mode. Column calibration was performed using Mono-Disperse Polystyrene Standards.

2.3.2. Gas chromatography-mass spectrometry (GC-MS)(paper I)

The individual compounds were identified by GC–MS by comparing with the commercial Wiley 10th/NIST 2012 database and in-house spectral database. The methods, instrumentation and derivatization of the different GC and GC–MS analysis have also been described elsewhere.[172,173]

2.3.2.1. Carbohydrate content (paper I)

The carbohydrate content was analyzed by GC after acid methanolysis and silylation, approximately 10 mg of samples were depolymerized by the addition of 2 mL 2 M HCl in anhydrous methanol. The samples were kept at 100 °C for 5 h before cooling to room temperature and neutralized with pyridine. A calibration solution containing equal amounts of the sugar monomers and uronic acids (except 4-*O*-MeGlcA) was also subjected to acid methanolysis under similar conditions. Additionally, 4 mL of methanol solution containing the internal standard sorbitol (0.1 mg/mL) was added to the samples. To exclude fibers during analysis, 1 mL of clear solution was then transferred to a test tube and evaporated to dryness. The dry samples were silylated and analyzed by GC-MS on a 25 m x 0.20 mm i.d., 0.11 um HP-1 column, according to literature procedures. [174,175]

2.3.2.2. Pyrolysis (*py*)-GC–MS and *py*-*THM*-GC–MS (thermally assisted hydrolysis and methylation) (paper I)

The *py*- and *THM*-GC–MS analyses were performed on a foil pulse Pyrola 2000 pyrolyzer. For py-GC–MS, approximately 100 µg of each sample was applied on the Pt filament and the samples were pyrolyzed at 650 °C for 2 s. For *THM*-GC-MS approximately 100 µg of each sample was dissolved in 10 µL of tetramethylammonium hydroxide (25% in methanol), whereafter the solution was added to the Pt filament and pyrolyzed at 380 °C for 2 s. The *py*-GC–MS was equipped with a 25 m x 0.20 mm i.d., 0.11 um HP-5 column.

2.3.2.3. Short column GC-MS analysis (papers I)

The composition of the MTBE-soluble fraction was analyzed using a short column GC, 6 m x 0.530 mm i.d., 0.15 um HP-1/SIMDIS column. For the

quantitative analysis by GC-FID, a solution containing internal standards was added before silylation.

2.3.3. Methoxy groups determination (paper I)

The determination of methoxy groups was done according to literature procedure.[176] The lignin sample (~5 mg) and the internal standard 4-methoxybenzoic acid-d3 were added to a headspace vial provided with a magnetic stirring bar. Hydroiodic acid (aq.) (1 mL, 57%) was added to the mixture and the vial was closed with a cap and heated at 130 °C under stirring. After 1 h the sample was allowed to cool to room temperature and the excess HI was neutralized. Headspace GC-MS analyses were performed on an Agilent 5890 N gas chromatograph (DB-5 ms column 30 m × 0.25 mm) coupled with an Agilent 5975B inert XL mass selective detector. Helium was used as a carrier gas with a constant column flow of 1 mL/min. The method was calibrated by responses from methyl iodide and deuterated methyl iodide obtained from vanillin and known amounts of the internal standard 4-methoxybenzoic acid-d3.

2.3.4. Elemental analysis (papers I & II)

Elemental analysis was performed on a FLASH 2000 organic elemental analyzer using cysteine and sulfanilamide as standards. A sample size of 2 mg; 950 °C reactor temperature; He gas carrier (140 L/min); O_2 oxidizer (250 L/min); during 6 min for CHNS-combustion. For O-pyrolysis (paper I): sample size of 2 mg; 1060 °C reactor temperature; He gas carrier (140 L/min). The oxygen content (paper II) was calculated by subtracting the sum of carbon, hydrogen and nitrogen from 100%. Quadruplicates of each sample were analyzed in paper I and triplicates of each sample in paper II.

2.3.5. Fourier transform infrared spectroscopy (FTIR) (paper I)

The FTIR spectra were recorded on a Bruker Alpha FTIR instrument using attenuated total reflection mode. The spectra were collected in the absorbance range from 4000 to 400 cm^{-1} over 32 scans per sample, at a resolution of 4 cm^{-1}

2.3.6. NMR spectroscopy (papers I-IV)

All the NMR experiments were performed at 298 K in DMSO-*d*6 on an AVANCE III spectrometer operating at 500.13 MHz for ^{1}H, 125.77 MHz for ^{13}C and 202.46 MHz for ^{31}P. The spectra were processed using Topspin 3.5 software.

2.3.6.1. ^{13}C NMR spectroscopy (papers I & II)

Sample preparation and parameters used for quantitative ^{13}C NMR in Paper I: To 150 mg lignin dissolved in 0.39 mL DMSO-d6 0.1 mL of a trioxane internal standard (IS) stock solution in DMSO-d6 (0.15 g/mL) and 0.06 mL of a stock

solution of $Cr(acac)_3$ in DMSO-d6 (50 mg/mL) was added. This yielded a 0.016 M concentration of the relaxation agent to ensure complete T1 relaxation according to published methods.[81] To ensure an accurate baseline, the spectra were recorded in the interval of 240-(-40) ppm according to Balakshin and Capanema.[94] A 1.4 s acquisition time and a 1.7 s relaxation delay were used. A total of 75,000 scans were collected. The solvent peak was used for calibration. The ^{13}C-NMR DEPT-90 experiment was calibrated to remove artefacts before sample measurements.

Quantitative ^{13}C NMR parameters used in Paper II: The quantitative ^{13}C NMR was measured with a spectral width of 35,714 Hz, 2 s acquisition and a 10 s relaxation delay with the Bruker pulse program zgig.

2.3.6.2. 2D HSQC NMR spectroscopy (papers I & II)

For quantification of the lignin linkages in paper I the Bruker's pulse program for adiabatic pulses for inversion and refocusing "hsqcetgpsisp.2" with a spectral width of 8012 Hz (from 0 to 16 ppm) and 20575 Hz (from 0 to 165 ppm) for the ^{1}H- and ^{13}C-dimensions was used. A 1.5 s recycle delay and 72 scans were collected. The quantification was done using the approach to combine quantitative ^{13}C NMR and HSQC suggested by Zhang and Gellerstedt.[116] A relative integration value is obtained from 2D HSQC by integrating the well-separated peaks and dividing that with the total integration of the region (for each typical linkage). Once the relative quantification was determined by HSQC the different linkages was multiplied by the integral of the cluster region in the quantitative ^{13}C NMR spectrum. The integral for the total aromatic carbons was set to 600 and compared with the integral values for the specific region cluster giving the amount of linkages per 100 aromatic moieties.

Linkage % = 2D(linkage) / 2D(linkage cluster) * ^{13}C(linkage cluster) / ^{13}C(163-101) * 600

Where the linkage % is the integration of C_α, $A_{o\beta}$, D_α, B_α, A_β (S and G), Y_α and E_γ and the region cluster was δ_C/δ_H (90.0-78.0/6.0-2.5). The integration value of B_α and E_γ was divided by two due to the symmetrical nature of the resinol structure and due to E_γ being a CH_2. The total aromatic integral value was set from 101.0 to 163.0 ppm. In paper II the HSQC experiment used the Bruker's pulse program "hsqcedetgpsisp2.3 for multiplicity edited with a spectral width of 8012 Hz (from 0–16 ppm) and 30,182 Hz (from 0–220 ppm) for the ^{1}H- and ^{13}C-dimensions. A semi quantitative method was used for calculating the amounts of lignin linkages by using the C_2-H integral as internal standard (IS). For qualitative HSQC analysis

experiments the multiplicity edited HSQC pulse program “hsqcedetgpsisp2.3” was used.

2.3.6.2. ^{31}P NMR spectroscopy (papers I & II)

A common standard protocol was used for ^{31}P NMR sample preparation.[83] To a solution of 20 or 40 mg lignin in a 0.4 mL mixture of pyridine and $CDCl_3$ (1.6:1, v/v) 0.100 mL of a IS solution (0.12 M) was added. After thorough stirring, 0.1 mL of phosphitylation reagent TMDP and 0.050 mL of a Cr(acac)3 solution (11.4 mg/mL) was added, and the sample was stirred at room temperature before transferred to a NMR tube. The ^{31}P NMR measurements were collected with a total of 500 scans with a 1.0 s acquisition time and a 5.0 s relaxation delay in paper I and with a 2.0 s acquisition time and a 5.0 s relaxation delay in paper II. The spectra were calibrated using the signal of the water-derivatized signal at 132.2 ppm. Cyclohexanol or N-hydroxy-5-norbornene-2,3-dicarboxylic acid imide (e-HNDI) was used as internal standard.

2.3.6.3. ^{31}P NMR spectroscopy (paper III)

The ^{31}P NMR measurements were carried out using a standard 90° pulse program with inverse-gated decoupling (Bruker’s pulse sequence zgig), and the 90° pulse was optimized by determining the pulse length corresponding to the 360° pulse and dividing it by four or by using Topspin’s automatic pulse calibrating program pulsecal p31.

Receiver gain (rg) value of 203, line broadening (lb) of 5 Hz, and 32 acquired scans between 117.2 and 166.5 ppm were used for the experiments. Tuning and matching of the probe was carried out automatically using the atma exact command for more accurate results. The chemical shifts of the ^{31}P NMR spectra were calibrated using the signal of the water-derivatized product at 132.2 ppm. Baseline corrections were performed automatically and phase corrections manually.

Receiver Gain. The correlation between signal intensity and receiver gain was investigated by analyzing a sample with increasing rg values from 1 to 203.

T1 Relaxation Times. The T1 relaxation times were measured using a standard inversion recovery experiment (Bruker pulse sequence t1ir). Triphenyl phosphate (TPP). When recording spectra of Bruker’s ^{31}P standard (0.0485 M triphenyl phosphate in acetone-d6), a longer relaxation delay (30 s) was used to accommodate the slower relaxation of the sample. The spectra were recorded between −45 and 5 ppm (in order to simplify the calculations the spectral width

was the same as for all other experiments, even though this is much wider than needed for the TPP sample).

90° Pulse. The 360° pulse was found using the parameter optimization ("popt") module in TopSpin. Once an approximate pulse length of 360° pulse was established, e.g., by initially using the pulsecal p31 program or by measuring a broader pulse length range, the popt module was set up to record one spectrum with a slightly too short pulse (with negative peaks) and one with a slightly too long pulse (with positive peaks). The actual 360° pulse, ideally with no peak, was interpolated from these two spectra. The reason why a 360° was sought instead of directly calibrating the 90° pulse is that the point when the signal crosses from negative to positive is easier to determine than the point where the signal is at maximum intensity. Additionally, radiation damping can cause asymmetry and phase distortion problems in the nutation curve, making the direct determination of a 90° (or 180° or 270°) pulse unreliable. To automate the calibration of the 90° pulse for iconnmr, the acquisition AU program au_zg was modified by adding a line XCMD("pulsecal p31") before the RGA line. The pulsecal program was found to consistently give pulses that were approximately 10–12% longer than the manually obtained 90° pulses, resulting in a 10–12% deviation in the flip. Since the signal strength is inversely proportional to the length of the 90° pulse, and the flip angle is directly proportional to the pulse length, the exact flip angle is not important, as long as it is consistent. Therefore, the pulsecal au program can be used for automating the PULCON methodology. Using a pulse that is not 90° will, however, result in lowered sensitivity, but even a deviation of 10° from the optimum value results in less than 2% signal loss.

Sample Preparation for ^{31}P NMR Spectroscopy. A known amount of lignin (20 mg) or vanillyl alcohol (1, 2, 5, 10, 15, and 20 mg, respectively) was dissolved in a 400 μL of a mixture of pyridine and $CDCl_3$ (1.6:1, v/v). To this solution, 100 μL of e-HNDI IS solution (0.12 M, in pyridine and $CDCl_3$ 1.6:1 v/v) and 50 μL of a $Cr(acac)_3$ solution (11.4 mg/mL in pyridine and $CDCl_3$ 1.6:1 v/v) were added. After thorough stirring, 100 μL of TMDP was added, and the sample was stirred at room temperature for 75 min before being transferred to an NMR tube and measured.

Sample Preparation for the verification of the automated procedure. The automated protocol was performed in triplicate for the birch and pine lignin as follows: The lignin (20 mg) was dissolved in 500 μL of a mixture of pyridine and $CDCl_3$ (1.6:1, v/v) and 50 μL of a $Cr(acac)_3$ solution (11.4 mg/mL). After thorough stirring, 100 μL of TMDP was added, and the sample was stirred at room temperature for 1 h before being transferred to an NMR tube. The samples were

put in an autosampler and queued for measurement using Bruker's iconnmr. The 90° pulse was calibrated for each sample using the AU program pulsecal prior to the ^{31}P NMR measurements.

2.3.7. Thermogravimetric Analysis (TGA) (paper II)

TGA was carried out using a STA 409 PG/1/G in the range of the temperature 23 to 600 °C at a rate of 10 °C/min under N2 atmosphere. As the different samples: unmodified lignin, acetylated lignin, and lignin with methylated phenolic groups had different workup procedures prior to drying under vacuum, the 100 wt% was set to the value when the samples had been heated to 120 °C during the analysis. Any prior weight losses correspond to the loss of moisture or volatile compounds, and it was concluded that at ~120 °C the weight loss had stabilized based on differential thermal analysis (DTG). To study the possible deacetylation two samples, unmodified pine lignin and acetylated pine lignin, was dried under vacuum at 60 °C over one week to ensure removal of any traces of acetic acid and then analyzed by TGA. The samples were also preheated to 100 °C and cooled prior to analysis to ensure removal of moisture that could have been absorbed on the lignin during transfer to the instrument.

3. Results and discussion

3.1. Isolation of lignin

To develop a lignin precipitation protocol, lignin was precipitated from the black liquor at pH 6.0, 5.0, 4.0, 3.5, 3.0, and 2.5, by addition of 1 M HCl, followed by centrifugation and decanting of the water phase. Precipitated lignin was then washed with water with the same pH as in the precipitation step. The precipitate was collected by centrifugation and the washing procedure was repeated four times. Precipitation at pH 2.5 yielded the largest amount of lignin, 12.4 wt% of the black liquor. Based on HPSEC analysis there were only small differences in the molar masses, but low molar mass lignin was also precipitated at a lower pH. The ash content for the lignin precipitated at pH 2.5, after four washes, was 0.15% according to TAPPI standard T 211 om-02. As such the protocol for precipitating lignin and subsequent wash was concluded to occur at pH 2.5 to yield the maximum amount of lignin.

3.1.1. Purification and solvent fractionation

Extractives and other organic impurities that could affect the analysis results were removed from the lignin. This was performed by extracting the final slurry from the precipitation and washing steps, with MTBE. This yielded MTBE insoluble lignin, referred to BLN lignin in this text, and a low molar mass MTBE-

soluble fraction. Approximately 15-20 wt% of the crude lignin was extracted by MTBE. The dried MTBE insoluble lignin could be further fractionated by stirring with *i*-PrOH to yield an insoluble high molar mass fraction (70 wt%) and a soluble medium molar mass fraction (30 wt%) (Scheme 7).

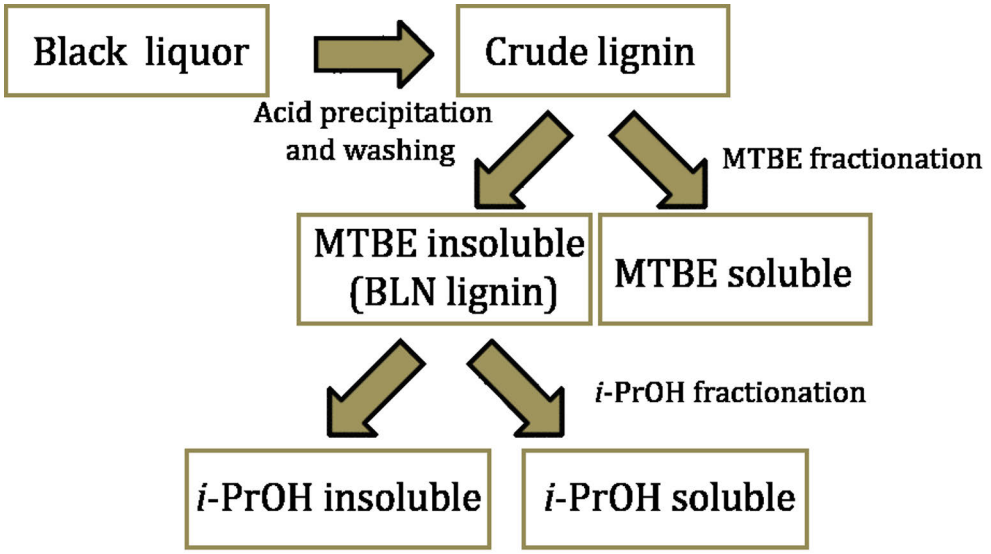

Scheme 7. Lignin precipitation, purification, and fractionation protocol.

3.2. Chemical composition and molar mass

To determine the structural changes that occurred during the fractionation process, the lignin (birch, spruce, and pine) was compared to MWL lignin, which was extracted from wood chips from the same wood species. As seen from (Table 1) the MTBE-soluble fraction mainly contained low molar mass compounds and as such did not remove excessive amounts of polymeric lignin. The molecular mass of all the lignin was all below 10 kDa, which can be considered relatively small and with a narrow dispersity (Đ) compared to other technical lignins.[177] The softwood lignins were fractionated with *i*-PrOH and the soluble fraction contained a low molar mass lignin fraction with low Đ. The number average (M_n) molecular mass was similar between the BLN lignin and MWL, which indicates that there might have been some degradation of the MWL during the milling process. The carbohydrate content in birch lignin was analyzed by methanolysis and it only consisted of small amounts of carbohydrates (~1% wt%), mainly xylans. MWL contained a larger amount of hemicelluloses that should be taken into consideration when comparing the lignin (~8% wt%).

Table 1. Molar mass of the different lignin fractions determined by HPSEC.

Lignin	M_n [g/mol]	M_w [g/mol]	Đ
Birch MWL	3300	4200	1.3
Birch BLN	3000	5300	1.8
Birch MTBE	900	1700	2.0
Pine MWL	1500	2700	1.7
Pine BLN	3200	6700	2.1
Pine MTBE	400	500	1.3
Pine iPrOH ins.	4200	8000	1.9
Pine iPrOH sol.	900	1500	1.7
Spruce MWL	2100	3000	1.5
Spruce BLN	2100	5600	2.7
Spruce MTBE	500	600	1.2
Spruce iPrOH ins.	3800	7000	1.9
Spruce iPrOH sol.	900	1200	1.3

The elemental analysis showed an enrichment of carbon and decrease of oxygen in the BLN lignin compared to the MWL lignins (Table 2). This trend is consistent with published results of birch MWL and kraft lignin[178] and can be partially explained by the higher amount of carbohydrates in the MWL, but mainly by the cleavage of the lignin alkyl side chains and subsequent condensation reactions. An important feature of the lignin is the lack of sulfur that possesses unwanted properties that limit the use of the lignin, which is the case for kraft lignin. Volatile sulfur-containing compounds acts as air pollutants and the unwanted odor can make it incompatible as an additive in polymers.[179] Sulfur can poison certain catalysts, which limits the possibilities for depolymerization, and sulfur contaminants can have a negative effect on lignin based carbon fibers[180,181] FTIR analysis of the birch lignin revealed an increase of carboxylic acids in the BLN

lignin by a band at 1697 cm^{-1}, while two separate bands were observed at 1725 and 1656 cm^{-1} from carbonyl groups in the spectrum from MWL. The BLN contained approximately 8% less methoxy groups compared to the MWL. While demethylation is common in kraft pulps, due to their usage of NaS_2, it has been shown that it occurs during pressurized hot-water extraction as well.[182]

Table 2. Elemental analysis of MWL and BLN lignin.

	C (%)	H (%)	S (%)	N (%)	O (%)
Birch MWL	58.5	6.6	0.0	0.1	33.0
Birch BLN	64.9	6.2	0.0	0.4	27.1
Pine MWL	60.6	5.9	0.0	0.2	33.3
Pine BLN	67.2	6.0	0.0	0.1	26.7
Spruce MWL	59.5	5.7	0.0	0.1	34.7
Spruce BLN	66.5	5.8	0.0	0.0	27.6
Lignoboost softwood[29]	65.1	5.8	2.5	0.1	27.5
Birch kraft lignin[178]	62.5	6.0	2.4	-	27.8

3.2.1. *Py*-GC-MS and *Py-THM*-GC-MS

The S/G ratio of the birch lignin was determined with *py*-GC-MS and had increased in the BLN lignin compared to the birch MWL from 1.8 to 2.2. Due to the similarities of the pyrograms and by the fact that the total peak area of the BLN is only 25% of the MWL it is a possibility that certain lignin fragments are more easily pyrolyzed, as the other analysis methods clearly show structural differences between MWL and BLN lignin. This indicates that more intact lignin bound together by ether bonds is more easily pyrolyzed and more condensed lignin is not detected by the pyrolysis methods. Even after the extensive MTBE-extraction to remove extractives from the lignin, still approximately 8% of the detected *Py-THM*-GC-MS peaks originated from fatty acids. The applied method is not quantitative and incomplete pyrolysis of the BLN lignin would also explain the high amounts of fatty acids detected, but it is still indicative of the remaining fatty acids having a high affinity to the lignin.

3.2.2. ^{31}P NMR

The amount of free hydroxyl groups in all the different lignin fractions and MWL can be seen in Table 3. The amount of aliphatic hydroxyl groups was greatly decreased and phenolic hydroxyl groups was increased in the MTBE washed BLN lignins compared to the MWL:s. This can be explained by cleavage of the aliphatic side chain, condensation reactions and formation of free phenolic hydroxyls groups from the cleavage of the aryl alkyl ether linkages, which is consistent with the results from the chemical composition analysis. The S/G ratios calculated for the MWL and BLN lignins were 1.6 and 3.0, thus in line with the values obtained by *py*-GC-MS, however, the ^{31}P NMR analysis method does not discriminate between free hydroxyl groups from 5-condensed- and S-units. In the softwood lignin the formation of condensed 5-substituted phenolic structures is seen as they are detected separately from the aliphatic hydroxyl groups and phenolic hydroxyl groups from G-units. The low molar mass *i*-PrOH fractionated softwood lignins had less aliphatic hydroxyl groups and more phenolic hydroxyl groups and carboxylic acids than the insoluble fraction. The increase in phenolic hydroxyl groups and carboxylic acids can be explained by the lower molar mass, which leads to more units per gram lignin, however, it does seem that the aliphatic hydroxyl groups are enriched in the higher molar mass fractions.

Table 3. Amount of free hydroxyl groups in mmol/g based on ^{31}P NMR analysis.

Lignin	Aliphatic	5-subs	G-units	Ph-OH_{tot}	OH_{tot}.	COOH
Birch MWL	4.5	0.8	0.5	1.2	5.8	0.2
Birch BLN	1.3	2.8	0.9	3.7	5.0	0.5
Birch MTBE	0.6	2.9	1.0	3.9	4.6	1.0
Pine MWL	4.7	0.8	1.2	2.0	6.7	0.3
Pine BLN	2.2	2.0	1.9	3.9	6.1	0.6
Pine MTBE	0.7	1.2	2.5	3.7	4.4	1.6
Pine *i*-PrOH ins.	1.9	1.8	1.5	3.3	5.2	0.4
Pine *i*-PrOH sol.	1.7	1.8	2.3	4.0	5.7	0.8
Spruce MWL	4.6	0.8	1.3	2.1	6.7	0.2

Spruce BLN	2.2	1.9	1.9	3.9	6.1	0.6
Spruce MTBE	1.0	1.3	2.3	3.6	4.6	1.4
Spruce *i*-PrOH ins.	2.1	1.9	1.6	3.5	5.6	0.5
Spruce *i*-PrOH sol.	1.6	1.7	2.1	3.8	5.4	0.8
OMe Pine BLN	2.0			0.8	2.8	0.7
OMe Spruce BLN	1.9			0.6	2.5	0.6
OMe Birch BLN	1.3			0.5	1.8	0.7

3.3. Thermal analysis

The lignin samples were analyzed by TGA to determine their thermal stability and decomposition. To investigate how esterification and etherification affects the thermal degradation also acetylated and selectively methylated derivatives were analyzed. As the different samples: unmodified lignin, acetylated lignin, and lignin with methylated phenolic groups had different workup procedures, the 100 wt% was set to the value when the samples had been heated to 120 °C during the analysis. Any weight losses prior correspond to the loss of moisture or volatile compounds, and it was concluded that at ~120°C the weight loss had stabilized based on differential thermal analysis (DTG). The decomposition starting temperature ($T_{dst\ 95\%}$), the maximum weight loss temperature (T_{max}) and char residue of the samples can be seen in Table 4. Birch lignin had slightly lower $T_{dst\ 95\%}$ and T_{max} than the softwoods and all three woods species had the same amount of char residue. The methylation of the phenolic groups slightly increased the stability of all the lignin samples compared to the unmodified lignin, however, the acetylation decreased the stability, which is contradictory to other studies.,[183] This indicates that the acetyl groups were cleaved or that the decrease in mass is due to evaporation of less volatile acetylated compounds. The cleavage could also be catalyzed by some impurities, such as minuscule amounts of acetic acid from the reaction. To ensure that volatile impurities did not affect the lower thermal stability of the acetylated lignin two samples of an acetylated lignin and an unmodified lignin were extensively dried under vacuum at 40°C for over a week and reanalyzed. While there was a small increase in stability it was still lower than the unmodified lignin. Acetylation has been used to increase the compatibility with other polymers in blends and as such deacetylation could potentially cause degradation of other polymers such as PLA.[184] All of the lignin

samples had lower $T_{dst\ 95\%}$ temperatures than normally used processing temperatures (~170°C).[185] The unmodified lignin had a higher char residue at 600 °C (wt%) than the methylated and acetylated lignin which could be due to the formation of more stable condensed structures in the unmodified lignin with free phenolic groups. The unmodified lignin could be a potential carbon source for carbon fiber applications due to the relatively high char residue.

Table 4. Thermal properties of pine, spruce, and birch lignin and their acetylated and methylated derivatives.

	T_{dst} 95% (°C)	T_{dst} 90% (°C)	T_{dmax} (°C)	Char residue[1]
Pine	302	347	401	49
OAc	233	324	398	44
OMe	317	360	411	48
Spruce	296	350	401	53
OAc	198	295	396	46
OMe	312	359	408	51
Birch	273	325	386	49
OAc	234	305	391	42
OMe	280	339	392	47
[1] at 600 °C (wt%)				

3.4. Structural analysis by NMR spectroscopy

The structural alteration, caused by the process to the lignin, can be seen by comparing the HSQC spectrum of the MWLs to BLN lignin (Figure 15 for hardwood) and (Figure 16 for softwood). The native lignin linkages are mostly cleaved during the process and the remaining amounts of the most common linkages (β-O-4, β-β and β-5) can be seen from Table 5**.** The softwood MWL had lower amount of β-O-4 linkages compared to other published studies,[65] which is in agreement with the molar mass analysis that there has been some degradation during the milling process. This degradation is also evident due to the presence of β-O-4'/α-CO (A_{ox}) linkage in the birch MWL. None of the other native lignin

linkages (dibenzodioxocin, γ-substituted β-O-4, Spirodienone) or end groups (cinnamyl alcohol, cinnamyl aldehyde), that can be detected in the MWLs are observed in the BLN lignins. Birch BLN lignin retained more carbohydrates compared to the softwood BLN lignin and the carbohydrate correlation peaks detected are from xylans, which agrees with the methanolysis results. However, no traditional LCC correlation peaks between the carbohydrates and lignin could be detected in the samples.[186] The process caused formation of aryl glycerol end groups in both hardwood and softwood lignin, which is known to form in alkaline pulping.[187,188] The chemical shifts of aryl glycerol are similar, or overlap, with signals from Xyl_4, Xyl_5 and 2-*O*-Ac-Xyl*p*, however, due to lack of acetyl groups in the BLN lignin and comparing the chemical shift of the unmodified and acetylated birch BLN lignin to previously published chemical shifts of lignin and xylose it was concluded that it was aryl glycerol end group signals.[189–192] Enol ethers and stilbenes were also formed during the process and could be detected in the aromatic region of the BLN lignin (Figure 17). The aromatic HSQC correlation peaks and ^{13}C NMR peaks are considerably broader in the BLN lignin compared to the MWL lignin and is typical for processed lignin.[193]

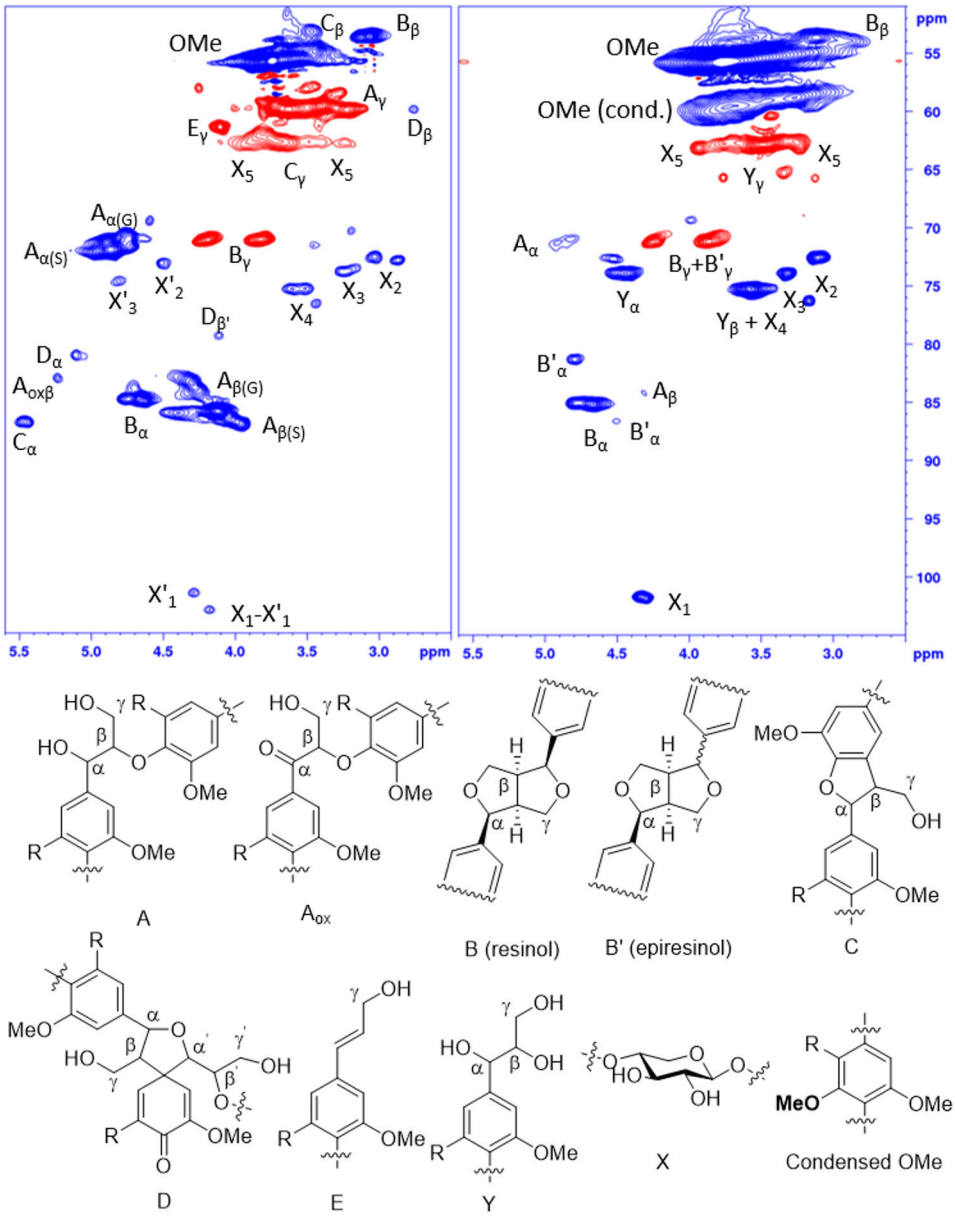

Figure 15. HSQC spectrum of the oxygenated aliphatic area of birch MWL (left), birch BLN lignin (right), and structures of lignin linkages and end groups (below) CH/CH_3 shown as positive (blue) and CH_2 as negative (red).

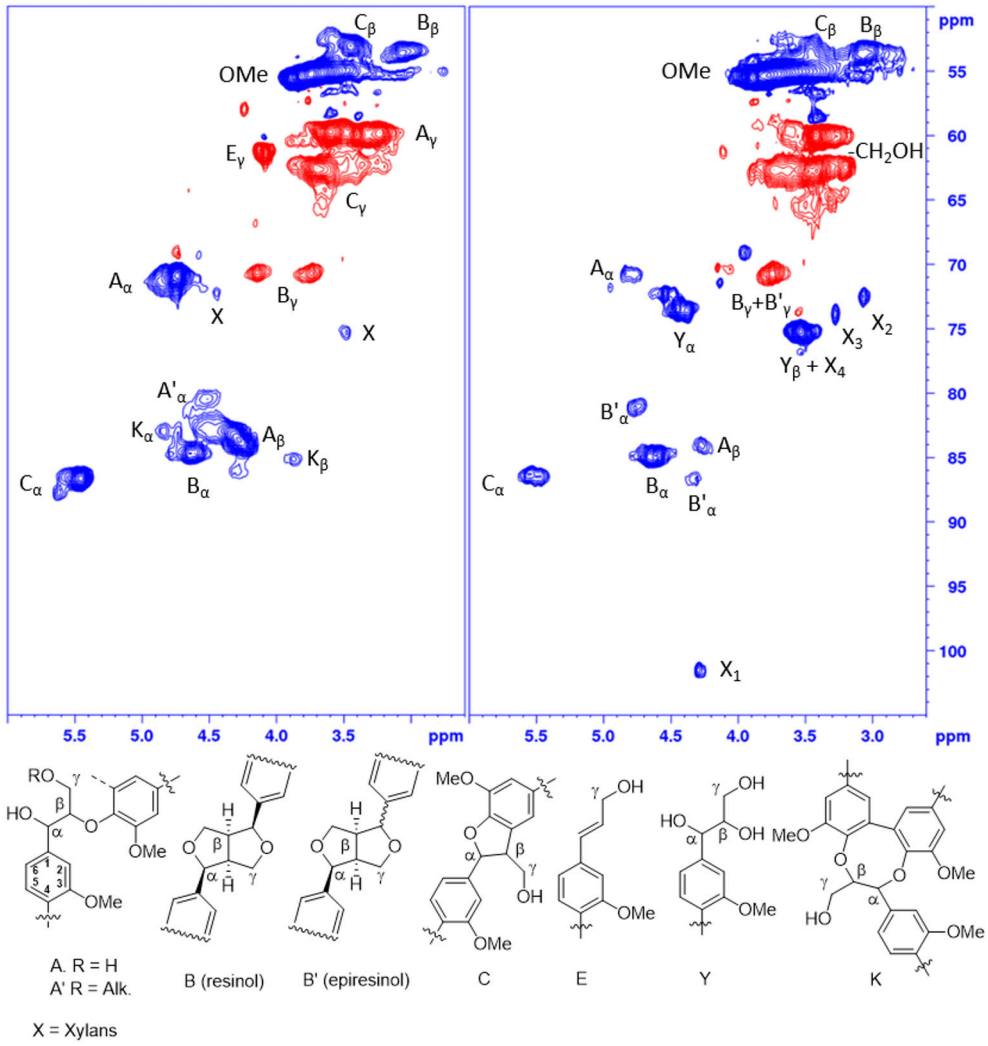

Figure 16. HSQC spectrum of the oxygenated aliphatic area of Spruce MWL (left), Spruce BLN lignin (right), and structures of lignin linkages and end groups (below) CH/CH_3 shown as positive (blue) and CH_2 as negative (red).

This can be attributed to increased heterogeneity of the lignin, which can be caused by several factors such as formation of non-etherified units due to the cleavage of the alkyl-aryl ether bonds. This can be as well seen in chemical shifts of model β-O-4 dimeric lignin compounds,[79] but it is also evident by comparing the ^{13}C NMR spectrum (Figure 9), where the ^{13}C chemical shifts are generally higher for etherified units compared to non-etherified units.[104,194] These results are in agreement with the results from the ^{31}P NMR, which showed an increase of free phenolic hydroxyl groups. Other factors that will affect the chemical shifts of the aromatic signals are condensation reactions to the rings and changes to

the propane side chain (oxidation, cleavage of C_1-C_α etc.).[195,196] The S/G ratio was calculated from both HSQC and ^{13}C NMR, by comparing the integrals of $S_{2,6}$ and $G_{5,6}$ in the birch lignins. The more homogenous MWL showed a more consistent S/G ratio of approximately 2.7 from both NMR experiments, slightly higher than the results from the *py*-GC-MS and ^{31}P NMR. The S/G ratio of the BLN birch lignin was 2.9, calculated from the HSQC spectrum, and a value of approximately 2.0 when calculated from the ^{13}C NMR. The inconsistency of the S/G ratio can be explained by the nature of the more heterogenous BLN lignin, which leads to considerably broader signals in the ^{13}C NMR spectrum that can lead to overlap of the signals and consequently interfere with the integration values. Any type of condensation of the aromatic rings will also affect the ratio due to possible changes in chemical shift of the relevant carbons. Difficulties of adjusting the baseline in the ^{13}C NMR spectrum will also lead to discrepancies in the integration. Some differences between the hardwood and softwoods were that guaiacyl propanol and secoisolariresinol could be detected in the aliphatic region of both the MWL and BLN softwood lignin but not in the hardwood samples. An unidentified structure was also detected in the oxygenated aliphatic region of the HSQC spectrum in the BLN softwood lignin (Figure 16). This was deduced from inconsistencies in integrals of the α-CH in the aryl glycerol subunits and in one of the two γ-CH in the β-β subunit. In the aldehyde region the cinnamyl aldehyde moiety and benzylic aldehyde unit could be detected in the softwood MWL but in the BLN lignin only the benzylic aldehyde correlation peak remained (Figure 17).

Table 5. Amounts (%) of lignin linkages in MWL and BLN lignin.

	β-O-4	β-β (resinol)	β-5
Birch MWL	49	12	3
Birch BLN	4	4	1
Pine MWL	22	6	11
Pine BLN	2	4	2
Spruce MWL	20	7	12
Spruce BLN	1	2	1

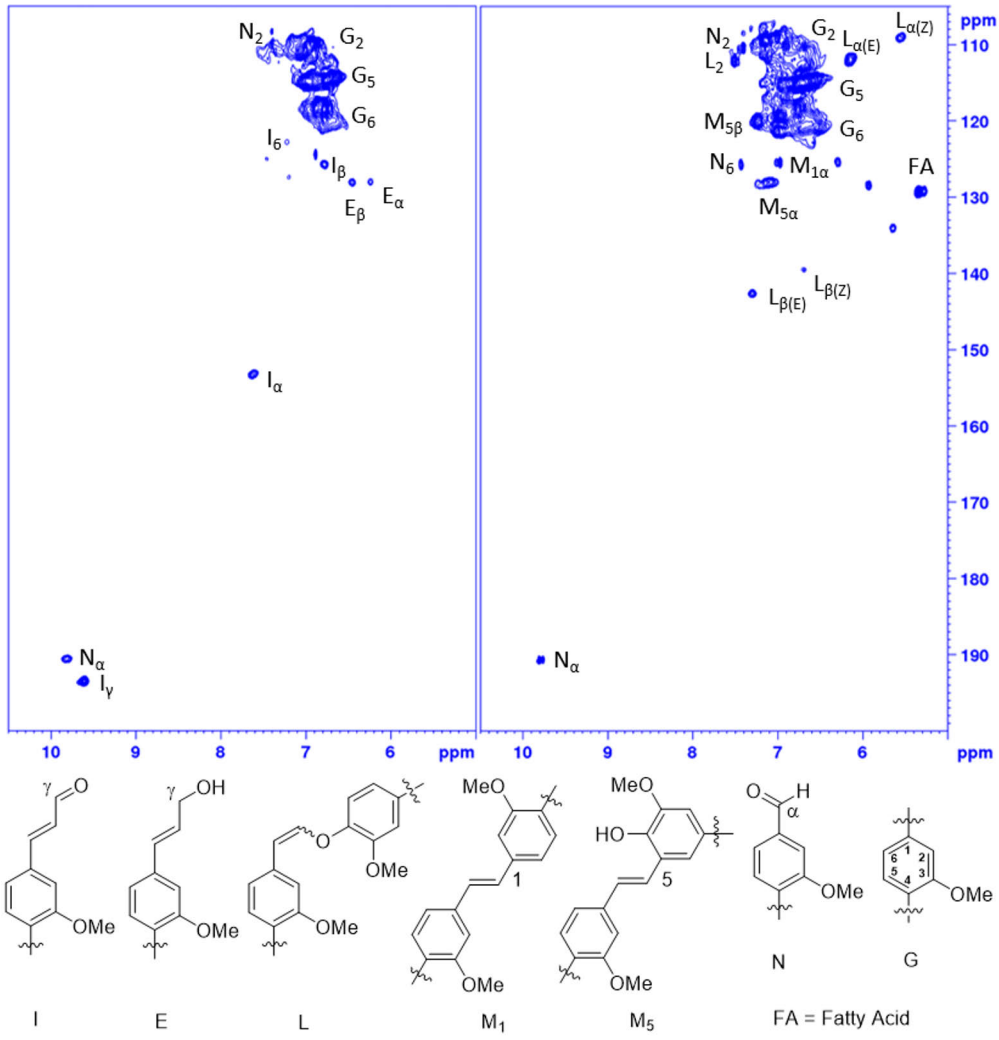

Figure 17. HSQC spectrum of the aromatic area of Spruce MWL (left), Spruce BLN lignin (right), and structures of lignin linkages and end groups (below).

3.4.1. Condensed structures

A broad correlation peak, at approximately δ_C/δ_H (60/3.8-3.3 ppm), was detected in the BLN birch lignin sample but not in the MWL nor in the softwood lignin samples (Figure 15). Correlation peaks in this region are normally assigned as primary alcohols, such as the γ-CH_2OH correlation peak from the β-O-4 linkage or primary alcohols from carbohydrates. However, due to the small amount of α- and β-CH cross-signals the peaks could not be explained entirely by γ-CH_2OH correlation peaks and seemed to be from a new type of structure formed during the process. This anomaly has been observed earlier but has been left unidentified or assumed to be from oligomeric or condensed γ-CH_2OH

units.[197–203] The formation of the correlation peak in the examples correlated with the pretreatment severity, as high temperatures were needed to form these structures in lignin. Multiplicity edited HSQC showed that the correlation peak was from a CH/CH_3, thus not from a primary alcohol, and chemical modification (acetylation or methylation) of the BLN lignin did not affect the chemical shift of the correlation peak either. The peak was analyzed with ^{13}C NMR DEPT experiments (DEPT-135 and DEPT-90) and based on these measurements it was concluded that the peak was a CH_3 group. Due to the relatively high chemical shift of the CH_3 it most probably originated from a methoxy group and not from an aliphatic CH_3. While the ^{13}C NMR chemical shift of methoxy groups in lignin moieties are typically at 56 ppm some uncommon structures in natural products, such as the C_4-OMe from 5-substituted veratryl units (3,4-dimethoxy substituted ring) and the C_5-OMe from C_6-substituted lignans, have been known to have an increased chemical shift (see examples Figure 18a and b).[204–207] In both cases the methoxy group, with an increased chemical shift, has substituents on both of its vicinal aromatic carbons. These types of structures are not naturally occurring in lignin but have been shown to form in sulfuric acid catalyzed condensation reactions with model lignin compounds (see examples Figure 18c and d).[208,209] The mechanism of these types of condensation reaction have been proposed to occur via repolymerization after degradation during autohydrolysis.[200,210] The same increase in ^{13}C chemical shift of the methoxy group can also occur in C_2-substituted guaiacyl units. This can be seen from a study by Kolehmainen et al.[211] who studied the chemical shifts of chlorovanillins with all possible aromatic substitution patterns (mono-, di- and trichlorinated) as well as all three monobrominated vanillin analogues. The ^{13}C chemical shift increase of the methoxy groups occurred in all instances, and only, when there was substitution at the vicinal C_2-position (see examples Figure 18e, f, and g). C_2-condensation was not observed in the BLN softwoods, this might be due to fact that guaiacyl units in lignin prefer the more available C_5 and C_6-positions to C_2-condensation. A secondary structural feature from this condensation pathway is a benzylic C-H between two aryl-units, the chemical shift of this type of benzylic C-H varies greatly depending on the chemical environment and while such a correlation peak was not detected in the HSQC spectrum, an unidentified C-H peak beneath the methoxy peak at 56 ppm was detected in the ^{13}C NMR DEPT 90 experiment, which could potentially originate from such a structure. Whether this is the mechanism of condensation, or the only type of condensation pathway, cannot be concluded from our studies. Considerable amounts of C_5-condensation could be detected in the ^{31}P NMR spectra of the softwoods and as such most likely both ionic and/or radical type mechanisms of condensation are occurring, possibly at the C_α, C_5, or C_6 positions. The shift of the methoxy groups to a higher ppm value

was investigated by comparing two different methods that quantified the amount of methoxy groups in lignin samples. One method used a published procedure that quantified all the methoxy groups in the sample and the other was determined by integrating the methoxy group peak in ^{13}C NMR spectroscopy, using a trioxane internal standard for quantification. When only integrating the methoxy peak at 56 ppm in the ^{13}C NMR method the birch MWL gave similar results between the methods but when analyzing the BLN sample the ^{13}C NMR method gave approximately 10% less methoxy groups, however, when integrating both the peak at 56 ppm and 60 ppm the results were almost identical between the methods.

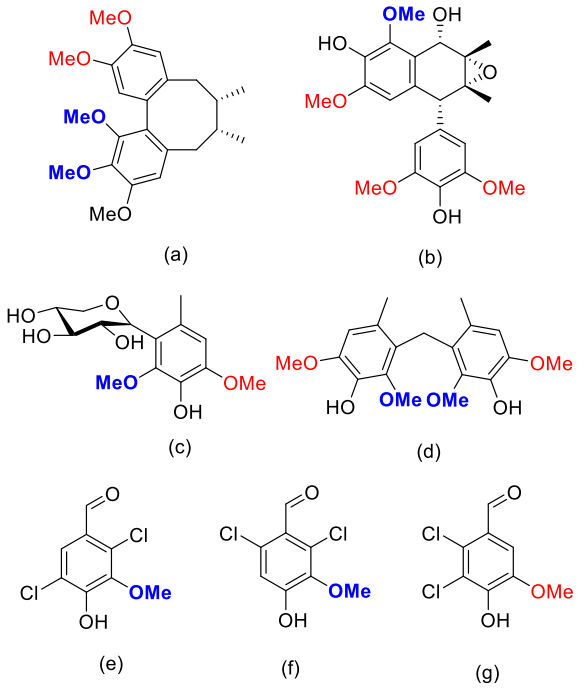

Figure 18. Examples of both natural products and synthetic compounds with different types of methoxy groups. Methoxy groups with substituents on both of its vicinal aromatic carbons in blue.

The premise that the chemical shift of a methoxy group is increased if it has substituents on both of its vicinal aromatic carbons was investigated by methylating the softwood lignin samples. While methylating a guaiacyl unit will yield a veratryl unit (3,4-dimethoxy substituted ring), with both methoxy group having identical chemical shifts, a guaiacyl unit with a condensed C_5-position will yield a methoxy group that has substituents on both of its vicinal aromatic carbons and should increase the chemical shift of the C_4-OMe to 60 ppm. This

would leave a similar correlation pattern as the birch sample. A method for selectively methylating the phenolic hydroxyl groups was used for the modification and to ensure that the formed methoxy group was not an aliphatic methyl ether group a different method that methylated all hydroxyl groups and acids was also used. From Figure 19 it can be seen, that compared to the starting material no other peaks besides the newly formed peak at 60 ppm is altered, however, in the fully methylated sample all the correlation peaks, besides the β-β signals that lack hydroxyl groups, were shifted to a higher ^{13}C chemical shift due to the methylation of the aliphatic hydroxyl groups. The methyl ester group and the aliphatic methyl ether groups were also clearly detected separately from the phenolic hydroxyl groups.

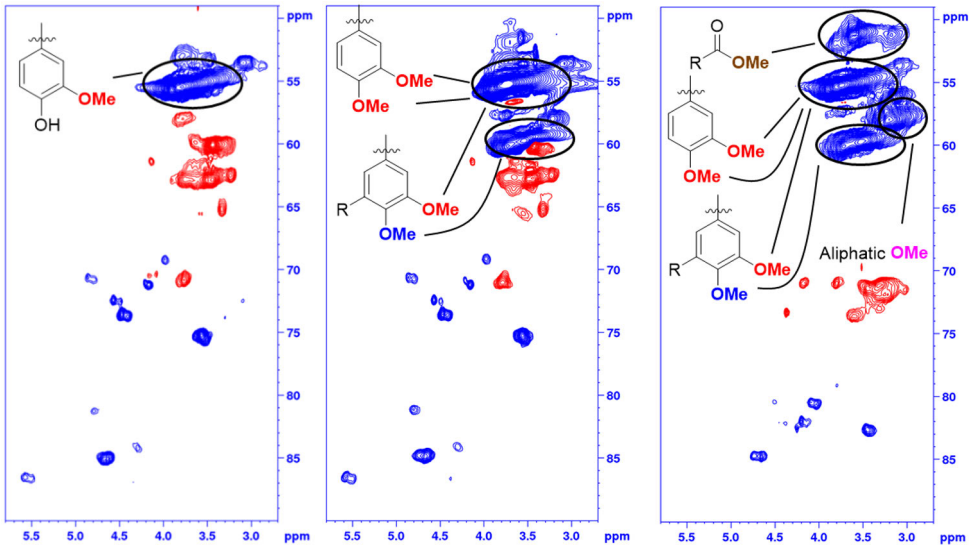

Figure 19. Multiplicity edited HSQC of the oxygenated aliphatic area of unmodified pine BLN lignin (left), pine BLN lignin with methylated phenolic hydroxyl groups (mid) and fully methylated pine BLN lignin (right). CH/CH_3 shown as positive (blue) and CH_2 as negative (red). Image from paper II.

3.4.2. Model compounds

To investigate how the substitution at the C_6-position affects the chemical shifts of the methoxy groups a small library of C_6-condensed syringylic model compounds was prepared (Figure 20). The synthesized model compounds were prepared from either syringyl methoxy methyl or syringyl aldehyde and had different substituents (aliphatic, carboxylic, phenylic, two benzylic alcohols with different -OMe substitution patterns and brominated) at the C_6-position.

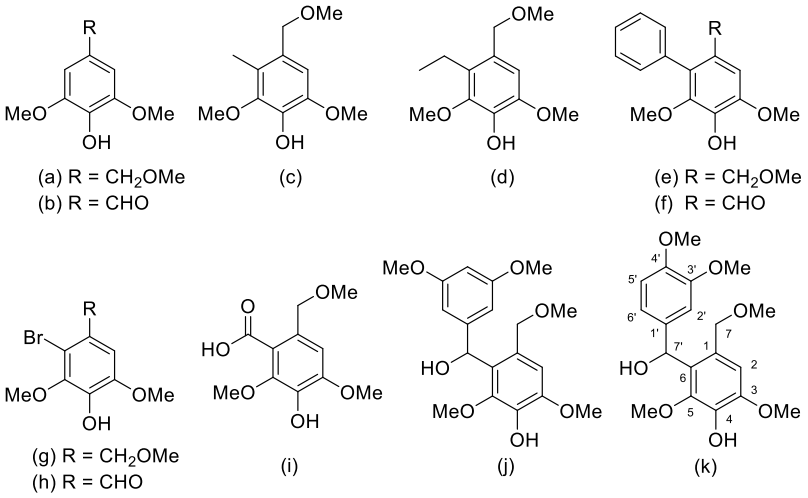

Figure 20. Structures of lignin model compounds.

In this way effects of the substitution could be seen and if the increase in chemical shift of the methoxy group only occurs with certain substituents. All the model compounds were synthesized, except the brominated and phenylated substrates, by a methodology developed by Costa and Saa.[168] The method proceeds by lithiation of the C_6-position with *n*-BuLi prior to the addition of the subsequent electrophile. The phenylated compounds were prepared by a Suzuki-coupling with phenyl boronic acid and brominated starting materials (Scheme 8).[171]

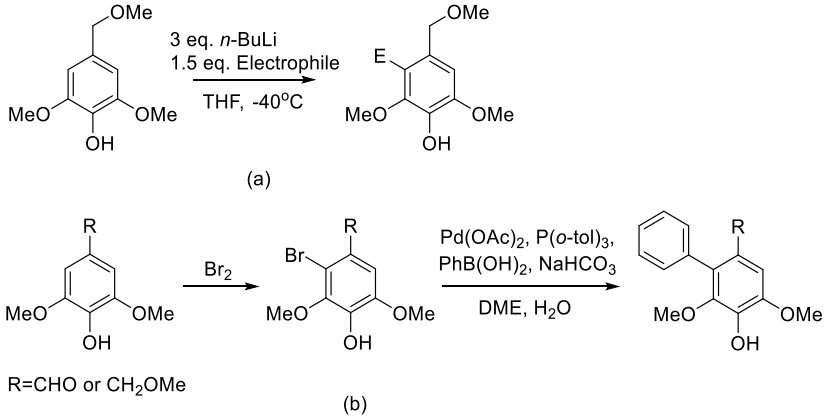

Scheme 8. Reaction scheme of the synthesis of 6-condensed model compounds. Lithiation (a), bromination and Suzuki-coupling (b).

From Figure 21 (cluster 2) it can be seen that all C_6-substituents caused an increase in the ^{13}C chemical shift, to a narrow (60.1-59.5 ppm) range of the C_5-OMe groups vicinal to the C_6-substitution. The ^{13}C chemical shifts of the aromatic

C_3-OMe (Figure 21 cluster 1) δ_C (56.1-55.8ppm) in the C_6-substituted rings were largely unaffected by the substitution and the methoxy groups of the aryl side chains in compounds Figure 20j (3,5-dimethoxy) and Figure 20k (3,4-dimethoxy) had a slightly lower chemical shift of ~55.0 ppm compared to the other methoxy groups (see top structures in Figure 21), due to the lack of the phenol functionality in these aromatic moieties. The aliphatic/benzylic C_7-OMe (Figure 21 cluster 3) δ_C/δ_H (57.7-57.2/3.32-3.10 ppm) did not overlap with the other methoxy group correlation peaks and the ^{13}C chemical shift was also largely unaffected by the substitution. The main differences in the ^{1}H NMR chemical shifts of the C_5-OMe groups was that the compounds with phenyl substituents (Figure 20e & f) had a lower chemical shift δ_H (3.38-3.44 ppm) compared to the other C_5-OMe groups (see bottom structure in Figure 21). This could potentially be used for discriminating between aryl-aryl and other 6-condensed bonds. Aryl-aryl bonds can be formed by radical coupling reactions between two lignin moieties at the C_2, C_5 and C_6 positions. Giummarella et al.[51,212] showed free C_1-H can form by retro aldol reactions in kraft lignin and consequently also form bonds between C_6-C_1 positions. The ^{13}C chemical shifts of C_1, C_2, C_3 and C_5 were affected by approximately 5 ppm by the C_6-substitution, however, the ^{13}C chemical shifts of C_6 varied greatly between the different substituents, methyl (Figure 20c) gives the lowest ppm value of 122.0 ppm, and the phenyl substituted (Figure 20f) the highest 134.4 ppm of the C_6-C substituents. This broad spread of the ^{13}C chemical shifts is consistent with ^{13}C NMR spectrum of the BLN lignin and makes it difficult to quantify the C_6-substituition based on the ^{13}C NMR peaks due to the general broadening of the peaks in the aromatic region. The benzylic alcohols (Figure 20j and k) from the condensation of the syringyl ring to an aldehyde was used as model for compounds that yield a benzylic carbon that is bonded to two aryl substituents. While these benzylic alcohols are unlikely in lignin motifs, other similar types of motifs such as that of the condensation of an aromatic ring and a benzyl carbocation/quinone methide could be formed during pulping processes. The chemical shifts of these types of benzylic C-H can vary quite drastically depending on the chemical environment as seen in other similar benzylic C-H motifs reported in literature, such as the condensation of an aromatic ring to a benzyl carbocation or the condensation reaction with formaldehyde (Figure 22).[49,213] Yasuda and Ota[209] reported similar structures with C_6-condensed syringyl moieties with similar chemical shifts of the benzylic C-H as seen in Figure 22, as there were no clear correlation peaks in BLN birch lignin sample at these chemical shifts the structures could not be detected. They cannot either explain the peak beneath the methoxy group detected by the ^{13}C NMR DEPT experiments. The aliphatic (Figure 20c and d) and carboxylic substituents

(Figure 20i), or similar type of structures, could potentially be C_6-substituents in the lignin as the correlation peaks of the aliphatic C-H could be overlapped with other aliphatic signals in the HSQC-spectrum and ^{31}P NMR spectroscopy showed an increase in carboxylic groups. However, it is difficult to determine a reaction mechanism of the formation of these hypothetical structures.

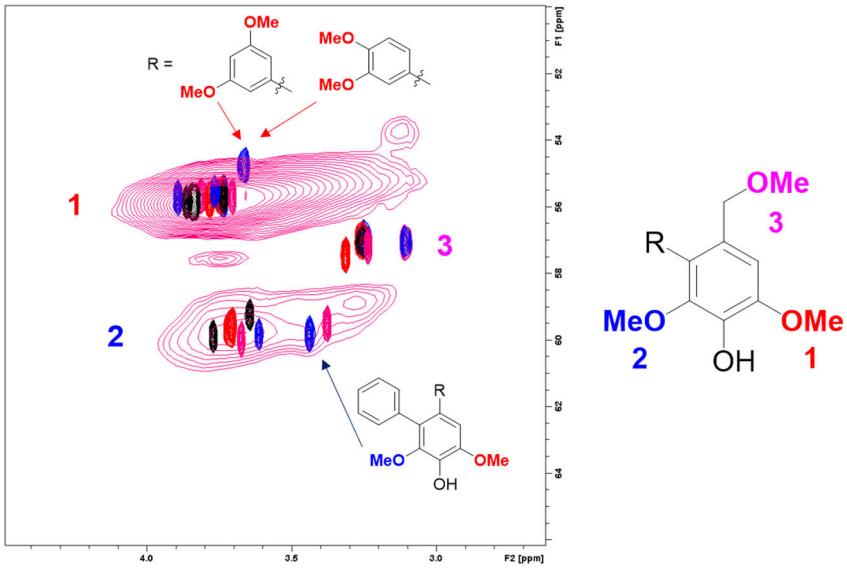

Figure 21. HSQC of the methoxy group correlation peaks. The top cluster (1) is from aromatic methoxy groups, the bottom cluster (2) is from C_5-methoxy groups next to C_6-substitution, the right cluster (3) is from benzylic methoxy groups, and the broad correlation peaks are from birch BLN lignin.

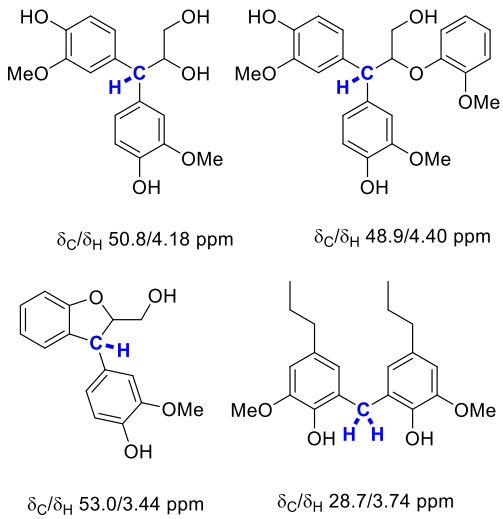

Figure 22. Structures and chemical shifts of benzylic C-H that is bonded to two aryl substituents.

3.5. MTBE and *i*-PrOH fractions

The MTBE-soluble fractions, approximately 15-20 wt% of the crude lignin (Scheme 7), was analyzed with HPSEC, ^{1}H NMR, ^{31}P NMR, ^{13}C NMR and 2D NMR. Birch MTBE soluble fraction was also analyzed with short column GC and GC-MS. It was concluded that the MTBE soluble compounds had lower molar mass than the insoluble lignin fraction and the extraction could remove the majority of the monomeric to oligomeric compounds (Table 1). From the ^{31}P NMR experiments (Table 3) it could be seen that the fraction contained considerably less aliphatic hydroxyl group and had been enriched with carboxylic groups in all three lignin samples. From the ^{1}H NMR, ^{13}C NMR and 2D NMR experiments a large amount of aliphatic and aromatic signal could be detected, most of these likely arise from lignin degradation products and extractives. Broad aromatic and methoxy group signals were also detected and can be from low molar mass lignin fragments. No correlation peaks from traditional lignin linkages could be detected in the samples except the correlation peaks from the β-β linkage. This indicates that the fragments are mainly bonded by condensed C-C bonds. This assumption is supported by the detection of the characteristic peak at δ_C 60 ppm in the birch sample. The short column GC analysis of the birch sample detected small amounts of 4-hydroxybutanoic acid and furfuryl alcohol, which could be carbohydrate degradation products, also lignin degradation products syringyl aldehyde and syringaresinol, and fatty acids were identified (Figure 23). The majority of the ~95 wt% of the sample was unidentified, broad baseline signals were detected and these could originate from heterogeneous lignin di- and

trimers. The GC-MS analysis showed similar results (carbohydrate and lignin degradation products, and fatty acids) and helped identifying more of the compounds than the short column GC.

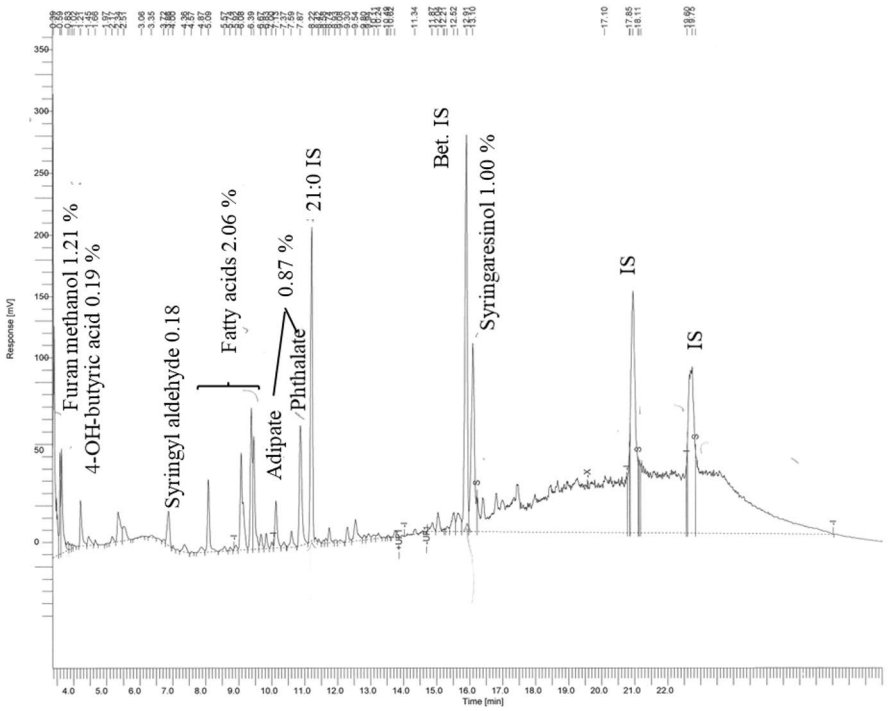

Figure 23. Short column GC of MTBE-soluble birch lignin fraction.

The BLN softwood lignins were fractionated with *i*-PrOH in an attempt to produce a more homogeneous fraction by simple solvent fractionation. By stirring the BLN lignin in *i*-PrOH and decanting of the solvent a *i*-PrOH insoluble (~70 wt%) and a *i*-PrOH soluble (~30 wt%) fraction could be collected. The M_w cut off was at approximately 1500 $gmol^{-1}$ based on HPSEC, yielding a high molar mass *i*-PrOH insoluble fraction and a lower molar mass *i*-PrOH soluble fraction, both fractions with narrow Đ values (Table 1). Structurally *i*-PrOH soluble fraction contained slightly lower amounts of aliphatic hydroxyl groups and carboxylic acids, and slightly higher amount of free phenolic groups than *i*-PrOH insoluble fraction based on ^{31}P NMR spectroscopy (Table 3).

3.6. ^{31}P NMR method development

The quantitative determination of hydroxyl groups in lignin by ^{31}P NMR spectroscopy was heavily used during the analysis of lignin from the CH-Bioforce process. During this time, a pulse length-based concentration determination (PULCON) methodology was investigated whether it could be applied for the ^{31}P

NMR spectroscopic method. PULCON is an established quantification method in biosciences and has been used to measure concentrations of biomolecules (e.g. proteins) and pharmaceuticals in complex mixtures.[214,215] The concentration determination by PULCON is based on the fact that the signal strength obtained with an NMR probe is inversely proportional to the 90° pulse length for the probe. By keeping experimental parameters identical between an unknown sample and an external reference sample the concentration of the unknown sample can be calculated according to:

$$c_u = c_r \frac{S_u \theta_u^{90}}{S_r \theta_r^{90}}$$

Where c stands for concentration, S for signal intensity and θ^{90} is the length of the 90° pulse. The subscripts u and r denote the sample of unknown concentration and reference sample (external standard), respectively. As such PULCON is capable of correlating signal intensities of two different spectra and does not need an internal standard. In practice this means that external standard can be used for the quantification of hydroxyl groups. This simplifies the sample preparation and eliminates problems associated with the use of an IS, such as overlapping signals, stability of the IS, and potential data processing errors regarding the IS signal. It was also investigated if the procedure could be simplified by using automated functions in the NMR software for optimization of the 90° pulse. The drawback of using PULCON methodology is slightly longer experimental times due to the need of calibrating the 90 °pulse and re-measuring the external standard at regular intervals.

First, the experimental parameters were determined and their effect on quantification was investigated. Here the signal intensity dependency on the receiver gain was investigated, the T_1 relaxation of the small-molecular samples were measured with and without relaxing agent so that a sufficiently long recycle delay could be determined and the phosphitylation reaction was investigated to ensure a complete derivatization of the lignin samples. For the concentration determination four, different methods were compared:

(1) The traditional method by calculating the concentration from the e-HNDI IS.

(2) The PULCON method when the 90° pulse was manually calibrated and the phosphitylated e-HNDI was used as an external standard.

(3) The PULCON method when the program pulsecal for automatic 90° pulse calibration was used with phosphitylated e-HNDI as an external standard.

(4) The PULCON method when the 90° pulse was manually calibrated and 0.0485 M triphenyl phosphate (TPP) in acetone-d6 was used as external standard. TPP is Bruker's ^{31}P standard and comes in a sealed sample that should be available for users of Bruker instruments, as such it is a good and stable external standard that is readily available.

The first comparison was done on six samples containing varying amount (1.0, 2.0, 5.0, 10.0, 15.0 and 20.0 mg) of vanillyl alcohol (VA). The known concentrations were then calculated with the four different concentration determination methods. All four methods had similar results, within <5% of the measured amount. The first method (1) gave slightly higher than the measured results for the samples with higher concentration of VA. This could be due to many factors that can influence the integration value of the IS peak, such as errors in measurement, the baseline, phase correction, integration range and S/N. However, the concentrations of these samples were considerably higher than what is used for lignin samples. A second comparison experiment was then conducted to calculate the amount of hydroxyl groups in VA (10.0 mg), BLN pine lignin (10, 20, 30 mg) and BLN birch lignin (20 mg) using concentration determination methods (1), (2), and (4) (Table 6). The results determined by PULCON were within the degree of accuracy of which was determined by the internal standard. The automated PULCON method was then verified by analyzing triplicate samples of both pine and birch lignin using TPP as external standard to ensure the reproducibility of the method. This makes the PULCON method a viable alternative for the hydroxyl group determination of lignin samples.

Table 6. Comparison of the amount of hydroxyl groups (in mmol/g) calculated from e-HNDI IS, PULCON with phosphitylated e-HNDI as external standard and PULCON with triphenyl phosphate (TPP) as external standard.

Method[1]	Substrate	Aliphatic[2]	5-sub[3]	G-units[4]	COOH[5]
1	VA (10.0 mg)[6]	6.5	-	6.7	-
2	VA (10.0 mg)[6]	6.4	-	6.5	-
4	VA (10.0 mg)[6]	6.2	-	6.4	-
1	Pine lignin (10 mg)	1.6	1.4	1.4	0.4
2	Pine lignin (10 mg)	1.5	1.3	1.3	0.4

4	Pine lignin (10 mg)	1.4	1.3	1.3	0.4
1	Pine lignin (20 mg)	1.8	1.7	1.6	0.5
2	Pine lignin (20 mg)	1.7	1.6	1.5	0.4
4	Pine lignin (20 mg)	1.6	1.5	1.5	0.4
1	Pine lignin (30 mg)	1.8	1.7	1.7	0.4
2	Pine lignin (30 mg)	1.6	1.6	1.5	0.4
4	Pine lignin (30 mg)	1.6	1.5	1.5	0.4
1	Birch lignin (20 mg)	1.1	2.5	0.6	0.4
2	Birch lignin (20 mg)	1.0	2.2	0.5	0.4
4	Birch lignin (20 mg)	0.9	2.2	0.5	0.4

[1] Manually calibrated 90° pulse, [2] (150.0-145.0 ppm), [3] (145.0-140.3 ppm), [4] (140.3-137.0 ppm), [5] (136.0-134.0 ppm), [6] theoretical value 6.5 mmol/g for each hydroxyl group.

4. Conclusions and prospects

4.1. Conclusions

The majority of the low molar mass compounds “impurities” could be removed from the precipitated lignin by MTBE-fractionation. The MTBE soluble fraction contained extractives, carbohydrate- and lignin degradation products, as well as heterogenous lignin fragments (M_n < 1000 Da). Small amounts of fatty acids and carbohydrates could still be detected in the isolated MTBE insoluble lignin fraction. The lignin was structurally altered compared to MWL from the same wood chips. The traditionally occurring alkyl-aryl ether linkages were reduced based on ^{13}C NMR and HSQC experiments. Results from the quantitative determination of hydroxyl groups by ^{31}P NMR spectroscopy showed a decrease in aliphatic hydroxyl groups and an increase in phenolic hydroxyl groups and carboxylic groups, elemental analysis showed an enrichment of carbon and decrease in oxygen. Several structural features were detected by NMR spectroscopy that were formed during the process such as aryl glycerol end group, enol ether and stilbene linkages, and evidence of condensation at both 5-

and 6-position on the aromatic ring. Due to all of these structural features it can be concluded that the lignin can be considered a technical lignin, similar to that of kraft lignin but without incorporated sulfur and with some different structural features. A tentative structure of BLN softwood lignin can be seen in Figure 24, with most of the detected structural features present. A previously unassigned HSQC correlation peak was identified as a so-called condensed structure in birch lignin. It was concluded that the correlation peak originated from a methoxy group that was vicinal to a condensed position in the aromatic ring. This type of structure has a methoxy group with two vicinal neighboring groups and causes its ^{13}C NMR chemical shift to increase from ~56 to ~60 ppm. This was deduced by comparing the chemical shift to molecules with the same structural motif from literature but also by synthesizing model compounds with the motif; analyzing the correlation peak and its ^{13}C NMR peak with DEPT experiments; comparing the quantitative amounts of methoxy groups based on different methods; chemically modifying lignin and comparing the chemical shifts to unmodified lignin. The lignin was also analyzed with TGA and it was concluded that the thermal decomposition temperature started at ~300 °C and the char residue at 600°C was ~50 wt%. Methylation of the phenolic hydroxyl groups increased the $T_{dst\ 95\%}$ by ~5% and acetylation decreased the $T_{dst\ 95\%}$ by ~15-30%. In this thesis we also showed that a PULCON methodology could be applied to the quantitative hydroxyl group determination in lignin by ^{31}P NMR spectroscopy. The method allows for the use of an external standard and therefore removes the problems associated with the use of an IS.

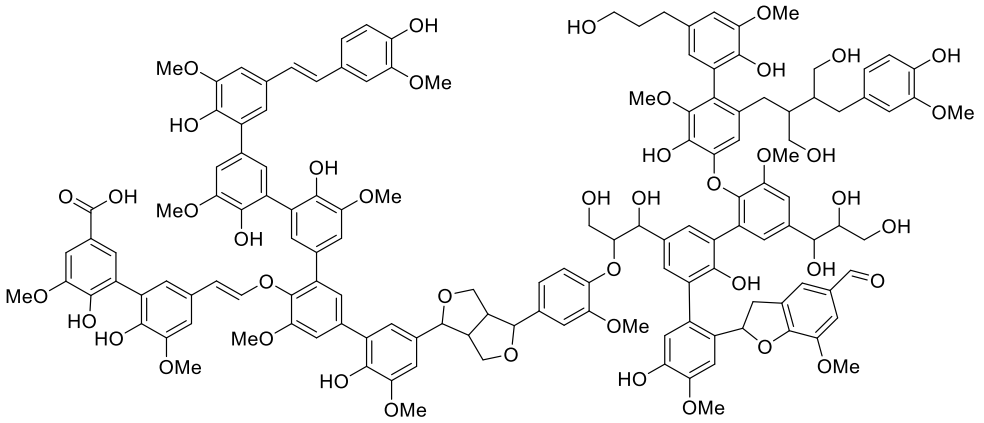

Figure 24. A tentative structure of BLN softwood lignin.

4.2. Prospects

The knowledge of lignin chemistry and analysis obtained during this thesis has already been applied to different projects. In supporting publication V Dr. A. Sokolov studied the non-thermal gas-phase pulsed corona discharge for lignin modification. Here we supplied the BLN lignin and then received the reactions mixture after the modifications. We then developed a lignin isolation protocol and analyzed the modified lignin. In supporting publication VII PhD student L. Wang studied the BLN lignin as a thermosetting lignin containing phenol-formaldehyde wood adhesive. Here she used, and further developed, the *i*-PrOH fractionation methodology by sequentially precipitated lignin fractions with different alcohols (*i*-PrOH, EtOH and MeOH), to obtain several homogenous fractions with increasing molar masses. These fractions could then be used to study the structure-performance correlation when using lignin in wood adhesive formulations. In this publication we assisted with analysis and took part in the discussions during the projects course. In supporting publication X Dr. X. Lu studied the reductive catalytic depolymerization of the BLN birch lignin and in this project, we were also actively taking part in analysis and discussions. In supporting publication IV & IX we assisted with analysis of lignin and other natural products, and in supporting publication VIII we assisted in discussions and planning synthetic methods of the lignan α-conidendrin.

The collaboration with the company CH-Bioforce Oy, as well as other companies, has continued in different industrial projects where we have performed analysis and various chemical modifications to modify the properties of lignin for different applications.

The PULCON methodology for the quantification of hydroxyl groups in lignin with ^{31}P NMR could find its use in routine measurements. The established method uses an internal standard for the quantification and there can be some reluctance to changing standard operational procedures, however, there are examples when PULCON could be applied e.g. for companies that need to prepare their samples in their facilities and then analyze the samples elsewhere or in laboratories that seldom use the analysis method and as such reduces the need of preparing an IS-standard solution, as these need to be redone at regular time intervals.

The identification of the condensed structure by NMR spectroscopy can be used for characterization of technical hardwood lignin. A wide variety of structural features in both native and technical lignin can already be identified and quantified in routine spectroscopic measurements. As such, it is important to

identify new structural features to be added to the already large library of lignin moieties to be able to describe different types of lignin. Technical lignin is especially difficult to characterize as many of the well-known alkyl aryl ether linkages are degraded and many of the proposed formed structures contain tertiary carbons. These structures cannot be detected by HSQC and are usually buried beneath the high abundance of aromatic peaks in ^{13}C NMR spectroscopy. Much of the current research on the structure of technical lignin has been performed on softwood lignin but now with the increased use of different types of lignocellulosic biomass, such as the hardwood *Eucalyptus grandis,* increases the importance of understanding syringyl containing technical lignins.

References

1. Ragauskas, A. J. *et al.* The path forward for biofuels and biomaterials. *Science (80-.).* **311**, 484–489 (2006).
2. de Jong, E. & Jungmeier, G. *Biorefinery Concepts in Comparison to Petrochemical Refineries*. *Industrial Biorefineries and White Biotechnology* (2015). doi:10.1016/B978-0-444-63453-5.00001-X.
3. de Jong, E., Higson, A., Walsch, P. & Wellisch, M. Bio-Based Chemicals: Value Added Products from Biorefineries. *In: IEA Bioenergy Task 42 report 2012* 1-36 date accessed 2019-05–29 https://www.ieabioenergy.com/wp-content/uploads/2013/10/Task-42-Biobased-Chemicals-value-added-products-from-biorefineries.pdf (2013).
4. Cherubini, F. *et al.* Toward a common classification approach for biorefinery systems. *Biofuels, Bioprod. Biorefining* **3**, 534–546 (2009).
5. Chambost, V. & Stuart, P. Selecting the most appropriate products for the forest biorefinery. *Ind. Biotechnol.* **3**, 112–119 (2007).
6. Menon, V. & Rao, M. Trends in bioconversion of lignocellulose: Biofuels, platform chemicals & biorefinery concept. *Prog. Energy Combust. Sci.* **38**, 522–550 (2012).
7. Habibi, Y., Lucia, L. A. & Rojas, O. J. Cellulose Nanocrystals: Chemistry, Self-Assembly, and Applications. *Chem. Rev.* **110**, 3479–3500 (2010).
8. Rubin, E. M. Genomics of cellulosic biofuels. *Nature* **454**, 841–845 (2008).
9. Scheller, H. V. & Ulvskov, P. Hemicelluloses. *Annu. Rev. Plant Biol.* **61**, 263–289 (2010).
10. Åkerholm, M. & Salmén, L. Interactions between wood polymers studied by dynamic FT-IR spectroscopy. *Polymer (Guildf).* **42**, 963–969 (2001).
11. Kang, X. *et al.* Lignin-polysaccharide interactions in plant secondary cell walls revealed by solid-state NMR. *Nat. Commun.* **10**, 1–9 (2019).
12. Nishimura, H., Kamiya, A., Nagata, T., Katahira, M. & Watanabe, T. Direct evidence for α ether linkage between lignin and carbohydrates in wood cell walls. *Sci. Rep.* **8**, 1–11 (2018).
13. Zakzeski, J., Bruijnincx, P. C. A., Jongerius, A. L. & Weckhuysen, B. M. The Catalytic Valorization of Lignin for the Production of Renewable Chemicals. *Chem. Rev.* **110**, 3552–3599 (2010).
14. Vanholme, R., Demedts, B., Morreel, K., Ralph, J. & Boerjan, W. Lignin Biosynthesis and Structure. *Plant Physiol.* **153**, 895–905 (2010).
15. Dimmel, D. R. Overview. in *Lignin and Lignans Advances in Chemistry* (eds. Heitner, C., Dimmel, D. R. & Schmidt, J. A.) 1–10 (CRC Press, Taylor & Francis, 2010).
16. Capanema, E. A., Balakshin, M. Y. & Kadla, J. F. A Comprehensive Approach for Quantitative Lignin Characterization by NMR Spectroscopy. *J. Agric. Food Chem.* **52**, 1850–1860 (2004).
17. Balakshin, M., Capanema, E., Gracz, H., Chang, H. min & Jameel, H. Quantification of lignin-carbohydrate linkages with high-resolution NMR spectroscopy. *Planta* **233**, 1097–1110 (2011).
18. Calvo-Flores, F. G., Dobado, J. A., Isac-García, J. & Martín-Martínez, F. J. *Lignin and lignans as renewable raw materials*. (Wiley, 2015).
19. Giummarella, N., Pu, Y., Ragauskas, A. J. & Lawoko, M. A critical review on the analysis of lignin carbohydrate bonds. *Green Chem.* **21**, 1573–1595 (2019).
20. Xie, Y., Yasuda, S., Wu, H. & Liu, H. Analysis of the structure of lignin-carbohydrate complexes by the specific 13C tracer method. *J. Wood Sci.* **46**, 130–136 (2000).
21. Björkman, A. Lignin and Lignin-Carbohydrate Complexes Extraction from Wood Meal with Neutral Solvents. *Ind. Eng. Chem.* **49**, 1395–1398 (1957).

22. Adler, E., Miksche, G. & Brown, W. Comparative studies on cellulolytic enzyme lignin and milled wood lignin of sweetgum and spruce. *Holzforschung* **29**, 153–159 (1975).

23. Capanema, E., Balakshin, M., Katahira, R., Chang, H. M. & Jameel, H. How well do MWL and CEL preparations represent the whole hardwood lignin? *J. Wood Chem. Technol.* **35**, 17–26 (2014).

24. Hu, Z., Yeh, T. F., Chang, H. M., Matsumoto, Y. & Kadla, J. F. Elucidation of the structure of cellulolytic enzyme lignin. *Holzforschung* **60**, 389–397 (2006).

25. Guerra, A., Filpponen, I., Lucia, L. A. & Argyropoulos, D. S. Comparative evaluation of three lignin isolation protocols for various wood species. *J. Agric. Food Chem.* **54**, 9696–9705 (2006).

26. Zinovyev, G., Sumerskii, I., Rosenau, T., Balakshin, M. & Potthast, A. Ball milling's effect on pine milled wood lignin's structure and molar mass. *Molecules* **23**, 1–10 (2018).

27. Chakar, F. S. & Ragauskas, A. J. Review of current and future softwood kraft lignin process chemistry. *Ind. Crops Prod.* **20**, 131–141 (2004).

28. Dessbesell, L., Paleologou, M., Leitch, M., Pulkki, R. & Xu, C. (Charles). Global lignin supply overview and kraft lignin potential as an alternative for petroleum-based polymers. *Renew. Sustain. Energy Rev.* **123**, 109768 (2020).

29. Tomani, P. The lignoboost process. *Cellul. Chem. Technol.* **44**, 53–58 (2010).

30. Kouisni, L., Holt-Hindle, P., Maki, K. & Paleologou, M. The LignoForce System™: A new process for the production of high-quality lignin from black liquor. *Pulp Pap. Canada* **115**, 18–22 (2014).

31. Watt, C. & Burgess, H. Patent No. 1448 and 1449. (1854).

32. Lora, J. H. Industrial commercial lignins: Sources, properties and applications. in *Monomers, Polymers and Composites from Renewable Resources* (eds. Balgacem, M. N. & Gandini, A.) 225–241 (Elsevier, 2008). doi:10.1016/B978-0-08-045316-3.00010-7.

33. Verardi, A., De Bari, I., Ricca, E. & Calabrò, V. Hydrolysis of Lignocellulosic Biomass: Current Status of Processes and Technologies and Future Perspectives. in *Bioethanol* (ed. Lima, M. A. P.) 95–122 (IntechOpen, 2012). doi:10.5772/23987.

34. Wang, H., Pu, Y., Ragauskas, A. & Yang, B. From lignin to valuable products–strategies, challenges, and prospects. *Bioresour. Technol.* **271**, 449–461 (2019).

35. Rabinovich, M. L. Lignin by-products of Soviet hydrolysis industry: Resources, characteristics, and utilization as a fuel. *Cellul. Chem. Technol.* **48**, 613–631 (2014).

36. Mussatto, S. I. *Biomass Fractionation Technologies for a Lignocellulosic Feedstock Based Biorefinery*. (Elsevier, 2016). doi:10.1016/C2014-0-01890-4.

37. Wei Kit Chin, D., Lim, S., Pang, Y. L. & Lam, M. K. Fundamental review of organosolv pretreatment and its challenges in emerging consolidated bioprocessing. *Biofuels, Bioprod. Biorefining* **14**, 808–829 (2020).

38. Rodríguez, A. *et al.* Different Solvents for Organosolv Pulping. in *Pulp and Paper Processing* (ed. Kazi, S. N.) 33–54 (IntechOpen, 2018). doi:10.5772/intechopen.79015.

39. Zhao, X., Cheng, K. & Liu, D. Organosolv pretreatment of lignocellulosic biomass for enzymatic hydrolysis. *Appl. Microbiol. Biotechnol.* **82**, 815–827 (2009).

40. Mesa, L., Albernas, Y., Morales, M., Corsano, G. & Gonza, E. Biomass Pretreatment in a Biorefinery. in *Biomass Fractionation Technologies for a Lignocellulosic Feedstock Based Biorefinery* (ed. Mussatto, S. I.) 229–254 (Elsevier, 2016).

41. Pye, E. K. & Lora, J. H. The Alcell process : a proven alternative to kraft pulping. *Tappi J.* **74**, 113–118 (1991).

42. Arato, C., Pye, E. K. & Gjennestad, G. The lignol approach to biorefining of woody biomass to produce ethanol and chemicals. *Appl. Biochem. Biotechnol. - Part A Enzym. Eng. Biotechnol.* **123**, 871–882 (2005).

43. Chempolis. Chempolis Seals Deal for Indian Biorefinery. Date accessed 2021-12-01

https://chempolis.com/chempolis-seals-deal-for-indian-biorefinery/ (2018).

44. Schutyser, W. *et al.* Chemicals from lignin: An interplay of lignocellulose fractionation, depolymerisation, and upgrading. *Chem. Soc. Rev.* **47**, 852–908 (2018).

45. Rinaldi, R. *et al.* Paving the Way for Lignin Valorisation: Recent Advances in Bioengineering, Biorefining and Catalysis. *Angew. Chemie - Int. Ed.* **55**, 8164–8215 (2016).

46. Gierer, J. Chemistry of delignification - Part 1: General concept and reactions during pulping. *Wood Sci. Technol.* **19**, 289–312 (1985).

47. Gellerstedt, G. Chemistry of Chemical Pulping. in *Pulping Chemistry and Technology : Pulping Chemistry and Technology* (eds. Ek, M., Gellerstedt, G. & Henriksson, G.) 91–120 (De Gruyter, Inc., 2009).

48. Balakshin, M. Y. & Capanema, E. A. Comprehensive structural analysis of biorefinery lignins with a quantitative ^{13}C NMR approach. *RSC Adv.* **5**, 87187–87199 (2015).

49. Lancefield, C. S., Wienk, H. J., Boelens, R., Weckhuysen, B. M. & Bruijnincx, P. C. A. Identification of a diagnostic structural motif reveals a new reaction intermediate and condensation pathway in kraft lignin formation. *Chem. Sci.* **9**, 6348–6360 (2018).

50. Miles-Barrett, D. M. *et al.* The synthesis and analysis of lignin-bound Hibbert ketone structures in technical lignins. *Org. Biomol. Chem.* **14**, 10023–10030 (2016).

51. Giummarella, N., Pylypchuk, I. V., Sevastyanova, O. & Lawoko, M. New Structures in Eucalyptus Kraft Lignin with Complex Mechanistic Implications. *ACS Sustain. Chem. Eng.* **8**, 10983–10994 (2020).

52. Crestini, C., Lange, H., Sette, M. & Argyropoulos, D. S. on the Structure of Softwood Kraft Lignin. *Green Chem.* **19**, 4104–4121 (2017).

53. Karhunen, P., Mikkola, J., Pajunen, A. & Brunow, G. The behaviour of dibenzodioxocin structures in lignin during alkaline pulping processes. *Nord. Pulp Pap. Res. J.* **14**, 123–128 (1999).

54. West, E., MacInnes, A. S. & Hibbert, H. Studies on Lignin and Related Compounds. LXIX. Isolation of 1-(4-Hydroxy-3-methoxyphenyl)-2-propanone and 1-Ethoxy-1-(4-hydroxy-3-methoxyphenyl)-2-propanone from the Ethanolysis Products of Spruce Wood. *J. Am. Chem. Soc.* **65**, 1187–1192 (1943).

55. Berthold, F., Lindfors, E. L. & Gellerstedt, G. Degradation of Guaiacylglycerol-β-Guaiacyl Ether in the Presence of NaHS or Polysulphide at Various Alkalinities. Part II. Liberation of Coniferyl Alcohol and Sulphur. *Holzforschung* **52**, 481–489 (1998).

56. Berthold, F., Lindfors, E. L. & Gellerstedt, G. Degradation of Guaiacylglycerol-β-Guaiacyl Ether in the Presence of NaHS or Polysulphide at Various Alkalinities. Part I. Degradation Rate and the Formation of Enol Ether. *Holzforschung* **52**, 398–404 (1998).

57. Feghali, E. *et al.* Thermosetting Polymers from Lignin Model Compounds and Depolymerized Lignins. *Top. Curr. Chem.* **376**, 1–25 (2018).

58. Lahive, C. W., Kamer, P. C. J., Lancefield, C. S. & Deuss, P. J. An Introduction to Model Compounds of Lignin Linking Motifs; Synthesis and Selection Considerations for Reactivity Studies. *ChemSusChem* **13**, 4238–4265 (2020).

59. Lupoi, J. S., Singh, S., Parthasarathi, R., Simmons, B. A. & Henry, R. J. Recent innovations in analytical methods for the qualitative and quantitative assessment of lignin. *Renew. Sustain. Energy Rev.* **49**, 871–906 (2015).

60. McCarthy, J. L. & Islam, A. Lignin Chemistry, Technology, and Utilization: A Brief History. in *Lignin: Historical, Biological, and Materials Perspectives* (eds. Glasser, W. G., Northey, R. A. & Schultz, T. P.) vol. 742 2–99 (American Chemical Society, 1999).

61. Chen, C. L., Lai, Y. Z. & Dence, C. . Functional Group Analysis. in *Methods in Lignin Chemistry* (eds. Lin, S. Y. & Dence, C. W.) 407–484 (Springer-Verlag, 1992). doi:10.1007/978-3-642-74065-7.

62. Chen, C. L., Gellerstedt, G., Rolando, C., Monties, B. & Lapierre, C. Characterization in Solution: Chemical Degradation Methods. in *Methods in Lignin Chemistry* (eds. Lin, S. & Dence, C.) 287–404 (Springer-Verlag, 1992).

63. Lapierre, C. Determining Lignin Structure by Chemical Degradations. in *Lignin and Lignans Advances in Chemistry* (eds. Heitner, C., Dimmel, D. R. & Schmidt, J. A.) 11–42 (CRC Press, Taylor & Francis, 2010).

64. Anderson, E. M. *et al.* Differences in S/G ratio in natural poplar variants do not predict catalytic depolymerization monomer yields. *Nat. Commun.* **10**, 1–10 (2019).

65. Balakshin, M. *et al.* Spruce milled wood lignin: Linear, branched or cross-linked? *Green Chem.* **22**, 3985–4001 (2020).

66. Yue, F., Lu, F., Regner, M., Sun, R. & Ralph, J. Lignin-Derived Thioacidolysis Dimers: Reevaluation, New Products, Authentication, and Quantification. *ChemSusChem* **10**, 830–835 (2017).

67. Harman-Ware, A. E. *et al.* A thioacidolysis method tailored for higher-throughput quantitative analysis of lignin monomers. *Biotechnol. J.* **11**, 1268–1273 (2016).

68. Ralph, J. & Landucci, L. L. NMR of Lignins. in *Lignin and Lignans Advances in Chemistry* (eds. Heitner, C., Dimmel, D. R. & Schmidt, J. A.) 138–222 (CRC Press, Taylor & Francis, 2010).

69. Meng, X. *et al.* Determination of hydroxyl groups in biorefinery resources via quantitative ^{31}P NMR spectroscopy. *Nat. Protoc.* **14**, 2627–2647 (2019).

70. Constant, S., Lancefield, C. S., Weckhuysen, B. M. & Bruijnincx, P. C. A. Quantification and Classification of Carbonyls in Industrial Humins and Lignins by ^{19}F NMR. *ACS Sustain. Chem. Eng.* **5**, 965–972 (2017).

71. Lancefield, C. S., Constant, S., de Peinder, P. & Bruijnincx, P. C. A. Linkage Abundance and Molecular Weight Characteristics of Technical Lignins by Attenuated Total Reflection-FTIR Spectroscopy Combined with Multivariate Analysis. *ChemSusChem* **12**, 1139–1146 (2019).

72. Lundquist, K. NMR Studies of Lignins. 5. Investigation of Non-derivatized Spruce and Birch Lignin by ^{1}H NMR spectroscopy. *Acta Chem. Scand. B* **35**, 497–501 (1981).

73. Lundquist, K. NMR studies of Lignins. 2. Interpretation of the ^{1}H NMR Spctrum of Acetylated Birch Lignin. *Acta Chem. Scand. B* **33**, 27–30 (1979).

74. Lundquist, K. NMR Studies pf Lignins. 4. Investigation of Spruce Lignin by ^{1}H NMR Spectroscopy. *Acta Chem. Scand. B* **34**, 21–26 (1980).

75. Shimatani, K., Sano, Y. & Sasaya, T. Preparation of moderate-temperature setting adhesives from softwood kraft lignin. Part 2. Effect of some factors on strength properties and chracteristics of lignin-based adhesives. *Holzforschung* **48**, 337–342 (1994).

76. Rönnols, J., Danieli, E., Freichels, H. & Aldaeus, F. Lignin analysis with benchtop NMR spectroscopy. *Holzforschung* **74**, 226–231 (2020).

77. Chen, C.-L. & Robert, D. Characterization of lignin by ^{1}H and ^{13}C NMR spectroscopy. *Methods Enzymol.* **161**, 137–174 (1988).

78. Kringstad, B. K. P. & Mörck, R. ^{13}C-NMR Spectra of Kraft Lignins. **37**, 237–244 (1983).

79. Ralph, S. A., Ralph, J. & Landucci, L. L. NMR Database of Lignin and Cell Wall Model Compounds. 109 (compound 89) date accessed 12-01–21 https://www.glbrc.org/databases_and_software/nmrdatabase/ (2009).

80. Xia, Z., Akim, L. G. & Argyropoulos, D. S. Quantitative ^{13}C NMR analysis of lignins with internal standards. *J. Agric. Food Chem.* **49**, 3573–3578 (2001).

81. Balakshin, M. Y., Capanema, E. A., Santos, R. B., Chang, H. M. & Jameel, H. Structural analysis of hardwood native lignins by quantitative ^{13}C NMR spectroscopy. *Holzforschung* **70**, 95–108 (2016).

82. Berlin, A. & Balakshin, M. Chapter 18 - Industrial Lignins: Analysis, Properties, and Applications. in *Bioenergy Research: Advances and Applications* (ed. Gupta, V. K.) 315–336 (Elsevier, 2014). doi:http://dx.doi.org/10.1016/B978-0-444-59561-4.00018-8.

83. Granata, A. & Argyropoulos, D. S. 2-Chloro-4,4,5,5-tetramethyl-1,3,2-dioxaphospholane, a Reagent for the Accurate Determination of the Uncondensed and Condensed Phenolic Moieties in Lignins. *J. Agric. Food Chem.* **43**, 1538–1544 (1995).

84. Schiff, D. E., Verkade, J. G., Metzler, R. M., Squires, T. G. & Venier, C. G. Determination of Alcohols, Phenols, and Carboxylic Acids Using Phosphorus-31 Nmr Spectroscopy. *Appl. Spectrosc.* **40**, 348–351 (1986).

85. Lensink, C., Markuszewski, R., Verkade, J. G. & Wroblewski, A. E. ^{31}P NMR Spectroscopic Analysis of Coal Pyrolysis Condensates and Extracts for Heteroatom Functionalities Possessing Labile Hydrogen. *Energy and Fuels* **2**, 765–774 (1988).

86. Lensink, C. & Verkade, J. G. ^{31}P NMR Spectroscopic Analysis of Labile Hydrogen Functional Groups: Identification with a Dithiaphospholane Reagent. *Energy and Fuels* **4**, 197–201 (1990).

87. Archipov, Y., Argyropoulos, D. S., Bolker, H. I. & Heitner, C. ^{31}P NMR Spectroscopy in Wood Chemistry Part I - Model Compounds. *J. Wood Chem. Technol.* **11**, 137–157 (1991).

88. Argyropoulos, D. S., Bolker, H. I., Heitner, C. & Archipov, Y. ^{31}P NMR Spectroscopy in Wood Chemistry Part V . Qualitative Analysis of Lignin Functional Groups. *J. Wood Chem. Technol.* **13**, 187–212 (1993).

89. Argyropoulos, D. S., Bolker, H. I., Heitner, C. & Archipov, Y. ^{31}P NMR Spectroscopy in Wood Chemistry Part IV. Lignin Models: Spin Lattice Relaxation Times and Solvent Effects in ^{31}P NMR. *Holzforschung* **47**, 50–56 (1993).

90. Argyropoulos, D. Quantitative phosphorus-31 NMR analysis of six soluble lignins. *J. wood Chem. Technol.* **14**, 65–82 (1994).

91. Argyropoulos, D. S. Quantitative phosphorus-31 nmr analysis of lignins, a new tool for the lignin chemist. *J. Wood Chem. Technol.* **14**, 45–63 (1994).

92. Zawadzki, M. & Ragauskas, A. N-hydroxy compounds as new internal standards for the ^{31}P-NMR determination of lignin hydroxy functional groups. *Holzforschung* **55**, 283–285 (2001).

93. Korntner, P., Sumerskii, I., Bacher, M., Rosenau, T. & Potthast, A. Characterization of technical lignins by NMR spectroscopy: Optimization of functional group analysis by 31P NMR spectroscopy. *Holzforschung* **69**, 807–814 (2015).

94. Balakshin, M. & Capanema, E. On the Quantification of Lignin Hydroxyl Groups With ^{31} P and ^{13} C NMR Spectroscopy. *J. Wood Chem. Technol.* **35**, 220–237 (2015).

95. Spyros, A. & Dais, P. Application of ^{31}P NMR spectroscopy in food analysis. 1. Quantitative determination of the mono- and diglyceride composition of olive oils. *J. Agric. Food Chem.* **48**, 802–805 (2000).

96. Stücker, A., Podschun, J., Saake, B. & Lehnen, R. A novel quantitative ^{31}P NMR spectroscopic analysis of hydroxyl groups in lignosulfonic acids. *Anal. Methods* **10**, 3481–3488 (2018).

97. Ben, H. *et al.* Characterization of Whole Biomasses in Pyridine Based Ionic Liquid at Low Temperature by ^{31}P NMR: An Approach to Quantitatively Measure Hydroxyl Groups in Biomass As Their Original Structures. *Front. Energy Res.* **6**, 1–7 (2018).

98. Crestini, C., Lange, H. & Bianchetti, G. Detailed Chemical Composition of Condensed Tannins via Quantitative ^{31}P NMR and HSQC Analyses: Acacia catechu, Schinopsis balansae, and Acacia mearnsii. *J. Nat. Prod.* **79**, 2287–2295 (2016).

99. Spyros, A. Phosphorus Derivatization as a Tool to Enhance Specificity of Quantitative NMR Analysis of Foods. in *Modern Magnetic Resonance* (ed. Webb, G. A.) 1–9 (Springer, Cham, 2017). doi:https://doi.org/10.1007/978-3-319-28275-6_7-1.

100. Fronimaki, P., Spyros, A., Christophoridou, S. & Dais, P. Determination of the diglyceride

content in Greek virgin olive oils and some commercial olive oils by employing ^{31}P NMR spectroscopy. *J. Agric. Food Chem.* **50**, 2207–2213 (2002).

101. Vigli, G., Philippidis, A., Spyros, A. & Dais, P. Classification of edible oils by employing 31P and ^{1}H NMR spectroscopy in combination with multivariate statistical analysis. A proposal for the detection of seed oil adulteration in virgin olive oils. *J. Agric. Food Chem.* **51**, 5715–5722 (2003).
102. Dais, P. *et al.* Comparison of analytical methodologies based on ^{1}H and ^{31}P NMR spectroscopy with conventional methods of analysis for the determination of some olive oil constituents. *J. Agric. Food Chem.* **55**, 577–584 (2007).
103. Wang, X., Guo, Y., Zhou, J. & Sun, G. Structural changes of poplar wood lignin after supercritical pretreatment using carbon dioxide and ethanol-water as co-solvents. *RSC Adv.* **7**, 8314–8322 (2017).
104. Wen, J. L., Sun, S. L., Xue, B. L. & Sun, R. C. Recent advances in characterization of lignin polymer by solution-state nuclear magnetic resonance (NMR) methodology. *Materials (Basel).* **6**, 359–391 (2013).
105. Yue, F., Lu, F., Ralph, S. & Ralph, J. Identification of 4-O-5-Units in Softwood Lignins via Definitive Lignin Models and NMR. *Biomacromolecules* **17**, 1909–1920 (2016).
106. Liu, L.-Y. *et al.* Valorization of Bark Using Ethanol–Water Organosolv Treatment: Isolation and Characterization of Crude Lignin. *ACS Sustain. Chem. Eng.* **8**, 4745–4754 (2020).
107. Kim, H. *et al.* Characterization and Elimination of Undesirable Protein Residues in Plant Cell Wall Materials for Enhancing Lignin Analysis by Solution-State Nuclear Magnetic Resonance Spectroscopy. *Biomacromolecules* **18**, 4184–4195 (2017).
108. Jawerth, M., Johansson, M., Lundmark, S., Gioia, C. & Lawoko, M. Renewable Thiol-Ene Thermosets Based on Refined and Selectively Allylated Industrial Lignin. *ACS Sustain. Chem. Eng.* **5**, 10918–10925 (2017).
109. Zhang, L. & Gellerstedt, G. NMR observation of a new lignin structure, a spiro-dienone. *Chem. Commun.* **1**, 2744–2745 (2001).
110. Karhunen, P., Rummakko, P., Sipilä, J., Brunow, G. & Kilpeläinen, I. The formation of dibenzodioxocin structures by oxidative coupling. A model reaction for lignin biosynthesis. *Tetrahedron Lett.* **36**, 4501–4504 (1995).
111. Karhunen, P., Rummakko, P., Sipilä, J., Brunow, G. & Kilpeläinen, I. Dibenzodioxocins; a novel type of linkage in softwood lignins. *Tetrahedron Lett.* **36**, 169–170 (1995).
112. Del Río, J. C. *et al.* Structural characterization of wheat straw lignin as revealed by analytical pyrolysis, 2D-NMR, and reductive cleavage methods. *J. Agric. Food Chem.* **60**, 5922–5935 (2012).
113. Ralph, J., Lapierre, C. & Boerjan, W. Lignin structure and its engineering. *Curr. Opin. Biotechnol.* **56**, 240–249 (2019).
114. Foston, M., Samuel, R., He, J. & Ragauskas, A. J. A review of whole cell wall NMR by the direct-dissolution of biomass. *Green Chem.* 608–621 (2016) doi:10.1039/C5GC02828K.
115. Mansfield, S. D., Kim, H., Lu, F. & Ralph, J. Whole plant cell wall characterization using solution-state 2D NMR. *Nat. Protoc.* **7**, 1579–1589 (2012).
116. Zhang, L. & Gellerstedt, G. Quantitative 2D HSQC NMR determination of polymer structures by selecting suitable internal standard references. *Magn. Reson. Chem.* **45**, 37–45 (2007).
117. Peterson, D. J. & Loening, N. M. QQ-HSQC: a quick, quantitative heteronuclear correlation experiment for NMR spectroscopy. *Magn. Reson. Chem.* **45**, 937–941 (2007).
118. Hu, K., Westler, W. M. & Markley, J. L. Simultaneous quantification and identification of individual chemicals in metabolite mixtures by two-dimensional extrapolated time-zero 1H-13C HSQC (HSQC0). *J. Am. Chem. Soc.* **133**, 1662–1665 (2011).

119. Heikkinen, S., Toikka, M. M., Karhunen, P. T. & Kilpeläinen, I. A. Quantitative 2D HSQC (Q-HSQC) via suppression of J-dependence of polarization transfer in NMR spectroscopy: Application to wood lignin. *J. Am. Chem. Soc.* **125**, 4362–4367 (2003).

120. Gellerstedt, G., Pla, F., Lin, S. Y., Chen, C. L. & Lewis, N. G. Determination of Molecular Weight, Size and Distribution. in *Methods in Lignin Chemistry* (eds. Lin, S. & Dence, C.) 485–568 (Spring-Verlag, 1992).

121. Alzahrani, Q. E. *et al.* Matrix-free hydrodynamic study on the size distribution and conformation of three technical lignins from wood and non-wood. *Holzforschung* **70**, 117–125 (2016).

122. Tolbert, A., Akinosho, H., Khunsupat, R., Naskar, A. K. & Ragauskas, A. J. Characterization and analysis of the molecular weight of lignin for biorefi ning studies. *Biofuels, Bioprod. Biorefining* **8**, 836–856 (2014).

123. Sulaeva, I. *et al.* Fast Track to Molar-Mass Distributions of Technical Lignins. *ChemSusChem* **10**, 629–635 (2017).

124. Cathala, B., Saake, B., Faix, O. & Monties, B. Association behaviour of lignins and lignin model compounds studied by multidetector size-exclusion chromatography. *J. Chromatogr. A* **1020**, 229–239 (2003).

125. Baumberger, S. *et al.* Molar mass determination of lignins by size-exclusion chromatography: Towards standardisation of the method. *Holzforschung* **61**, 459–468 (2007).

126. Asikkala, J., Tamminen, T. & Argyropoulos, D. S. Accurate and reproducible determination of lignin molar mass by acetobromination. *J. Agric. Food Chem.* **60**, 8968–8973 (2012).

127. Lange, H., Rulli, F. & Crestini, C. Gel Permeation Chromatography in Determining Molecular Weights of Lignins: Critical Aspects Revisited for Improved Utility in the Development of Novel Materials. *ACS Sustain. Chem. Eng.* **4**, 5167–5180 (2016).

128. Zinovyev, G. *et al.* Getting Closer to Absolute Molar Masses of Technical Lignins. *ChemSusChem* **11**, 3259–3268 (2018).

129. Gaugler, E. C., Radke, W., Vogt, A. P. & Smith, D. A. Molar mass determination of lignins and characterization of their polymeric structures by multi-detector gel permeation chromatography. *J. Anal. Sci. Technol.* **12**, (2021).

130. Mattinen, M. L. *et al.* Polymerization of different lignins by laccase. *BioResources* **3**, 549–565 (2008).

131. Yoshioka, K., Ando, D. & Watanabe, T. A comparative study of matrix- and nano-assisted laser desorption/ ionisation time-of-flight mass spectrometry of isolated and synthetic lignin. *Phytochem. Anal.* **23**, 248–253 (2012).

132. Rönnols, J., Jacobs, A. & Aldaeus, F. Consecutive determination of softwood kraft lignin structure and molar mass from NMR measurements. *Holzforschung* **71**, 563–570 (2017).

133. Montgomery, J. R. D., Bazley, P., Lebl, T. & Westwood, N. J. Using Fractionation and Diffusion Ordered Spectroscopy to Study Lignin Molecular Weight. *ChemistryOpen* **8**, 601–605 (2019).

134. Suota, M. J. *et al.* Lignin Functionalization Strategies and the Potential Applications of Its Derivatives - A Review. *BioResources* vol. 16 6471–6511 (2021).

135. Holladay, J. E., White, J. F., Bozell, J. J. & Johnson, D. *Top Value-Added Chemicals from Biomass - Volume II—Results of Screening for Potential Candidates from Biorefinery Lignin*. https://www.osti.gov/biblio/921839 (2007) doi:10.2172/921839.

136. Löfstedt, J. *et al.* Green Diesel from Kraft Lignin in Three Steps. *ChemSusChem* **9**, 1392–1396 (2016).

137. Duval, A. & Lawoko, M. A review on lignin-based polymeric , micro- and nano-structured materials. *React. Funct. Polym.* **85**, 78–96 (2014).

138. Laurichesse, S. & Avérous, L. Chemical modification of lignins: Towards biobased

polymers. *Prog. Polym. Sci.* **39**, 1266–1290 (2014).

139. Matsushita, Y. Conversion of technical lignins to functional materials with retained polymeric properties. *J. Wood Sci.* **61**, 230–250 (2015).
140. Upton, B. M. & Kasko, A. M. Strategies for the Conversion of Lignin to High-Value Polymeric Materials: Review and Perspective. *Chem. Rev.* **116**, 2275–2306 (2016).
141. Baker, D. A. & Rials, T. G. Recent advances in low-cost carbon fiber manufacture from lignin. *J. Appl. Polym. Sci.* **130**, 713–728 (2013).
142. Sun, Z., Fridrich, B., De Santi, A., Elangovan, S. & Barta, K. Bright Side of Lignin Depolymerization: Toward New Platform Chemicals. *Chem. Rev.* **118**, 614–678 (2018).
143. Deuss, P. J. & Barta, K. From models to lignin: Transition metal catalysis for selective bond cleavage reactions. *Coord. Chem. Rev.* **306**, 510–532 (2016).
144. Li, C., Zhao, X., Wang, A., Huber, G. W. & Zhang, T. Catalytic Transformation of Lignin for the Production of Chemicals and Fuels. *Chemical Reviews* vol. 115 11559–11624 (2015).
145. Kärkäs, M. D., Matsuura, B. S., Monos, T. M., Magallanes, G. & Stephenson, C. R. J. J. Transition-metal catalyzed valorization of lignin: The key to a sustainable carbon-neutral future. *Org. Biomol. Chem.* **14**, 1853–1914 (2016).
146. Korányi, T. I., Fridrich, B., Pineda, A. & Barta, K. Development of 'Lignin-First' Approaches for the Valorization of Lignocellulosic Biomass. *Molecules* **25**, 1–22 (2020).
147. Renders, T., Van Den Bosch, S., Koelewijn, S. F., Schutyser, W. & Sels, B. F. Lignin-first biomass fractionation: The advent of active stabilisation strategies. *Energy Environ. Sci.* **10**, 1551–1557 (2017).
148. Shuai, L. *et al.* Formaldehyde stabilization facilitates lignin monomer production during biomass depolymerization. *Science (80-.).* **354**, 329–333 (2016).
149. Lan, W., Amiri, M. T., Hunston, C. M. & Luterbacher, J. S. Protection Group Effects During α,γ-Diol Lignin Stabilization Promote High-Selectivity Monomer Production. *Angew. Chemie - Int. Ed.* **57**, 1356–1360 (2018).
150. Wagner, A. *et al.* Syringyl lignin production in conifers: Proof of concept in a Pine tracheary element system. *Proc. Natl. Acad. Sci. U. S. A.* **112**, 6218–6223 (2015).
151. Li, Y. *et al.* An ideal lignin facilitates full biomass utilization. *Sci. Adv.* **4**, (2018).
152. Wilkerson, C. G. *et al.* Monolignol ferulate transferase introduces chemically labile linkages into the lignin backbone. *Science (80-.).* **344**, 90–93 (2014).
153. Dumont, C., Gauvin, R. M., Belva, F. & Sauthier, M. Palladium-Catalyzed Functionalization of Kraft Lignin: Ether Linkages through the Telomerization Reaction. *ChemSusChem* **11**, 1649–1655 (2018).
154. Ganewatta, M. S., Lokupitiya, H. N. & Tang, C. Lignin Biopolymers in the Age of Controlled Polymerization. *Polymers (Basel).* **11**, 1176 (2019).
155. Moreno, A. & Sipponen, M. H. Lignin-based smart materials: A roadmap to processing and synthesis for current and future applications. *Mater. Horizons* **7**, 2237–2257 (2020).
156. Gioia, C., Lo Re, G., Lawoko, M. & Berglund, L. Tunable Thermosetting Epoxies Based on Fractionated and Well-Characterized Lignins. *J. Am. Chem. Soc.* **140**, 4054–4061 (2018).
157. Karaaslan, M. A., Cho, M., Liu, L.-Y., Wang, H. & Renneckar, S. Refining the Properties of Softwood Kraft Lignin with Acetone: Effect of Solvent Fractionation on the Thermomechanical Behavior of Electrospun Fibers. *ACS Sustain. Chem. Eng.* **9**, 458–470 (2021).
158. Sadeghifar, H. & Ragauskas, A. Perspective on Technical Lignin Fractionation. *ACS Sustain. Chem. Eng.* **8**, 8086–8101 (2020).
159. Österberg, M., Sipponen, M. H., Mattos, B. D. & Rojas, O. J. Spherical lignin particles: A review on their sustainability and applications. *Green Chem.* **22**, 2712–2733 (2020).
160. Sipponen, M. H., Lange, H., Crestini, C., Henn, A. & Österberg, M. Lignin for Nano- and

Microscaled Carrier Systems: Applications, Trends, and Challenges. *ChemSusChem* **12**, 2039–2054 (2019).

161. von Schoultz, S. Method for extracting biomass. WO 2014/009604 A1 (2014).

162. von Schoultz, S. Method for extracting lignin. WO 2015/104460 A1 (2015).

163. Leppänen, K. *et al.* Pressurized hot water extraction of Norway spruce hemicelluloses using a flow-through system. *Wood Sci. Technol.* **45**, 223–236 (2011).

164. Björkman, A. Studies on Finely Divided Wood. Part I. Extraction of Lignin with Neutral Solvents. *Sven. Papperstidning* **59**, 477–485 (1956).

165. Zwierzak, A. Cyclic organophosphorus compounds. I. Synthesis and infrared spectral studies of cyclic hydrogen phosphites and thiophosphites. *Can. J. Chem.* **45**, 2501–2512 (1967).

166. Sadeghifar, H., Cui, C. & Argyropoulos, D. S. Toward thermoplastic lignin polymers. Part 1. Selective masking of phenolic hydroxyl groups in kraft lignins via methylation and oxypropylation chemistries. *Ind. Eng. Chem. Res.* **51**, 16713–16720 (2012).

167. Saá, J., Llobera, A., García-Raso, A., Costa, A. & Deyá, P. M. Metalation of Phenols. Synthesis of Benzoquinones by the Oxidative Degradation Approach. *J. Org. Chem.* **53**, 4263–4273 (1988).

168. Costa, A. & Saá, J. M. On the Metalation of Phenolic Compounds: Ready Access to Highly Substituted Phenols. *Tetrahedron Lett.* **28**, 5551–5554 (1987).

169. Ellerbrock, P., Armanino, N., Ilg, M. K., Webster, R. & Trauner, D. An eight-step synthesis of epicolactone reveals its biosynthetic origin. *Nat. Chem.* **7**, 879–882 (2015).

170. Davidson, S. J. & Barker, D. Total Synthesis of Ovafolinins A and B: Unique Polycyclic Benzoxepin Lignans through a Cascade Cyclization. *Angew. Chemie - Int. Ed.* **56**, 9483–9486 (2017).

171. Priestley, E. S. *et al.* Discovery and gram-scale synthesis of BMS-593214, a potent, selective FVIIa inhibitor. *Bioorganic Med. Chem. Lett.* **23**, 2432–2435 (2013).

172. Smeds, A. I., Eklund, P. C., Monogioudi, E. & Willför, S. Chemical characterization of polymerized products formed in the reactions of matairesinol and pinoresinol with the stable radical 2,2-diphenyl-1- picrylhydrazyl. *Holzforschung* **66**, 283–294 (2012).

173. Smeds, A. I., Eklund, P. C. & Willför, S. Chemical characterization of high-molar-mass fractions in a Norway spruce knotwood ethanol extract. *Phytochemistry* **130**, 207–217 (2016).

174. Sundberg, A., Sundberg, K., Lillandt, C. & Holmbom, B. Determination of hemicelluloses and pectins in wood and pulp fibres by acid methanolysis and gas chromatography. *Nord. Pulp Pap. Res. J.* **11**, 216–219 (1996).

175. Willför, S. *et al.* Carbohydrate analysis of plant materials with uronic acid-containing polysaccharides-A comparison between different hydrolysis and subsequent chromatographic analytical techniques. *Ind. Crops Prod.* **29**, 571–580 (2009).

176. Sumerskii, I. *et al.* Fast track for the accurate determination of methoxyl groups in lignin. in *RSC Advances* vol. 7 22974–22982 (Royal Society of Chemistry, 2017).

177. Constant, S. *et al.* New insights into the structure and composition of technical lignins: a comparative characterisation study. *Green Chem.* **18**, 2651–2665 (2016).

178. Gellerstedt, G., Pranda, J. & Lindfors, E. L. Structural and Molecular-Properties of Residual Birch Kraft Lignins. *J. Wood Chem. Technol.* **14**, 467–482 (1994).

179. Kalliola, A., Savolainen, A., Ohra-aho, T. & Faccio, G. Reducing the Content of Vocs of Softwood Kraft. *BioResources* **7**, 2871–2882 (2012).

180. Bartholomew, C. H. Mechanisms of catalyst deactivation. *Appl. Catal. A Gen.* **212**, 17–60 (2001).

181. Compere, A. L., Griffith, W. L., Leitten, C. F. & Pickel, J. M. *Evaluation of Lignin from Alkaline-Pulped Hardwood Black Liquor*. *Reports of the Oak Ridge National Laboratory*

(2005).

182. Sumerskiy, I., Pranovich, A., Holmbom, B. & Willför, S. Lignin and Other Aromatic Substances Released from Spruce Wood During Pressurized Hot-Water Extraction, Part 1: Extraction, Freactionation and Physio-Chemical Characterization. *J. Wood Chem. Technol.* **35**, 398–411 (2015).

183. Gordobil, O., Delucis, R., Egüés, I. & Labidi, J. Kraft lignin as filler in PLA to improve ductility and thermal properties. *Ind. Crops Prod.* **72**, 46–53 (2015).

184. Kim, Y. *et al.* All Biomass and UV Protective Composite Composed of Compatibilized Lignin and Poly (Lactic-acid). *Sci. Rep.* **7**, 1–11 (2017).

185. Cicala, G. *et al.* Polylactide / lignin blends. *J. Therm. Anal. Calorim.* **130**, 515–524 (2017).

186. Giummarella, N. & Lawoko, M. Structural Insights on Recalcitrance during Hydrothermal Hemicellulose Extraction from Wood. *ACS Sustain. Chem. Eng.* **5**, 5156–5165 (2017).

187. Gierer, J. Chemical Aspects of Kraft Pulping. *Wood Sci. Technol.* **14**, 241–266 (1980).

188. Lundquist, K. & Von Unge, S. Stability of arylglycerols during alkaline cooking. *Holzforschung* **58**, 330–333 (2004).

189. Ede, R. M. *et al.* Application of Two-Dimensional NMR Spectroscopy to Wood Lignin Structure Determination and Identification of Some Minor Structural Units of Hard- and Softwood Lignins. *J. Agric. Food Chem.* **42**, 2790–2794 (1994).

190. Ralph, J., Akiyama, T., Coleman, H. D. & Mansfield, S. D. Effects on Lignin Structure of Coumarate 3-Hydroxylase Downregulation in Poplar. *Bioenergy Res.* **5**, 1009–1019 (2012).

191. Teleman, A., Lundqvist, J., Tjerneld, F., Stålbrand, H. & Dahlman, O. Characterization of acetylated 4-O-methylglucuronoxylan isolated from aspen employing ^{1}H and ^{13}C NMR spectroscopy. *Carbohydr. Res.* **329**, 807–815 (2000).

192. Zhao, C., Li, S., Zhang, H., Yue, F. & Lu, F. Structural insights into the alkali lignins involving the formation and transformation of arylglycerols and enol ethers. *Int. J. Biol. Macromol.* **152**, 411–417 (2020).

193. Fernández-Costas, C., Gouveia, S., Sanromán, M. A. & Moldes, D. Structural characterization of Kraft lignins from different spent cooking liquors by 1D and 2D Nuclear Magnetic Resonance spectroscopy. *Biomass and Bioenergy* **63**, 156–166 (2014).

194. Duarte, A. P., Robert, D. & Lachenal, D. Eucalyptus globulus kraft pulp residual lignin. Part 2. Modification of residual lignin structure in oxygen bleaching. *Holzforschung* **55**, 645–651 (2001).

195. Sun, S., Yang, H., Sun, R. & Tu, M. The strong association of condensed phenolic moieties in isolated lignins with their inhibition of enzymatic hydrolysis. *Green Chem.* **18**, 4276–4286 (2016).

196. Landucci, L. L. & Ralph, S. A. Assessment of lignin model quality in lignin chemical shift assignments - Substituent and solvent effects. *J. Wood Chem. Technol.* **17**, 361–382 (1997).

197. Araya, F., Troncoso, E., Mendonça, R. T. & Freer, J. Condensed lignin structures and re-localization achieved at high severities in autohydrolysis of Eucalyptus globulus wood and their relationship with cellulose accessibility. *Biotechnol. Bioeng.* **112**, 1783–1791 (2015).

198. Brandt, A., Chen, L., van Dongen, B. E., Welton, T. & Hallett, J. P. Structural changes in lignins isolated using an acidic ionic liquid water mixture. *Green Chem.* **17**, 5019–5034 (2015).

199. Kangas, H. *et al.* Characterization of dissolved lignins from acetic acid Lignofibre (LGF) organosolv pulping and discussion of its delignification mechanisms. *Holzforschung* **69**, 247–256 (2015).

200. Samuel, R. *et al.* Investigation of the fate of poplar lignin during autohydrolysis

pretreatment to understand the biomass recalcitrance. *RSC Adv.* **3**, 5305 (2013).

201. Shen, X.-J., Wang, B., Pan-li, H., Wen, J.-L. & Sun, R. C. Understanding the structural changes and depolymerization of Eucalyptus lignin under mild conditions in aqueous AlCl 3. *RSC Adv.* **6**, 45315–45325 (2016).
202. Xiao, L. P., Shi, Z. J., Xu, F. & Sun, R. C. Characterization of Lignins Isolated with Alkaline Ethanol from the Hydrothermal Pretreated Tamarix ramosissima. *Bioenergy Res.* **6**, 519–532 (2013).
203. Zhu, M. Q., Wen, J. L., Su, Y. Q., Wei, Q. & Sun, R. C. Effect of structural changes of lignin during the autohydrolysis and organosolv pretreatment on Eucommia ulmoides Oliver for an effective enzymatic hydrolysis. *Bioresour. Technol.* **185**, 378–385 (2015).
204. Ikeya, Y. *et al.* A Lignan from Schizandra chinensis. *Phytochemistry* **27**, 569–573 (1988).
205. Gan, L. S., Yang, S. P., Fan, C. Q. & Yue, J. M. Lignans and their degraded derivatives from Sarcostemma acidum. *J. Nat. Prod.* **68**, 221–225 (2005).
206. Ikeya, Y., Taguchi, H. & Yosioka, I. The Constituents of Schizandra chinensis BAILL. VII. The Structures of Three New Lignans, (-)-Gomisin K1 and (+)-Gomisins K2 and K3. *Chem. Pharm. Bull.* **28**, 2422–2427 (1980).
207. Agrawal, P. K. & Thakur, R. S. ^{13}C NMR Spectroscopy of lignan and neolignan derivatives. *Magn. Reson. Chem.* **23**, 389–418 (1985).
208. Yasuda, S. & Murase, N. Chemical Structures of Sulfuric Acid Lignin Part XII. Reaction of Lignin Models with Carbohydrates in 72% H2SO4. *Holzforschung* **49**, 418–422 (1995).
209. Yasuda, S. & Ota, K. Chemical Structures of Sulfuric Acid Lignin. *Holzforschung* **41**, 59–65 (1987).
210. Li, J. & Gellerstedt, G. Improved lignin properties and reactivity by modifications in the autohydrolysis process of aspen wood. *Ind. Crops Prod.* **27**, 175–181 (2008).
211. Kolehmainen, E., Laihia, K., Knuutinen, J. & Hyötyläinen, J. 1H, ^{13}C and ^{17}O NMR study of chlorovanillins and some related compounds. *Magn. Reson. Chem.* **30**, 253–258 (1992).
212. Giummarella, N., Lindén, P. A., Areskogh, D. & Lawoko, M. Fractional Profiling of Kraft Lignin Structure: Unravelling Insights on Lignin Reaction Mechanisms. *ACS Sustain. Chem. Eng.* **8**, 1112–1120 (2020).
213. Li, N. *et al.* An uncondensed lignin depolymerized in the solid state and isolated from lignocellulosic biomass: A mechanistic study. *Green Chem.* **20**, 4224–4235 (2018).
214. Wider, G. & Dreier, L. Measuring protein concentrations by NMR spectroscopy. *J. Am. Chem. Soc.* **128**, 2571–2576 (2006).
215. Monakhova, Y. B., Kohl-Himmelseher, M., Kuballa, T. & Lachenmeier, D. W. Determination of the purity of pharmaceutical reference materials by ^{1}H NMR using the standardless PULCON methodology. *J. Pharm. Biomed. Anal.* **100**, 381–386 (2014).

ISBN 978-952-12-4195-6